UNIVERSITY OF OKLAHOMA

GRADUATE COLLEGE

DYNAMICS AND STABILITY OF BUOYANCY-INDUCED FLOWS

A DISSERTATION

SUBMITTED TO THE GRADUATE FACULTY

in partial fulfillment of the requirements for the

Degree of

DOCTOR OF PHILOSOPHY

By

DANIA SHEAIB
Norman, Oklahoma
2019

DYNAMICS AND STABILITY OF BUOYANCY-INDUCED FLOWS

A DISSERTATION APPROVED FOR THE
DEPARTMENT OF MATHEMATICS

BY

Dr. Alexander Grigo, Chair

Dr. Nikola Petrov, Co-Chair

Dr. Kurt Marfurt

Dr. John Albert

Dr. Christian Remling

Acknowledgments

"Reflect upon your present blessings, of which every man has plenty; not on your past misfortunes, of which all men have some." – **Charles Dickens**

When I count my blessings, I count my family twice and so I dedicate this dissertation to my Mom, Wafaa, my Dad Wafic, my brother Bilal and his lovely wife Marwa. You all have taught me the true meaning of love, perseverance, hard work and resilience. You have embraced me when I was at my lowest and supported me both financially and emotionally. I cannot be thankful enough for my parents who chose to invest the little money they have in educating me and my brother because they believe that education is the best legacy to leave behind and the most powerful tool to get us through the hurdles of life. I hope I made you all proud.

Words cannot express my ultimate gratitude to have Dr. Nikola Petrov as my advisor. He goes above and beyond the call of duty to ensure the well-being of his students. He has been an advisor, a mentor and most importantly a friend who has built my intuition about a great deal of mathematics and taught me a lot about life by sharing his valuable life experiences. I cannot thank him enough for his continuous encouragement, support and patience especially in the deepest frustrations of my research life and graduate school. None of this would have been possible without him. His lovely family gave me

a home away from home and I will greatly miss Adriana and Rossi because they have truly become family to me.

I would also like to thank my committee members Dr. John Albert, Dr. Alexander Grigo, Dr. Christian Remling, and Dr. Kurt Marfurt for overlooking my progress in the doctoral program, giving me constructive feedback on my dissertation and making themselves available whenever I needed advice. It has been a pleasure to be around such caring and friendly faculty at the mathematics department. Special thanks go to Dr. Ralf Schmidt for being an incredible graduate director, for all the valuable advice and for all the time and effort he constantly put in serving the graduate student community. Thank you Dr. Sepideh Stewart for all the conversations we had, for helping me become the teacher I am today and for your genuine heartfelt recommendation letters. Thank you Dr. Tomasz Przebinda, Dr. Kevin Grasse, Dr. Leonard Rubin, Dr. Jonathan Kujawa and Dr. Noel Brady for your kind support.

I want to express my sincere appreciation to Dr. Evgeni Fedorovich and Dr. Alan Shapiro from the School of Meteorology who did not hesitate to take the time of their busy schedules to reach out, offer valuable advice and help me overcome the challenges of my research. I am beyond grateful for having the chance to work with Dr. Shapiro whose conversations, long emails and guidance have added a unique perspective into my research and opened the door to many interesting future research problems.

This journey would not have been easy if it were not for the help of the sweet mathematics department staff. Thank you Lorraine Inkster for the motherly and caring figure you are. Thank you Dr. Catherine Hall for giving me professional advice on how to best handle tricky teaching situations. Thank you Cristin Yates for your patience, understanding and help all these years. Most

importantly, thank you for your valuable friendship and for always listening when I needed someone to vent to; you are amazing.

I would also like to take a moment to thank all the teachers from elementary to graduate school who shaped the person I am today; you are too many to name and I appreciate each one of you. Special thanks to my Master's thesis advisor Dr. Nabil Nassif for teaching me a lot about research and for pushing me to continuously improve and become a better version of myself.

I am very fortunate to be a part of a welcoming mathematics community at the University of Oklahoma. I would like first to thank Houssein and Salam for encouraging me to apply for the PhD program and for their hospitality and support especially during my early years in Oklahoma. Thank you to the ladies that started the program with me (Jieru, Rebecca, Fatma, Yan, and Emily) for all the memories and the fun moments. Thank you to my colleagues and friends Ignat, Garret, Sean, Bryan, Lee, Elizabeth, Connor, Martin, Tetsuya, Jeff, Tia, Manami, Chloe and Jessi.

Thank you Ore for being there during all the ups and downs of graduate school and the job hunt; I am truly grateful that we got through this together and I will definitely miss your sassy personality. I cannot be thankful enough for everything that Mahesh does for me, whether it is a ride from the airport or covering my classes and math center shifts; you will always be my 'little' brother and I wish you the best in the next chapter of your life.

They say friends are the family that we choose for ourselves and I am very blessed to have such kind spirits in my life. Thank you James for always being there for me, believing in me, uplifting my spirit, sharing your experiences, and giving me the extra push to reach my full potential. Thank you Lucas for always taking the time to check on me and give me advice; I am glad that our

paths crossed because you have become one of my best friends.

Thank you Hiba and Hayat for the endless phone calls, for your sincere advice and for being such an inspiration for me; I look up to both of you and I am so proud to have you in my life. Thank you to Rami Akkari, Kamel and Emad for everything; I know I can count on you whenever I need help and to that I am truly thankful. I am extremely blessed to have Karim, Wassim and Rami Haddad in my life; you are my brothers and I cannot imagine how life in Norman would have been without the joy you brought into my life. Thank you all for the support you have given me over the years, for believing in me, for the long conversations, and for the precious moments.

Despite all the stress, my last year of graduate school would not have gone smoothly if it were not for Hrsito. Although I have known you for only a short time, you have definitely left a great impact on my life. Thank you for giving me the strength to keep going and never give up. I am blessed that we had the chance to share many of our happy moments together.

To my beautiful friends in Lebanon, Iman, Nisreen, Salam and Rana, although we are thousands of miles apart, you will always be the closest to my heart. Thank you for being my optimum support system; I could not have asked for better sisters. I miss you all so much.

Contents

List of Figures

Abstract

The present dissertation tackles two different problems in fluid mechanics. In the first problem, we study the stability of free or natural convection of a compressible fluid over a heated plate underlying a semi-infinite vertical slot and underlying a closed vessel. For both settings, we show linear and nonlinear stability of the reference solution by constructing respective Lyapunov functions and using LaSalle's Invariance Principle. The construction of the Lyapunov function is motivated by the assumption that the fluid particles evolve according to a Markov chain. In the second problem, we study the flow dynamics of a viscous stably stratified fluid in a channel with time-periodic temperature variations applied at the sidewalls. Seeking solutions in the form of simple harmonic oscillations, we obtain analytical temperature and velocity profiles for the one-dimensional time-dependent flow. We then use these solutions to study the possibility of resonance of the fluid flow with the periodic oscillations of the externally supplied temperatures at the walls. Results indicate the existence of resonance depicted as prominent peaks of physical quantities at certain frequencies of the external temperature oscillations.

Chapter 1

Introduction

Natural or free convection is a mechanism in which the motion or mixing of the fluid is caused only by temperature differences within the fluid and not by an external source (such as a turbine or fan). These temperature differences result in density variation and thus give rise to the driving force of free convection known as buoyancy. Understanding free convection and buoyancy-induced flows in fluids is critical because of their abundance in nature and engineering applications. A very common industrial application of natural convection is free air cooling without the aid of fans. In nature, convection is the principle motor of cloud formation and circulation.

Chapters 2, 3 and 4, in collaboration with Dr. Alexander Grigo, study the stability analysis of free convection of a compressible fluid over a heated plate in two different regimes: semi-infinite vertical slot as well as a closed vessel. In contrast to previous work, we use the exact non-linear Navier-Stokes equations without imposing the Boussinesq approximation. Doing so increases the complexity of the problem as the fluid in this case is compressible and flow dynamics could be driven by the continuity equation.

The plan of Part I is as follows: In Chapter 2, we discuss the problem set-up and its boundary conditions and describe the reference state whose stability is under study. In Chapter 3, we apply a numerical model based on the finite element method to study the linear stability of the problem. Although the numerical results obtained in this chapter cannot be used as a proof of stability of the reference solution in the linear case, we choose to include them in this dissertation for their importance in building our intuition about the behaviour of perturbations of the reference state. Finally, in Chapter 4, we prove the stability of the reference solution in both the linear and non-linear settings by constructing respective Lyapunov functions that decrease over solutions of the corresponding systems. Since there is no systematic way for constructing Lyapunov functions, we dedicate section 4.3.1 to motivate the choice of the Lyapunov function that works in the non-linear setting.

The second part of this dissertation (Chapters 5, 6 and 7) is a collaborative work with Dr. Nikola Petrov and Dr. Alan Shapiro. In this part, we study the flow dynamics in a stratified fluid along an infinite vertical channel with temporally periodic surface temperature variations. Although a big part of the literature has been devoted for studying stratified and non-stratified fluids in various geometrical configurations, most of the research has been done numerically and very few discuss the interesting physical phenomena that arise due to the complexity of the problem setting. What makes our research unique is the fact that we obtained analytic solutions of the coupled system of partial differential equations with the corresponding boundary conditions; thus opening the door to exploring the sensitivity of the fluid behaviour to the physical parameters.

The structure of Part II is as follows: In Chapter 5, we give a brief literature

review, describe the governing equations and what fluid stratification means in this case, derive the energy balance equations to interpret some of the physical quantities that appear in the problem, and non-dimensionalize the system in a way that makes it easier to study and interpret the physical observations. In Chapter 6, we transform the system of partial differential equations into two decoupled higher order boundary value problems whose solutions then give the required temperature and vertical velocity profiles. Finally, in Chapter 7, we present some interesting and somewhat surprising physical observations and discuss possible interpretations for these behaviours.

Part I

Stability of Free Convection Over a Heated Plate

Chapter 2

Problem Formulation

2.1 Introduction

Using statistical mechanics to study dissipative hydrodynamic systems which exchange energy with an external source has increasingly gained interest over the years. Some common, everyday examples are the fascinating growing patterns found in snowflakes or bacteria colonies, ripples in sandy deserts and the complex turbulent flow patterns found in the atmosphere. But what causes such patterns to exist and how can one characterize this phenomenon mathematically? Apparently, systems that show a complex pattern-formation process share three main ingredients:

1. *exchange of energy* to drive the system;
2. *instability* in order to start the pattern;
3. *non-linearity* in order to choose the pattern.

A huge proportion of the early work on pattern formation was motivated by the study of *convection*, which is the overturning of a fluid that is heated from below. Heat at the bottom of a container causes the fluid there to ex-

pand, become less dense and more buoyant and so to rise through the colder fluid above. As the fluid rises away from the heat source, it cools, becoming denser than the fluid below, and so falls back down to the bottom of the container under the influence of gravity. The cycle repeats, so the fluid is constantly overturning. The rising and falling fluid forms spatial patterns, most commonly stripes or convection rolls, though more complicated patterns such as hexagons and squares are also possible, depending on the details of the physical system and fluid properties. Convection is important because it occurs naturally in the environment: in the Earth's mantle convection leads to 'continental drift' and in the atmosphere convection creates thunderclouds.

One of the most commonly studied convection phenomena is the Rayleigh-Bénard convection occurring in an incompressible fluid placed between horizontal parallel plates in the gravitational field in which a temperature gradient is always maintained (Figure 2.1). Literature studies based on the Boussinesq approximation [9, 17] show that when the temperature difference across the fluid exceeds a critical value, the rest state becomes unstable and the fluid breaks into convective flow cells that occur periodically in space. However, the situation becomes more complicated if the fluid is compressible as some of the dynamics would be driven by the continuity equation. Moreover, if we use a container which is open at the top, the fluid has a free surface where temperature-induced variations in the surface tension can drive motion.

The research problem we are interested in is motivated by modelling the turbulent flow found in the atmosphere and studying the onset of complex convective patterns caused mainly by the interactions of solar radiation with the Earth's surface. In this chapter, we introduce the governing equations for the problem, describe the reference state and derive the linearized equations.

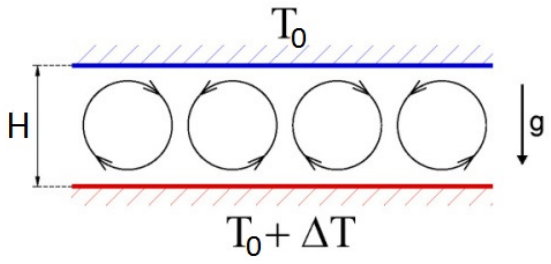

Figure 2.1: Rayleigh-Bénard Convection

2.2 Governing Equations

Consider a Cartesian coordinate system in which the z-axis opposes the gravity vector and the (x, z)-plane coincides with a semi-infinite vertical plate. We consider two different geometrical configurations: In the first set-up, the fluid fills the semi-infinite region $\Omega_\infty = \{(x, z),\, 0 \le x \le L,\, z \ge 0\}$ whereas in the second the fluid lies in a finite vessel $\Omega_H = \{(x, z),\, 0 \le x \le L,\, 0 \le z \le H\}$ of height H as shown in Figures 2.2 and 2.3, respectively. We maintain a constant temperature across the domain so that the value of the temperature at the bottom plate is T_0.

In the notation of Cartesian tensors with position vector $\mathbf{x} = (x_j) = (x, z)$ and velocity vector $\mathbf{u} = (u_j) = (u, w)$ ($j = 1,\, 2$), the hydrodynamic equations for a *compressible* fluid are given by the full non-linear Navier-Stokes equations written as

$$\partial_t\, n = -\nabla\cdot(n\mathbf{u}), \tag{2.1}$$

$$\partial_t\,(n u_i) = -\sum_j \partial_{x_j}\Pi_{ij} - \nabla\cdot((n\mathbf{u})\,u_i) + g_i\, n, \tag{2.2}$$

$$n\,\partial_t\, T = -(n\mathbf{u}\cdot\nabla)\,T - \sum_i\sum_j \Pi_{ij}\,\partial_{x_j} u_i + \nabla\cdot[\kappa\,\nabla T], \tag{2.3}$$

where $\partial_t = \dfrac{\partial}{\partial t}$, $\partial_{x_j} = \dfrac{\partial}{\partial x_j}$, n is the particle count per unit volume, $T = \dfrac{k_B}{m}\,\theta$

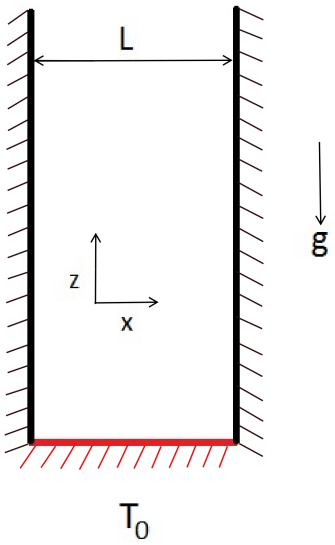

Figure 2.2: Semi-infinite Domain Ω_∞

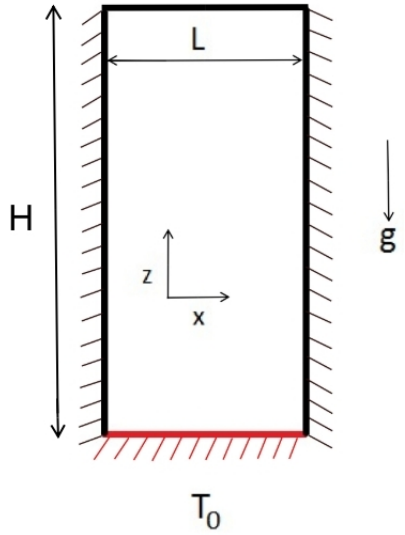

Figure 2.3: Finite Domain Ω_H

with k_B being the Boltzmann constant, m is the mass, and θ is the temperature. For simplicity, we will refer to T as the temperature. In this case, the z-axis is the upward vertical, $\mathbf{g} = \begin{pmatrix} 0 \\ -G \end{pmatrix}$ is the (constant) acceleration due to gravity, the stress tensor Π_{ij} is given by

$$\Pi_{ij} = nT\,\delta_{ij} - \nu\,\left[\,\partial_{x_j} u_i + \partial_{x_i} u_j - \delta_{ij}\;\nabla\cdot\mathbf{u}\,\right],$$

ν is the viscosity which is a measure of the fluid's internal resistance to flow and κ is the thermal conductivity which measures the rate of heat conduction through the fluid. Equations (2.1)-(2.3) are referred to as the continuity, momentum and thermal equations, respectively.

In this set-up, the total count per unit volume is kept fixed, that is, for any fixed time t and for $\Omega = \Omega_H$ or Ω_∞,

$$\int_\Omega n(\mathbf{x}, t)\,\mathrm{d}\mathbf{x} = N \equiv Constant. \tag{2.4}$$

2.3 Boundary Conditions

As for the case of the Rayleigh-Bénard, we should specify boundary conditions before we talk about the reference state and apply the stability analysis.

To suppress the effect of the vertical walls at $x = 0$ and $x = L$ on the dynamics of the flow, we impose the periodic boundary conditions in the horizontal x-direction; that is, for all $t \geq 0$ and $0 \leq z \leq H$ or $z \geq 0$, we take

$$n(0, z; t) = n(L, z; t), \tag{2.5}$$

$$\mathbf{u}(0, z; t) = \mathbf{u}(L, z; t), \tag{2.6}$$

$$T(0, z; t) = T(L, z; t). \tag{2.7}$$

As for the velocity, it is reasonable to consider the no-slip boundary condition on the surfaces $z = 0$ and $z = H$ in the case of the finite domain Ω_H; that is, for all $t \geq 0$ and $0 \leq x \leq L$, we have

$$\mathbf{u}(x, 0; t) = \mathbf{0}, \tag{2.8}$$

$$\mathbf{u}(x, H; t) = \mathbf{0}, \tag{2.9}$$

whereas, for the semi-infinite domain Ω_∞, we consider the no-slip boundary condition on the surface $z = 0$ and assume that the fluid is at rest far away from this surface; that is, for all $t \geq 0$ and $0 \leq x \leq L$, we write

$$\mathbf{u}(x, 0; t) = \mathbf{0}, \tag{2.10}$$

$$\lim_{z \to \infty} \mathbf{u}(x, z; t) = \mathbf{0}. \tag{2.11}$$

Moreover, in order to ensure that the only way energy can enter the system is through the bottom layer, we impose a zero flux boundary condition far away

from this layer; that is, for all $t \geq 0$ and $0 \leq x \leq L$, we take the boundary conditions on Ω_H to be

$$T(x, 0; t) = T_0, \tag{2.12}$$

$$\kappa \, \nabla T(x, z; t)\Big|_{z=H} = \mathbf{0}, \tag{2.13}$$

and on the domain Ω_∞ to be

$$T(x, 0; t) = T_0, \tag{2.14}$$

$$\lim_{z \to \infty} \kappa \, \nabla T(x, z; t) = \mathbf{0}. \tag{2.15}$$

2.4 Reference State

For the steady state and in the absence of any macroscopic flow; that is, $\mathbf{u} = \mathbf{0}$, equations (2.1)-(2.3) give for $i = 1, 2$,

$$\partial_{x_i} (nT) = g_i \, n, \tag{2.16}$$

$$\partial_{x_i} [\kappa \, \partial_{x_i} T] = 0. \tag{2.17}$$

Using (2.16), we get

$$\partial_x(nT) = 0 \qquad \Longrightarrow \ (nT) \text{ is independent of } x,$$

$$\partial_z(nT) = -Gn \quad \Longrightarrow \ n \text{ is independent of } x \quad \Longrightarrow \ T \text{ is independent of } x.$$

Therefore, both n and T are independent of x.

Using (2.17) and the fact that T is independent of x, we get

$$\partial_z [\kappa \, \partial_z T] = 0 \implies \kappa \, \partial_z T = C_1 \equiv \text{Constant}.$$

Since we're assuming that there is no heat flux far away from $z = 0$ using

conditions (2.13) and (2.15) then

$$\kappa\, \partial_z T = 0 \implies T(z) = T_0 \equiv \text{Constant} \quad \forall\, z \geq 0,$$

where T_0 is the temperature at the bottom plate (see Figures 2.2 and 2.3).

Moreover, $\dfrac{\mathrm{d}}{\mathrm{d}z}\Big(n(z)T(z)\Big) = -G\, n(z)$ and $T(z) = T_0$ give

$$\frac{1}{n(z)}\frac{\mathrm{d}n(z)}{\mathrm{d}z} = -\frac{G}{T_0} \quad \text{and} \quad n(z) = n(0)\, \exp\left(-\frac{G}{T_0}\, z\right).$$

To determine $n(0)$, we integrate both sides of equation $T_0 \dfrac{\mathrm{d}n(z)}{\mathrm{d}z} = -G\, n(z)$ with respect to z from 0 to ∞ if $\Omega = \Omega_\infty$ (and similarly from 0 to H in the case when $\Omega = \Omega_H$) to get

$$\lim_{z\to\infty}\Big(T_0\, n(z)\Big) - T_0\, n(0) = -G \int_0^\infty n(z)\, dz.$$

Using (2.4), $\displaystyle\int_0^\infty n(z)\, dz = \frac{N}{L}$ and given the exponential decay profile of $n(z)$ we get

$$n(0) = \frac{G}{T_0}\frac{N}{L}.$$

Thus, the reference state solutions when the fluid does not convect are

$$\bar{\mathbf{u}} = \mathbf{0}, \tag{2.18}$$

$$\bar{T}(z) = T_0, \tag{2.19}$$

$$\bar{n}(z) = \bar{n}(0) \exp\left(\frac{-G}{T_0}\, z\right), \tag{2.20}$$

where $\bar{n}(0) = \dfrac{G}{T_0}\dfrac{N}{L}$.

2.5 Linearized Equations

To study the stability of the reference state, we perturb the solutions (2.18)-(2.20) slightly and study the resulting linearized equations for the perturbations. Thus we write

$$\begin{aligned}
\mathbf{u}(\mathbf{x},t) &= \mathbf{u}'(\mathbf{x},t),\\
T(\mathbf{x},t) &= \bar{T}(z) + T'(\mathbf{x},t),\\
n(\mathbf{x},t) &= \bar{n}(z) + n'(\mathbf{x},t),
\end{aligned}$$

where $\mathbf{u}(\mathbf{x},t)$ is a first-order perturbation from equilibrium and $\mathbf{u}'$, T' and n' are infinitesimal perturbations of velocity, temperature and particle count, respectively.

It should be noted that in general, the equations of state for a fluid specify ν and κ as functions of the pressure $p = nT$ and temperature T. For layers of real fluid in which the pressure does not vary much, these functions are almost independent of p [17]. Moreover, since the reference state temperature is constant, it is reasonable to assume that $\kappa = \kappa(T_0) \equiv \kappa_0$ and $\nu = \nu(T_0) \equiv \nu_0$ are constants.

Let's now substitute these expressions into the hydrodynamic equations (2.1)-(2.3) and get the linearized equations for the perturbations n', $\mathbf{u}'$ and T'. From (2.1), we get

$$\partial_t\, n' = -\nabla\cdot(\bar{n}\,\mathbf{u}') = \bar{n}\left[\frac{G}{T_0}w' - \nabla\cdot\mathbf{u}'\right].$$

Substituting the perturbations in (2.2) gives

$$\partial_t\left(\bar{n}\,u_i'\right) = -\sum_j \partial_{x_j}\delta\Pi_{ij} + g_i\,n'\ ,$$

where $\delta\Pi_{ij} = \left(\bar{n}\,T' + \bar{T}\,n'\right)\delta_{ij} - \nu_0\left[\partial_{x_j}u_i' + \partial_{x_i}u_j' - \delta_{ij}\nabla\cdot\mathbf{u}'\right]$ and

$$\sum_j \partial_{x_j} \delta\Pi_{ij} = \partial_{x_i}\left(\bar{n}\,T' + \bar{T}\,n'\right) - \nu_0 \left[\sum_j \partial^2_{x_j} u'_i + \sum_j \partial_{x_j}\partial_{x_i} u'_j - \partial_{x_i}\nabla\cdot\mathbf{u}'\right]$$
$$= \partial_{x_i}\left(\bar{n}\,T' + \bar{T}\,n'\right) - \nu_0 \left[\nabla^2 u'_i + \partial_{x_i}\sum_j \partial_{x_j} u'_j - \partial_{x_i}\nabla\cdot\mathbf{u}'\right]$$
$$= \partial_{x_i}\left(\bar{n}\,T' + \bar{T}\,n'\right) - \nu_0\ \nabla^2 u'_i.$$

Therefore,

$$\partial_t\left(\bar{n}\,u'_i\right) = -\partial_{x_i}\left(\bar{n}\,T' + \bar{T}\,n'\right) + g_i\,n' + \nu_0\ \nabla^2 u'_i\ .$$

Finally, the linearized version of (2.3) is given by

$$\bar{n}\ \partial_t T' = -\sum_i \sum_j \delta\left(\Pi_{ij}\ \partial_{x_j} u'_i\right) + \nabla\cdot\left[\kappa_0\,\nabla T'\right],$$

where

$$\sum_i \sum_j \delta\left(\Pi_{ij}\ \partial_{x_j} u'_i\right) = \sum_i \sum_j \bar{n}\bar{T}\ \ \partial_{x_j} u'_i\ \ \delta_{ij} = \bar{n}\bar{T}\ \sum_i \partial_{x_i} u'_i$$
$$= \bar{n}\bar{T}\ \nabla\cdot\mathbf{u}' = \bar{n}T_0\ \nabla\cdot\mathbf{u}'.$$

and

$$\bar{n}\ \partial_t T' = -\bar{n}T_0\ \nabla\cdot\mathbf{u}' + \kappa_0\ \nabla^2 T'\ .$$

Thus, the linearized system of Navier-Stokes equations (2.1)-(2.3) about the reference steady state solution (2.18)-(2.20) is given by

$$\partial_t\, n' = \bar{n}\left[\frac{G}{T_0}\ w' - \nabla\cdot\mathbf{u}'\right], \tag{2.21}$$

$$\partial_t\left(\bar{n}\,u'\right) = -\partial_x\left(\bar{n}\,T' + \bar{T}\,n'\right) + \nu_0\ \nabla^2 u', \tag{2.22}$$

$$\partial_t\left(\bar{n}\,w'\right) = -\partial_z\left(\bar{n}\,T' + \bar{T}\,n'\right) - G\,n' + \nu_0\ \nabla^2 w', \tag{2.23}$$

$$\bar{n}\ \partial_t T' = -\bar{n}T_0\ \nabla\cdot\mathbf{u}' + \kappa_0\ \nabla^2 T', \tag{2.24}$$

with the periodic boundary conditions in the horizontal x-direction given by

$$n'(0,z;t) = n'(L,z;t), \tag{2.25}$$

$$\mathbf{u}'(0,z;t) = \mathbf{u}'(L,z;t), \tag{2.26}$$

$$T'(0,z;t) = T'(L,z;t), \tag{2.27}$$

and the boundary conditions in the vertical direction given by

$$\mathbf{u}'(x,0;t) = \mathbf{0}, \qquad \mathbf{u}'(x,H;t) = \mathbf{0}, \qquad \text{on } \Omega_H, \tag{2.28}$$

$$\mathbf{u}'(x,0;t) = \mathbf{0}, \qquad \lim_{z\to\infty} \mathbf{u}'(x,z;t) = \mathbf{0}, \qquad \text{on } \Omega_\infty, \tag{2.29}$$

$$T'(x,0;t) = 0, \qquad \kappa_0 \nabla T'(x,z;t)\Big|_{z=H} = \mathbf{0}, \qquad \text{on } \Omega_H, \tag{2.30}$$

$$T'(x,0;t) = 0, \qquad \lim_{z\to\infty} \kappa_0 \nabla T'(x,z;t) = \mathbf{0}, \qquad \text{on } \Omega_\infty. \tag{2.31}$$

Chapter 3

Numerical Approach

To get an intuition about the linear stability of the hydrodynamic problem, we utilize a numerical model that incorporates the boundary conditions and uses the Galerkin approximation to write our linearized system in matrix form as $M\frac{dC}{dt} = A\,C$. Studying the solutions of the linearized system reduces then to studying the eigenvalues of the matrix $M^{-1}\,A$: if the real part of one (or more) of the eigenvalues of this matrix turns positive as we change the parameters of the hydrodynamic problem then the perturbations (for this set of parameters) would grow exponentially and hence instabilities occur.

Although this problem seems similar to the Rayleigh-Bénard convection, there are subtle differences that add complexity to the problem and make it hard to predict, on a first encounter, the stability of the reference solution even in the linear setting. Having access to this numerical model gives us means to test the dependence of linear stability on the parameters of the hydrodynamic problem. Although the numerics presented in this chapter cannot serve as a proof of linear stability, it should be noted that these results have given us the intuition that the reference steady state solution is stable in this setting.

3.1 Numerical Set-up

For numerical purposes, we choose to scale the perturbation n' by the reference $\bar{n}$ and use the expressions for the reference state solutions

$$\bar{T}(z) = T_0,$$
$$\bar{n}(z) = \bar{n}(0)\, exp\left(-\frac{G}{T_0}z\right),$$

to rewrite the linearized equations (2.21)-(2.24) in terms of the rescaled particle count as

$$\partial_t \left(\frac{n'}{\bar{n}}\right) = \frac{G}{T_0}w' - \nabla\cdot\mathbf{u}', \tag{3.1}$$

$$\partial_t u' = -\partial_x T' - T_0\ \partial_x\left(\frac{n'}{\bar{n}}\right) + \frac{\nu_0}{\bar{n}}\ \nabla^2 u', \tag{3.2}$$

$$\partial_t w' = -\partial_z T' + \frac{G}{T_0}T' - T_0\ \partial_z\left(\frac{n'}{\bar{n}}\right) + \frac{\nu_0}{\bar{n}}\ \nabla^2 w', \tag{3.3}$$

$$\partial_t T' = -T_0\ \nabla\cdot\mathbf{u}' + \frac{\kappa_0}{\bar{n}}\ \nabla^2 T'. \tag{3.4}$$

Imposing the periodic boundary conditions in the horizontal x-direction, we have

$$\left(\frac{n'}{\bar{n}}\right)(0,z;t) = \left(\frac{n'}{\bar{n}}\right)(L,z;t), \tag{3.5}$$

$$\mathbf{u}'(0,z;t) = \mathbf{u}'(L,z;t), \tag{3.6}$$

$$T'(0,z;t) = T'(L,z;t). \tag{3.7}$$

Since infinite domains can pose computational challenges, we choose to work with the finite spatial domain $\Omega_H = [0,L]\times[0,H]$ that imposes the boundary conditions:

$$\mathbf{u}'(x,0;t) = \mathbf{u}'(x,H;t) = \mathbf{0}, \tag{3.8}$$

$$T'(x,0;t) = \kappa_0\ \partial_z T'(x,H;t) = 0. \tag{3.9}$$

3.2 Fourier Transform in x-direction

To remove the explicit x-dependence from equations (3.1)-(3.4), we impose the periodic boundary conditions and take a Fourier Transform in the horizontal x-direction. Thus, we introduce a horizontal Fourier mode k and write

$$\begin{aligned}
\frac{n'}{\bar{n}} &= \sum_{k\in\mathbb{Z}} n'_k(z,t)\ e^{\mathrm{i}\frac{2\pi k x}{L}}, \\
u' &= \sum_{k\in\mathbb{Z}} u'_k(z,t)\ e^{\mathrm{i}\frac{2\pi k x}{L}}, \\
w' &= \sum_{k\in\mathbb{Z}} w'_k(z,t)\ e^{\mathrm{i}\frac{2\pi \mathrm{k x}}{\mathrm{L}}}, \\
T' &= \sum_{k\in\mathbb{Z}} T'_k(z,t)\ e^{\mathrm{i}\frac{2\pi k x}{L}}.
\end{aligned}$$

Substituting in the linearized equations (3.1)-(3.4), we get

$$\partial_t n'_k = \frac{G}{T_0}\, w'_k - \mathrm{i}\, k_x\, u'_k - \partial_z w'_k\ , \tag{3.10}$$

$$\partial_t u'_k = -\mathrm{i}\, T_0\, k_x\, n'_k - \mathrm{i}\, k_x\, T'_k + \frac{\nu_0}{\bar{n}}\ \left[\partial_z^2 - k_x^2\right] u'_k\ , \tag{3.11}$$

$$\partial_t w'_k = -T_0\, \partial_z n'_k + \frac{G}{T_0}\, T'_k - \partial_z T'_k + \frac{\nu_0}{\bar{n}}\ \left[\partial_z^2 - k_x^2\right] w'_k\ , \tag{3.12}$$

$$\partial_t T'_k = -\mathrm{i} T_0\, k_x u'_k - T_0\, \partial_z w'_k + \frac{\kappa_0}{\bar{n}}\ \left[\partial_z^2 - k_x^2\right] T'_k\ , \tag{3.13}$$

where $k_x = \dfrac{2\pi k}{L}$.

3.3 Weak Formulation of Linearized System

After incorporating the periodic boundary condition in the horizontal direction by taking the Fourier transform in the x-direction, it is convenient to write a weak formulation for the system of equations (3.10)-(3.13) with the boundary

conditions given for all $t \geq 0$ by

$$\mathbf{u}_k'(0,t) = \mathbf{u}_k'(H,t) = 0, \tag{3.14}$$

$$T_k'(0,t) = \partial_z T_k'(z,t)\,|_{z=H} = 0\ . \tag{3.15}$$

To derive the weak formulation, let $\psi \in L^2([0,H])$ be a test function and let $\langle\,\cdot,\cdot\,\rangle$ denote the inner product in $L^2([0,H])$, that is, for f and g in $L^2([0,H])$,

$$\langle\, f, g\,\rangle = \int_0^H f(z)\, g(z)\, dz.$$

We are going to multiply both sides of equations (3.10)-(3.13) by the test function ψ and integrate from 0 to H. Thus, (3.10) becomes

$$\langle\,\psi\,,\,\partial_t n_k'\,\rangle = -\,\mathrm{i}\,k_x\,\langle\,\psi\,,\,u_k'\,\rangle + \frac{G}{T_0}\langle\,\psi\,,\,w_k'\,\rangle - \langle\,\psi\,,\,\partial_z\, w_k'\,\rangle. \tag{3.16}$$

From equation (3.11), we get

$$\begin{aligned}\langle\,\psi\,,\,\partial_t\, u_k'\,\rangle = &-\,\mathrm{i}\,k_x\,T_0\ \langle\,\psi\,,n_k'\,\rangle - \mathrm{i}\ k_x\ \langle\,\psi\,,\,T_k'\,\rangle \\ &+\,\nu_0\ \langle\,\psi\,,\,\frac{1}{\bar{n}}\,\partial_z^2 u_k'\,\rangle -\ \nu_0\,k_x^2\ \langle\,\psi\,,\,\frac{1}{\bar{n}}\ u_k'\,\rangle.\end{aligned}$$

By integration by parts,

$$\begin{aligned}\langle\,\psi\,,\,\frac{1}{\bar{n}}\,\partial_z^2\, u_k'\,\rangle &= \langle\,\psi\,\frac{1}{\bar{n}}\,,\,\partial_z^2 u_k'\,\rangle \\ &= -\langle\,\partial_z\left(\psi\frac{1}{\bar{n}}\right),\,\partial_z u_k'\,\rangle + \big[\psi\,\frac{1}{\bar{n}}\,\partial_z u_k'\,\big]_{z=0}^{z=H} \\ &= -\langle\,\partial_z\left(\frac{1}{\bar{n}}\,\psi\right),\,\partial_z u_k'\,\rangle \\ &\quad +\ \frac{1}{\bar{n}(H)}\,\psi(H)\,\big[\,\partial_z u_k'\,\big]_{z=H} - \frac{1}{\bar{n}(0)}\,\psi(0)\,\big[\partial_z u_k'\,\big]_{z=0},\end{aligned}$$

and so (3.11) becomes

$$\begin{aligned}\langle\,\psi\,,\,\partial_t u_k'\,\rangle = &-\mathrm{i}\,k_x\,T_0\,\langle\,\psi\,,n_k'\,\rangle - \mathrm{i}\;k_x\,\langle\,\psi\,,\,T_k'\,\rangle \\ &-\nu_0\,\langle\,\partial_z\left(\frac{1}{\bar n}\,\psi\right)\,,\,\partial_z u_k'\,\rangle \\ &+\frac{\nu_0}{\bar n(H)}\,\psi(H)\left[\,\partial_z u_k'\,\right]_{z=H} - \frac{\nu_0}{\bar n(0)}\,\psi(0)\left[\partial_z u_k'\right]_{z=0} \\ &-\nu_0\;k_x^2\,\langle\,\psi\,,\,\frac{1}{\bar n}\;u_k'\,\rangle.\end{aligned} \tag{3.17}$$

Similarly, equation (3.12) becomes

$$\begin{aligned}\langle\,\psi\,,\,\partial_t w_k'\,\rangle = &-\;T_0\,\langle\,\psi\,,\,\partial_z n_k'\,\rangle + \frac{G}{T_0}\,\langle\,\psi\,,\,T_k'\,\rangle - \langle\,\psi\,,\,\partial_z T_k'\,\rangle \\ &-\nu_0\,\langle\,\partial_z\left(\frac{1}{\bar n}\,\psi\right)\,,\,\partial_z w_k'\,\rangle \\ &+\frac{\nu_0}{\bar n(H)}\,\psi(H)\left[\,\partial_z w_k'\,\right]_{z=H} - \frac{\nu_0}{\bar n(0)}\,\psi(0)\left[\partial_z w_k'\,\right]_{z=0} \\ &-\nu_0\,k_x^2\,\langle\,\psi\,,\,\frac{1}{\bar n}\;w_k'\,\rangle.\end{aligned} \tag{3.18}$$

Now, from equation (3.13), we get

$$\begin{aligned}\langle\,\psi\,,\,\partial_t\,T_k'\,\rangle = &-\mathrm{i}\,k_x\,T_0\,\langle\,\psi\,,\,u_k'\,\rangle - T_0\,\langle\,\psi\,,\,\partial_z w_k'\,\rangle \\ &+\kappa_0\,\langle\,\psi\,,\,\frac{1}{\bar n}\,\partial_z^2 T_k'\,\rangle - \kappa_0\,k_x^2\langle\,\psi\,,\,\frac{1}{\bar n}\,T_k'\,\rangle.\end{aligned}$$

By integration by parts and using (3.15), we get

$$\begin{aligned}\langle\,\psi\,,\,\frac{1}{\bar n}\,\partial_z^2 T_k'\,\rangle &= \langle\,\psi\,\frac{1}{\bar n}\,,\,\partial_z^2 T_k'\,\rangle \\ &= -\langle\,\partial_z\left(\psi\,\frac{1}{\bar n}\right)\,,\,\partial_z T_k'\,\rangle + \left[\psi\,\frac{1}{\bar n}\,\partial_z T_k'\right]_{z=0}^{z=H} \\ &= -\langle\,\partial_z\left(\psi\,\frac{1}{\bar n}\right)\,,\,\partial_z T_k'\,\rangle - \psi(0)\frac{1}{\bar n(0)}\left[\partial_z T_k'\right]_{z=0},\end{aligned}$$

and hence equation (3.13) becomes

$$\begin{aligned}\langle\,\psi\,,\,\partial_t T_k'\,\rangle = &-\mathrm{i}\,k_x\,T_0\,\langle\,\psi\,,\,u_k'\,\rangle - T_0\,\langle\,\psi\,,\,\partial_z w_k'\,\rangle \\ &-\kappa_0\,\langle\,\partial_z\left(\psi\,\frac{1}{\bar{n}}\right)\,,\,\partial_z T_k'\,\rangle - \frac{\kappa_0}{\bar{n}(0)}\,\psi(0)\left[\partial_z T_k'\right]_{z=0} \\ &-k_x^2\langle\,\psi\,,\,T_k'\,\rangle.\end{aligned} \tag{3.19}$$

3.4 Numerical Scheme

At this stage, we are going to apply the Petrov-Galerkin procedure to study the weak formulation (3.16)-(3.19) as follows.

Discretize the interval $[0, H]$ into J equal subintervals of length h to get

$$\bar{\Omega}_h = \{z_j,\, z_j = j\cdot h,\, 0 \le j \le J\}.$$

For u_k', w_k' and T_k', use the finite element functions on the domain $[0, H]$, namely the head test functions, given by

$$\phi_0(z) = \begin{cases} -\frac{z-z_1}{z_1-z_0}, & z \in [z_0, z_1] \\ 0, & \text{otherwise} \end{cases} \qquad \phi_J(z) = \begin{cases} \frac{z-z_{J-1}}{z_J-z_{J-1}}, & z \in [z_{J-1}, z_J] \\ 0, & \text{otherwise} \end{cases}$$

and $$\phi_j(z) = \begin{cases} \frac{z-z_{j-1}}{z_j-z_{j-1}}, & z \in [z_{j-1}, z_j] \\ -\frac{z-z_{j+1}}{z_{j+1}-z_j}, & z \in [z_j, z_{j+1}], \\ 0, & \text{otherwise} \end{cases} \qquad \text{for } j = 1, \cdots, J-1$$

and for n'_k, we use the finite element functions on the domain $[0, H]$ given by

$$\chi_j(z) = \begin{cases} 1, & z \in [z_j, z_{j+1}] \\ & \text{for } j = 0, \cdots, J-1. \\ 0, & \text{otherwise} \end{cases}$$

Since we are dealing with each Fourier mode separately, we will drop the k^{th} index in the coefficients to simplify the notation and write

$$\begin{aligned} n'_k(z,t) &= \sum_{j=0}^{J-1} \rho_j(t)\, \chi_j(z), \\ u'_k(z,t) &= \sum_{j=0}^{J} V_{x,j}(t)\, \phi_j(z), \\ w'_k(z,t) &= \sum_{j=0}^{J} V_{z,j}(t)\, \phi_j(z), \\ T'_k(z,t) &= \sum_{j=0}^{J} S_j(t)\, \phi_j(z). \end{aligned}$$

Now, on $z = 0$, using the boundary condition (3.14) for $u'_k(z,t)$ and $w'_k(z,t)$ and the boundary condition (3.15) for $T'_k(z,t)$ we get

$$\begin{aligned} u'_k(0,t) = 0 \quad &\Longrightarrow \quad \sum_{j=0}^{J} V_{x,j}(t)\phi_j(0) = 0 \quad \Longrightarrow \quad V_{x,0}(t) = 0 \\ w'_k(0,t) = 0 \quad &\Longrightarrow \quad \sum_{j=0}^{J} V_{z,j}(t)\phi_j(0) = 0 \quad \Longrightarrow \quad V_{z,0}(t) = 0 \\ T'_k(0,t) = 0 \quad &\Longrightarrow \quad \sum_{j=0}^{J} S_j(t)\phi_j(0) = 0 \quad \Longrightarrow \quad S_0(t) = 0, \end{aligned}$$

where we used the fact that $\phi_0(0) = 1$ and $\phi_j(0) = 0$ for all $j = 1, \cdots, J$.

Similarly, on $z = H$, the boundary condition (3.14) for $u'_k(z,t)$ and $w'_k(z,t)$ implies that

$$V_{x,J}(t) = 0 \qquad \text{and} \qquad V_{z,J}(t) = 0,$$

where here we used that $\phi_J(H) = 1$ and $\phi_j(H) = 0$ for all $j = 0, \cdots, J-1$.

Thus, incorporating the proper boundary conditions, we get the following representations of the Fourier coefficients in terms of the finite element functions

$$\begin{aligned} n'_k(z,t) &= \sum_{j=0}^{J-1} \rho_j(t)\, \chi_j(z), \\ u'_k(z,t) &= \sum_{j=1}^{J-1} V_{x,j}(t)\, \phi_j(z), \\ w'_k(z,t) &= \sum_{j=1}^{J-1} V_{z,j}(t)\, \phi_j(z), \\ T'_k(z,t) &= \sum_{j=1}^{J} S_j(t)\, \phi_j(z). \end{aligned} \tag{3.20}$$

Substituting these representations in equations (3.16)-(3.19), we can write the numerical scheme in matrix form as

$$M\ \frac{d\,C}{dt} = A\ C\ .$$

The coefficient matrices M, A and C are defined in Appendix A.

In fact, we are trying to solve a problem of the form

$$\partial_t\, v(z,t) = L\, v(z,t)$$

where L is a linear operator. After incorporating the right boundary conditions, the solution can be written as

$$v(z,t) = v(z,0)\, e^{L\,t}.$$

Thus, if the real part of one (or more) of the eigenvalues of L is positive then the perturbations grow exponentially and we see instabilities.

In the discretized version, our linear operator is the matrix $M^{-1}A$ and that's why we turn our attention to studying the eigenvalues of this matrix as they carry information about when an instability can occur relative to changing the parameters of the hydrodynamic problem.

3.5 Numerical Results and Discussion

Before starting our numerical analysis, we need a way to choose the height H that best describes the hydrodynamic problem with infinite vertical extent. Since

$$1 - exp\left(-\frac{G}{T_0}H\right) = \alpha$$

gives the fraction of particles that lie *inside* the column $[0, L] \times [0, H]$, it is enough to choose α as close as possible to 1 (say $\alpha = 0.9999$) and solve for the numerical cut-off for H in this case. This says that even if not all the particles are in $[0, H]$ but say 99.99% are, it's a good estimate for what happens if we were to consider that all of them are actually there. In fact, the 0.01% of particles outside this column would not cause dramatic change in the stability analysis.

This discussion implies that it is reasonable to choose $\frac{G}{T_0}H$ as a parameter and use it to get a quantification on how big the height H should be. For most of these numerical computations (except those in which we change the temperature T_0 of the hot plate), we will set this parameter to a fixed value 10 and choose the height H that satisfies the relation $\frac{G}{T_0}H = 10$.

Recall that our parameters are: gravitational acceleration G, temperature of the plate T_0, height H (computed from the formula $\frac{G}{T_0}H = 10$), width L, viscosity ν_0, thermal diffusivity κ_0 and the horizontal mode k. Throughout this discussion, we set the gravitational acceleration G to 9.81. Rather than specifying both k and L, we choose to specify the combination $k_x = \frac{2\pi k}{L}$ since it is the one showing up after taking the Fourier transform in the horizontal direction. Moreover, although we are referring to T_0 as the temperature, recall that in our case $T = \frac{k_B}{m}\theta$ where k_B is the Boltzmann constant, m is the mass and θ is the true temperature so T_0 is a scaled version of the temperature θ.

3.5.1 Choosing Reasonable Number of Nodes

Since our numerical scheme depends on discretizing the vertical extent $[0, H]$ into J subintervals, it is crucial to conduct an experiment to find the number of nodes J that produces eigenvalues with reasonable accuracy. Below we fix the parameters $\nu_0 = 0.01827$ and $\kappa_0 = 0.0261$ (so that the Prandtl number $\mathsf{Pr} = \frac{\nu_0}{\kappa_0} = 0.7$ corresponding to air) and consider two scenarios in which we determine the height H by solving $\frac{G}{T_0}H = 10$: In Experiment 1 we consider $H = 3.65$, $T_0 = 3.58065$ and set $k_x = 2.7$ and in Experiment 2 we take $H = 70$, $T_0 = 68.7$ and set $k_x = 0.15$.

In Figures 3.1 and 3.2, we plot the real part of the leading eigenvalue as a function of the number of nodes J as well as the respective log-log plot for Experiments 1 and 2, respectively. Although increasing the number of nodes J has the advantage of enhancing the accuracy of the computed eigenvalue, we notice that we do not get significant changes in the values past $J = 250$ for either of the experiments. For this reason, we choose to fix the number of

nodes J to 250 for all the subsequent numerical experiments presented in this chapter.

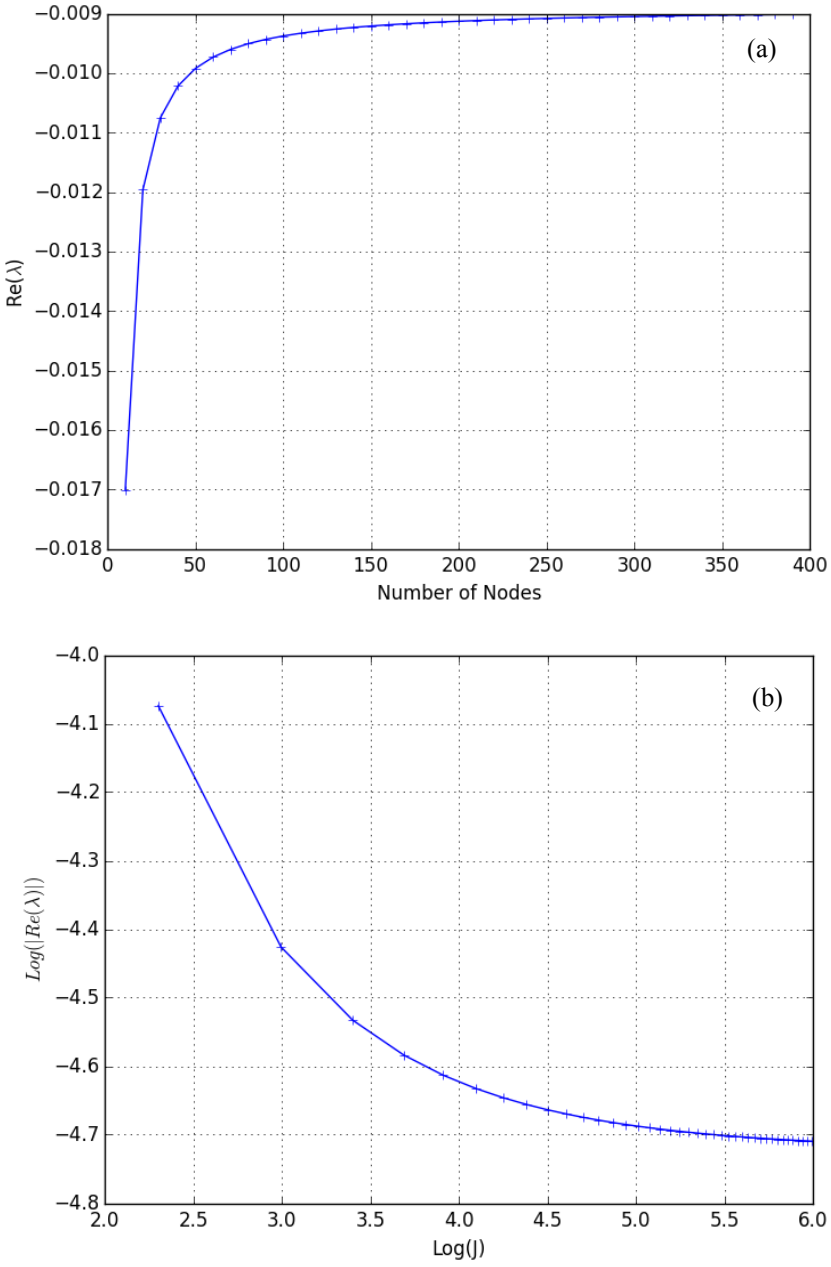

Figure 3.1: Testing the change of $\Re(\lambda_{Top})$ vs. Number of Nodes for $H = 3.65$, $T_0 = 3.58065$ and $k_x = 2.7$: (a) $\Re(\lambda_{Top})$ vs. number of nodes and (b) Log-log Plot of $\Re(\lambda_{Top})$ vs. number of nodes.

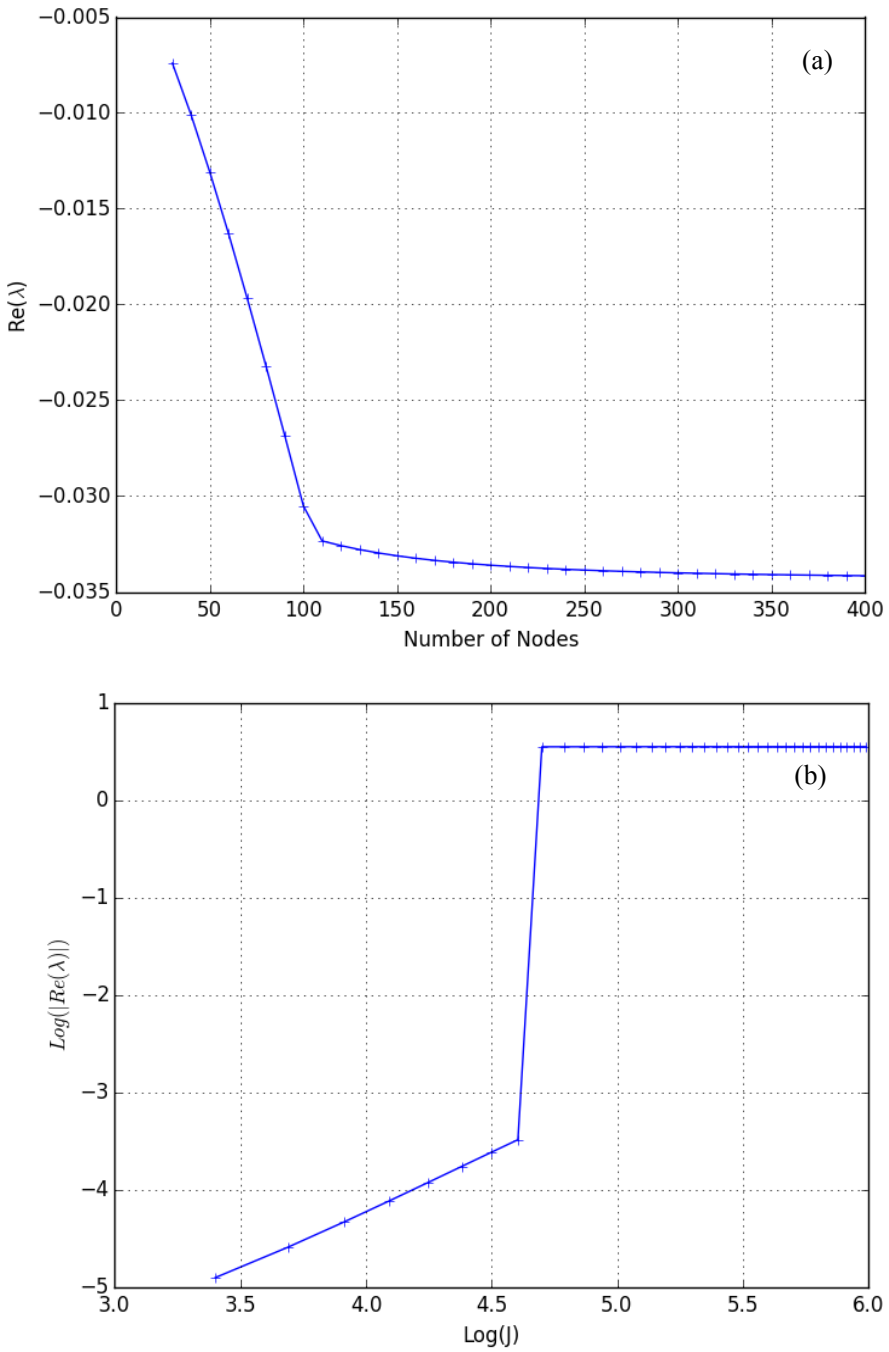

Figure 3.2: Testing the change of $\Re(\lambda_{Top})$ vs. Number of Nodes for $H = 70$, $T_0 = 68.7$ and $k_x = 0.15$: (a) $\Re(\lambda_{Top})$ vs. number of nodes and (b) Log-log Plot of $\Re(\lambda_{Top})$ vs. number of nodes.

3.5.2 Validation of Numerical Results

In order to make sure that the numerical model produces reliable results, we will derive a limiting case and check the accuracy of the model in approximating these analytic results. To do so, recall first that after taking the Fourier transform in the horizontal x-direction the linearized equations are given by (3.10)-(3.13) writtten as

$$\begin{aligned}
\partial_t n'_k &= \frac{G}{T_0}\, w'_k - \mathrm{i}\, k_x\, u'_k - \partial_z w'_k,\\
\partial_t u'_k &= -\mathrm{i}\, T_0\, k_x\, n'_k - \mathrm{i}\, k_x\, T'_k + \frac{\nu_0}{\bar{n}}\, \left[\partial_z^2 - k_x^2\right] u'_k,\\
\partial_t w'_k &= -T_0\, \partial_z n'_k + \frac{G}{T_0}\, T'_k - \partial_z T'_k + \frac{\nu_0}{\bar{n}}\, \left[\partial_z^2 - k_x^2\right] w'_k,\\
\partial_t T'_k &= -\mathrm{i} T_0\, k_x u'_k - T_0\, \partial_z w'_k + \frac{\kappa_0}{\bar{n}}\, \left[\partial_z^2 - k_x^2\right] T'_k,
\end{aligned}$$

where $k_x = \dfrac{2\pi k}{L}$ and n'_k, u'_k, w'_k and T'_k are the Fourier coefficients of $\left(\dfrac{n'}{\bar{n}}\right)$, u', w' and T' respectively. To transform this system into an eigenvalue problem, we write

$$\begin{aligned}
n'_k(z,t) &= \widehat{n'}(z)\, e^{\lambda t},\\
u'_k(z,t) &= \widehat{u'}(z)\, e^{\lambda t},\\
w'_k(z,t) &= \widehat{w'}(z)\, e^{\lambda t},\\
T'_k(z,t) &= \widehat{T'}(z)\, e^{\lambda t},
\end{aligned}$$

and substituting in the above equations to get

$$\lambda\, \widehat{n'} = \frac{G}{T_0}\, \widehat{w'} - \mathrm{i}\, k_x\, \widehat{u'} - \partial_z \widehat{w'}, \tag{3.21}$$

$$\lambda\, \widehat{u'} = -\mathrm{i}\, T_0\, k_x\, \widehat{n'} - \mathrm{i}\, k_x\, \widehat{T'} + \frac{\nu_0}{\bar{n}}\, \left[\partial_z^2 - k_x^2\right] \widehat{u'}, \tag{3.22}$$

$$\lambda\, \widehat{w'} = -T_0\, \partial_z \widehat{n'} + \frac{G}{T_0}\, \widehat{T'} - \partial_z \widehat{T'} + \frac{\nu_0}{\bar{n}}\, \left[\partial_z^2 - k_x^2\right] \widehat{w'}, \tag{3.23}$$

$$\lambda\, \widehat{T'} = -\mathrm{i}\, T_0\, k_x\, \widehat{u'} - T_0\, \partial_z \widehat{w'} + \frac{\kappa_0}{\bar{n}}\, \left[\partial_z^2 - k_x^2\right] \widehat{T'}. \tag{3.24}$$

First observe that for $k = 0$, $\lambda^* = 0$ is an eigenvalue of the system corresponding to the eigenfunction

$$\begin{pmatrix} \widehat{n'} \\ \widehat{u'} \\ \widehat{w'} \\ \widehat{T'} \end{pmatrix} = \begin{pmatrix} 1 \\ 0 \\ 0 \\ 0 \end{pmatrix}.$$

Proof. To prove this, set $k = 0$ and $\lambda = 0$ in equations (3.21)-(3.24) and study the resulting system

$$0 = \frac{G}{T_0}\ \widehat{w'} - \partial_z \widehat{w'}, \tag{3.25}$$

$$0 = \frac{\nu_0}{\bar{n}}\ \partial_z^2 \widehat{u'}, \tag{3.26}$$

$$0 = -T_0\ \partial_z \widehat{n'} + \frac{G}{T_0}\ \widehat{T'} - \partial_z \widehat{T'} + \frac{\nu_0}{\bar{n}}\ \partial_z^2 \widehat{w'}, \tag{3.27}$$

$$0 = -T_0\ \partial_z \widehat{w'} + \frac{\kappa_0}{\bar{n}}\ \partial_z^2 \widehat{T'}. \tag{3.28}$$

1. Using (3.26), we solve the boundary value problem

$$\begin{cases} \dfrac{\nu_0}{\bar{n}}\ \partial_z^2 \widehat{u'} = 0, \\ \widehat{u'}(0) = \widehat{w'}(H) = 0. \end{cases}$$

   and get $\widehat{u'}(z) = 0$ as the only solution.

2. Similarly, (3.25) together with the boundary conditions $\widehat{w'}(0) = \widehat{w'}(H) = 0$ gives $\widehat{w'}(z) = 0$.

3. Moreover, we get $\widehat{T'}(z) = 0$ using (3.28) together with the boundary conditions $\widehat{T'}(0) = \partial_z \widehat{T'}(z)|_{z=H} = 0$.

4. Finally, (3.27) suggests that $\widehat{n'}(z) = C$ where C is any constant.

This shows that $\lambda^* = 0$ is an eigenvalue of the system obtained by setting the horizontal Fourier mode k to zero. $\square$

At this point, we want to study how the eigenvalue λ behaves for small changes of the zero horizontal mode k. Therefore, with attention restricted to Fourier modes near zero and with ϵ defined as the deviation of k from zero, we seek solutions of (3.21)-(3.24) combined with the appropriate boundary conditions for λ, $\widehat{n'}$, $\widehat{u'}, \widehat{w'},$ and $\widehat{T'}$ in the form of regular perturbation expansions in ϵ:

$$\begin{aligned}
\lambda &= \lambda_0 + \epsilon\,\lambda_1 + \epsilon^2\,\lambda_2 + \ldots = \sum_{j=0}^{\infty} \epsilon^j\,\lambda_j, \\
\widehat{n'} &= \widehat{n'}_0 + \epsilon\,\widehat{n'}_1 + \epsilon^2\,\widehat{n'}_2 + \ldots = \sum_{j=0}^{\infty} \epsilon^j\,\widehat{n'}_j, \\
\widehat{u'} &= \widehat{u'}_0 + \epsilon\,\widehat{u'}_1 + \epsilon^2\,\widehat{u'}_2 + \ldots = \sum_{j=0}^{\infty} \epsilon^j\,\widehat{u'}_j, \\
\widehat{w'} &= \widehat{u'}_0 + \epsilon\,\widehat{w'}_1 + \epsilon^2\,\widehat{w'}_2 + \ldots = \sum_{j=0}^{\infty} \epsilon^j\,\widehat{w'}_j, \\
\widehat{T'} &= \widehat{T'}_0 + \epsilon\,\widehat{T'}_1 + \epsilon^2\,\widehat{T'}_2 + \ldots = \sum_{j=0}^{\infty} \epsilon^j\,\widehat{T'}_j,
\end{aligned} \tag{3.29}$$

with $\lambda_0 = 0$, $\widehat{n'}_0 = 1$ and $\widehat{u'}_0 = \widehat{w'}_0 = \widehat{T'}_0 = 0$.

It is easy to see that the differential equations and boundary conditions for $\widehat{n'}_j$, $\widehat{u'}_j$, $\widehat{w'}_j$, and $\widehat{T'}_j$ are independent of ϵ. Applying (3.29) into equations (3.21)-(3.24) and collecting terms in common powers of ϵ, we obtain a sequence of differential equations for $\widehat{n'}_j$, $\widehat{u'}_j$, $\widehat{w'}_j$, and $\widehat{T'}_j$. Since our objective is to find λ for any Fourier mode k near zero, we simultaneously solve for $\widehat{n'}_j$, $\widehat{u'}_j$, $\widehat{w'}_j$, and $\widehat{T'}_j$ as well as λ_j from the resulting equations for successive j's.

ϵ^1-terms:

Collecting the terms multiplying ϵ, we get

$$\lambda_1 = \frac{G}{T_0}\ \widehat{w'}_1 - \partial_z \widehat{w'}_1, \tag{3.30}$$

$$0 = -\mathrm{i}T_0 + \frac{\nu_0}{\bar{n}}\ \partial_z^2 \widehat{u'}_1, \tag{3.31}$$

$$0 = -T_0\ \partial_z \widehat{n'}_1 + \frac{G}{T_0}\ \widehat{T'}_1 - \partial_z \widehat{T'}_1 + \frac{\nu_0}{\bar{n}}\ \partial_z^2 \widehat{w'}_1, \tag{3.32}$$

$$0 = -T_0\ \partial_z \widehat{w'}_1 + \frac{\kappa_0}{\bar{n}}\ \partial_z^2 \widehat{T'}_1. \tag{3.33}$$

1. Solving (3.30) for $\widehat{w'}_1$, we get

$$\widehat{w'}_1(z) = Ce^{\frac{G}{T_0}z} + \lambda_1 \frac{T_0}{G}.$$

   Using the boundary condition $\widehat{w'}_1(0) = 0$, we get

$$C = -\lambda_1 \frac{T_0}{G} \quad \text{and} \quad \widehat{w'}_1(z) = -\frac{\lambda_1 T_0}{G}\left[e^{\frac{G}{T_0}z} - 1\right].$$

   However, imposing the boundary condition $\widehat{w'}_1(H) = 0$ forces λ_1 to be zero. Therefore, $\lambda_1 = 0$ and $\widehat{w'}_1(z) = 0$.

2. Since $\widehat{w'}(z) = 0$, equation (3.33) gives the boundary value problem

$$\begin{cases} \dfrac{\kappa_0}{\bar{n}}\ \partial_z^2 \widehat{T'}_1 = 0, \\ \widehat{T'}_1(0) = \partial_z \widehat{T'}_1(z)|_{z=H} = 0, \end{cases}$$

   which implies that $\widehat{T'}_1(z) = 0$.

3. Also, equation (3.32) gives

$$-T_0\ \partial_z \widehat{n'}_1 = 0 \quad \Longrightarrow \quad \widehat{n'}_1(z) = C,$$

   where C is a constant.

4. Finally, from (3.31), we have

$$\widehat{u'}_1(z) = C_1 + C_2\, z + \mathrm{i}\ \frac{T_0^3\ \bar{n}(0)}{\nu_0\ G^2}\ e^{-\frac{G}{T_0}z},$$

where C_1 and C_2 are determined by imposing the boundary conditions $\widehat{u'}_1(0) = \widehat{u'}_1(H) = 0$ and hence we get

$$\widehat{u'}_1(z) = -\mathrm{i}\ \frac{T_0^3\ \bar{n}(0)}{\nu_0\ G^2}\ \left[\left(1 - e^{-\frac{G}{T_0}z}\right) + \left(e^{-\frac{G}{T_0}H} - 1\right)\frac{z}{H}\right].$$

Therefore, the first order terms λ_1, $\widehat{n'}_1\,\widehat{u'}_1$, $\widehat{w'}_1$, and $\widehat{T'}_1$ are given by

$$\begin{aligned}
\lambda_1 &= 0,\\
\widehat{n'}_1(z) &= C,\\
\widehat{u'}_1(z) &= -\mathrm{i}\ \frac{T_0^3\ \bar{n}(0)}{\nu_0\ G^2}\ \left[\left(1 - e^{-\frac{G}{T_0}z}\right) + \left(e^{-\frac{G}{T_0}H} - 1\right)\frac{z}{H}\right],\\
\widehat{w'}_1(z) &= \widehat{T'}_1(z) = 0.
\end{aligned} \tag{3.34}$$

ϵ^2-terms:

Collecting the terms multiplying ϵ^2, we get

$$\lambda_2 = \frac{G}{T_0}\,\widehat{w'}_2 - \mathrm{i}\,\widehat{u'}_1 - \partial_z\widehat{w'}_2\ , \tag{3.35}$$

$$0 = -\mathrm{i}\,T_0\,\widehat{n'}_1 + \frac{\nu_0}{\bar{n}}\,\partial_z^2\widehat{u'}_2\ , \tag{3.36}$$

$$0 = -T_0\,\partial_z\widehat{n'}_2 + \frac{G}{T_0}\,\widehat{T'}_2 - \partial_z\widehat{T'}_2 + \frac{\nu_0}{\bar{n}}\partial_z^2\widehat{w'}_2\ , \tag{3.37}$$

$$0 = -\mathrm{i}\,T_0\,\widehat{u'}_1 - T_0\,\partial_z\widehat{w'}_2 + \frac{\kappa_0}{\bar{n}}\partial_z^2\widehat{T'}_2\ , \tag{3.38}$$

where $\widehat{n'}_1$ and $\widehat{u'}_1$ are given by (3.34).

We solve for λ_2 using (3.35) and solving

$$\begin{cases} \partial_z \widehat{w'}_2 - \dfrac{G}{T_0}\ \widehat{w'}_2 = -\mathrm{i}\,\widehat{u'}_1 - \ \lambda_2, \\ \widehat{w'}_2(0) = \widehat{w'}_2(H) = 0, \end{cases}$$

we get

$$\lambda_2 = -\,\frac{T_0^4\ \bar{n}(0)}{2\,\nu_0\ G^3\ H}\ e^{-\frac{G}{T_0}H}\left[\left(1+e^{\frac{G}{T_0}H}\right)\frac{G}{T_0}H - 2\left(e^{\frac{G}{T_0}H}-1\right)\right]. \tag{3.39}$$

Since we're restricting our attention to small horizontal modes k and ϵ represents the deviation from zero, using (3.34) and (3.39), we can write λ up to the 2nd-oder correction in k as

$$\lambda = -\,\frac{T_0^4\ \bar{n}(0)}{2\,\nu_0\ G^3\ H}\ e^{-\frac{G}{T_0}H}\left[\left(1+e^{\frac{G}{T_0}H}\right)\frac{G}{T_0}H - 2\left(e^{\frac{G}{T_0}H}-1\right)\right]k^2 + \mathcal{O}(k^3), \tag{3.40}$$

and we focus our attention to studying the sign of λ_2 as this would give us information about the graph of λ as a function of k.

Since $\dfrac{T_0^4\ \bar{n}(0)}{2\,\nu_0\ G^3\ H}\ e^{-\frac{G}{T_0}H} \geq 0$, it is enough to study the sign of

$$\left[\left(1+e^{\frac{G}{T_0}H}\right)\frac{G}{T_0}H - 2\left(e^{\frac{G}{T_0}H}-1\right)\right].$$

Note that the function

$$f(\zeta) = \left(1+e^{\zeta}\right)\zeta - 2\left(e^{\zeta}-1\right) \geq 0 \quad \forall\,\zeta \geq 0,$$

because $f(0) = 0$ and $\dfrac{df}{d\zeta}(\zeta) = (\zeta-1)\ e^{\zeta} + 1 \geq 0 \quad \forall\,\zeta \geq 0.$

This implies that

$$\left[\left(1+e^{\frac{G}{T_0}H}\right)\frac{G}{T_0}H-2\left(e^{\frac{G}{T_0}H}-1\right)\right]\geq 0 \qquad \text{and} \qquad \lambda_2\leq 0.$$

Therefore, for small values of k, the graph of λ behaves like a parabola that starts at the origin, has a horizontal tangent there and is concave downward.

In Figure 3.3, we plot the real part of the computed leading eigenvalue as well as the asymptotic curve presented in equation (3.40) against "small" values of the scaled horizontal Fourier mode k_x for $\nu_0 = 0.01827$ and $\kappa_0 = 0.0261$ and in two different scenarios: Experiment 1 with $H = 3.65$ and $T_0 = 3.58065$ and Experiment 2 with $H = 70$ and $T_0 = 68.7$. Note that the "smallness" of k_x depends on the set of parameters we choose to work with. For this reason, we see that although the numerics match the asymptotic analytic curve, the level of accuracy differs with the size of the domain. Moreover, since $k_x = \dfrac{2\pi k}{L}$, then taking small k_x does not reflect whether the smallness comes from small k or large width L.

3.5.3 Numerical Experiments

Since instabilities occur when one (or more) of the eigenvalues turn positive as we vary the parameters governing the hydrodynamic problem, it is enough then to study the sign of the real part of the *leading* eigenvalue of the matrix $M^{-1}A$ in several regimes. Given that our parameter space is big, we conduct experiments that vary each parameter (or certain combination of parameters) individually while keeping the rest fixed and study how the sign of the real part of the leading eigenvalue evolves as a function of the varying parameter.

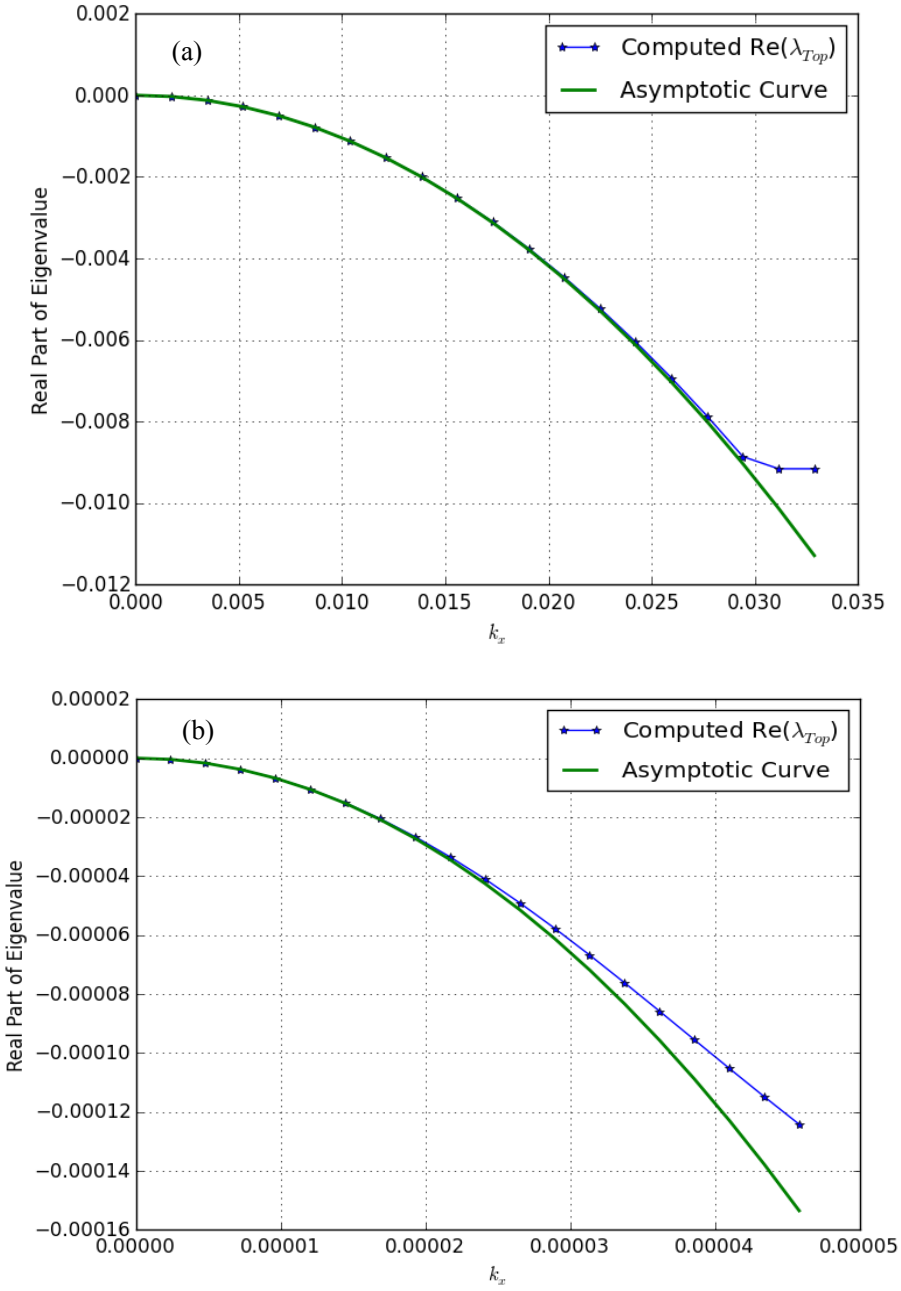

Figure 3.3: Computed $\Re(\lambda_{Top})$ and the asymptotic curve vs. k_x for $\nu_0 = 0.01827$ and $\kappa_0 = 0.0261$: (a) Experiment 1 with $H = 3.65$ and $T_0 = 3.58065$, and (b) Experiment 2 with $H = 70$ and $T_0 = 68.7$.

In what follows, we present several test cases that can help us understand the linear stability of the reference state under study. Namely, we study the behaviour of the real part of the leading eigenvalue as we change individually the conductivity κ_0, viscosity ν_0 and temperature T_0.

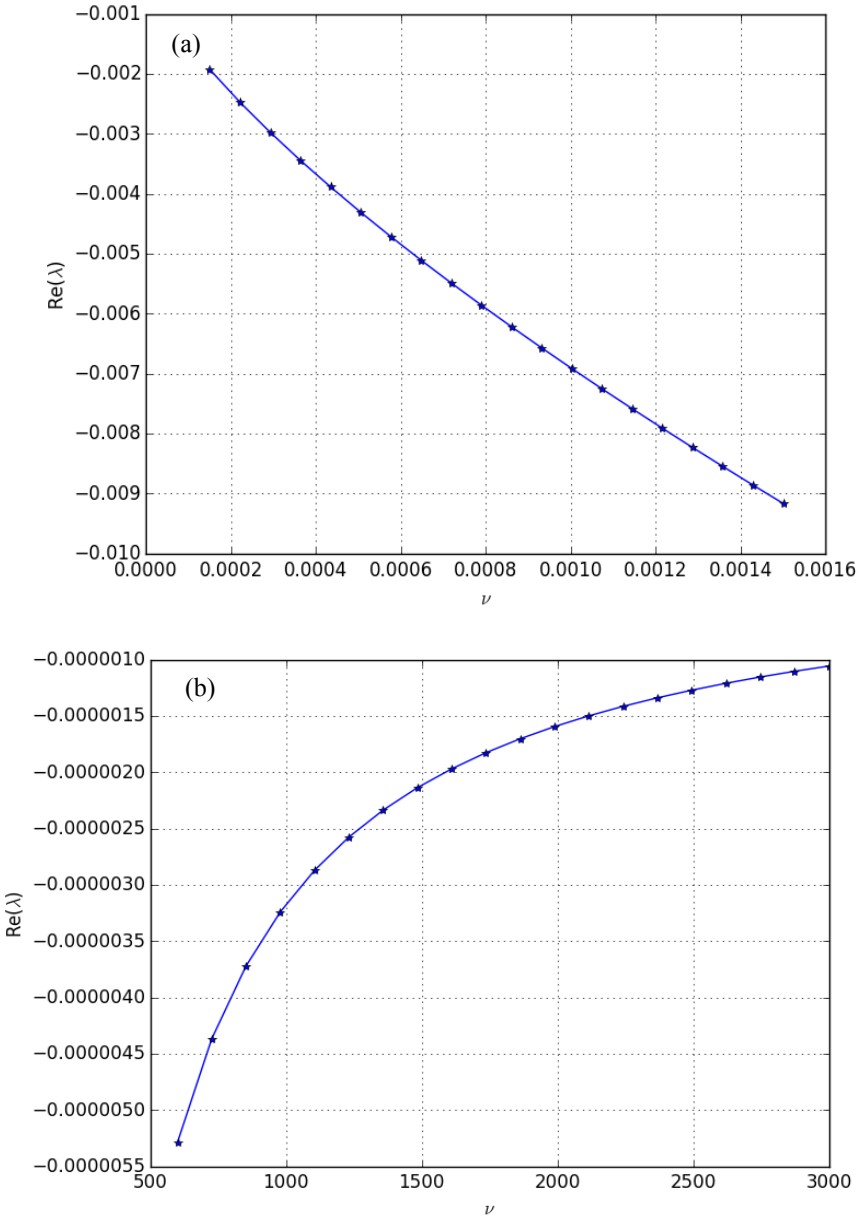

Figure 3.4: $\Re(\lambda_{Top})$ vs. ν_0 for $\kappa_0 = 1.5$, $H = 70$, $T_0 = 68.7$, $k_x = 0.15$ and (a) small ν_0-values and (b) big ν_0-values.

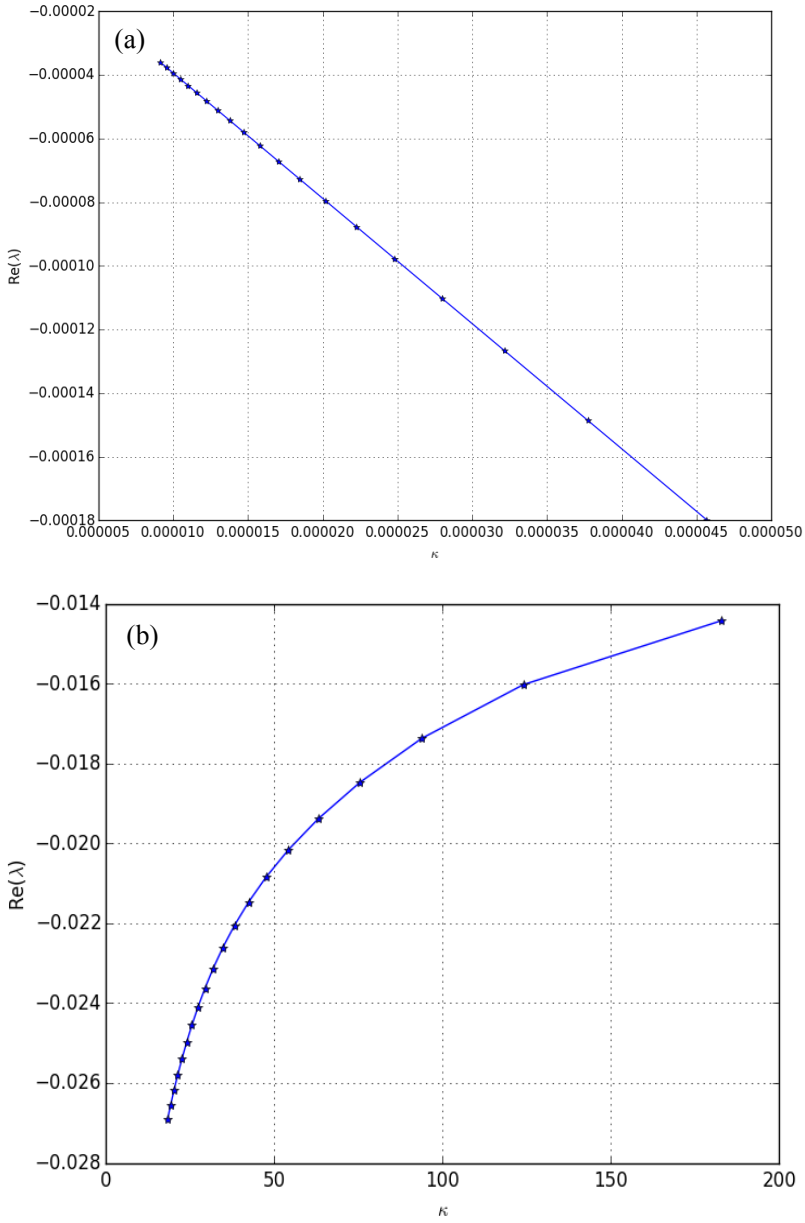

Figure 3.5: $\Re(\lambda_{Top})$ vs. κ_0 for $\nu_0 = 0.01827$, $H = 70$, $T_0 = 68.7$, $k_x = 0.15$ and (a) small κ_0-values and (b) big κ_0-values.

In Figures 3.4 and 3.5, we study the sign of the real part of the leading eigenvalue for small as well as large values of ν_0 and κ_0, respectively. To see how the perturbations behave in the presence of high temperature, we consider a spatial domain whose bottom plate is at temperature $T_0 = 68.7$. This then implies from $\dfrac{G}{T_0} H = 10$ that the height $H = 70$ and we set the scaled

horizontal Fourier mode to $k_x = 0.15$. Although we tested the eigenvalues for both small and big values of ν_0 and κ_0, from a physical point of view, we expect instabilities to occur for small viscosity while keeping κ_0 relatively big (in Figure 3.4 we set $\kappa_0 = 1.5$) or high conductivity while maintaining small viscosity (in Figure 3.5 we set $\nu_0 = 0.01827$). However, no matter how much we increase the range of ν_0 and κ_0, the observed real part of the top eigenvalue remains negative and so we cannot see instabilities in this case.

Since increasing the temperature at the bottom plate would heat the fluid there and cause it to move, we want to investigate how increasing T_0 would affect the sign of $\Re(\lambda_{Top})$. For this reason, for the experiment in Figure 3.6 we choose a fluid with viscosity $\nu_0 = 0.01827$ and conductivity $\kappa_0 = 0.0261$ (Prandtl number $\mathsf{Pr} = 0.7$ represents air at room temperature) and we set $k_x = 2.7$. To avoid numerical instabilities, we choose a spatial domain of height $H = 3.65$ so that when we increase T_0 the fraction $\dfrac{G}{T_0} H$ remains bounded away from 10 (remember, this term appears as the argument of the exponential function and we want to maintain it within a reasonable range). We conduct the experiment searching for a critical temperature T_0 above which the perturbations will grow exponentially and hence the fluid would convect. These instabilities would be seen as a change in the sign of $\Re(\lambda_{Top})$ from negative to positive and we want to inspect when the first crossing would occur. However, as we observe from Figure 3.6, no matter how much we increase the temperature, $\Re(\lambda_{Top})$ remains negative and bounded away from zero.

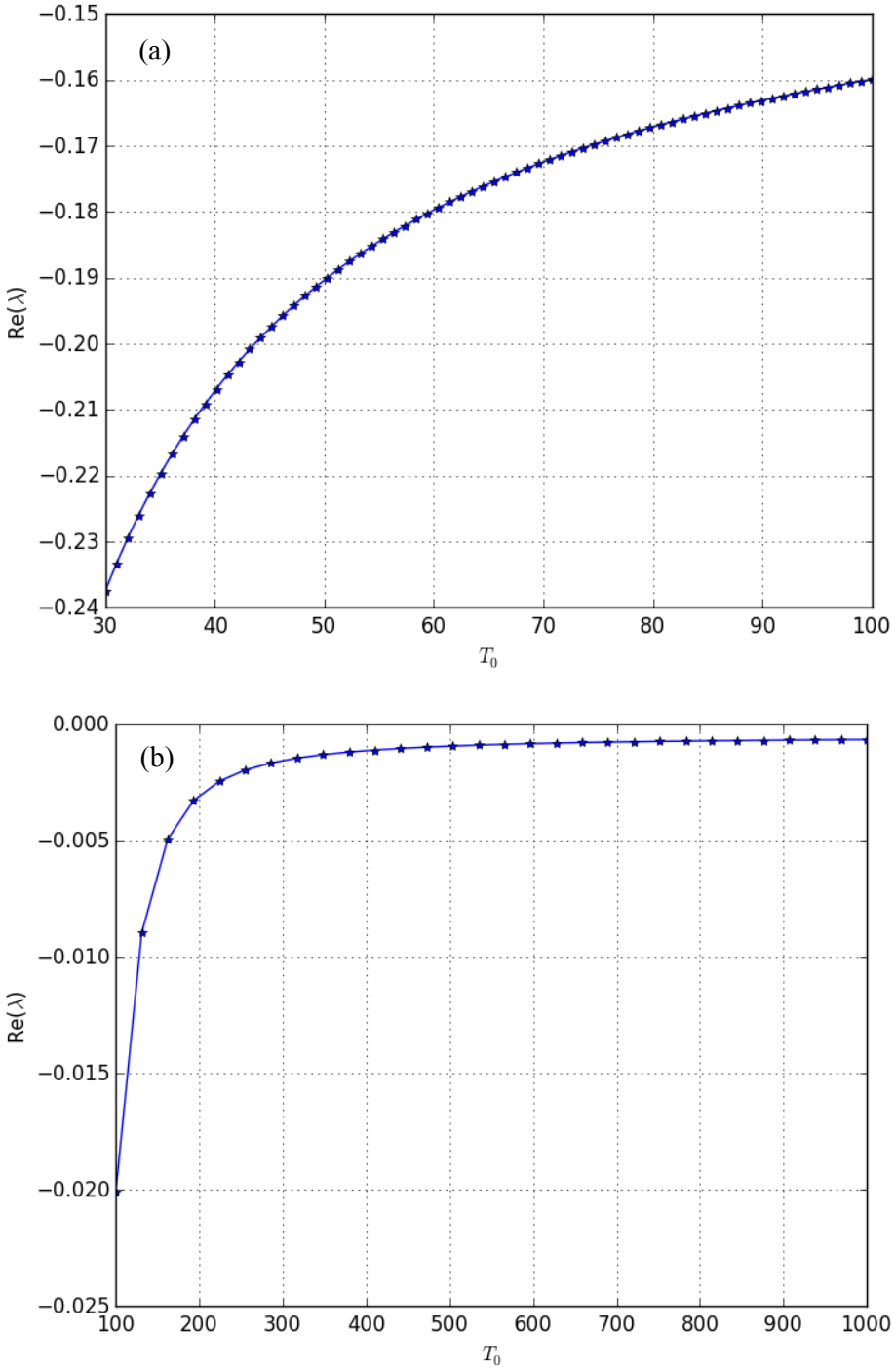

Figure 3.6: $\Re(\lambda_{Top})$ vs. T_0 for $\nu_0 = 0.01827$ and $\kappa_0 = 0.0261$: (a) Small T_0-values with $H = 3.65$ and $k_x = 2.7$ and (b) Big T_0-values with $H = 70$ and $k_x = 0.15$.

3.5.4 Concluding Remarks

Although we cannot treat these numerical experiments as a concrete proof that the reference solution under study is stable in the linear case, they give a good indication that there is very little chance for instabilities to occur. Note that once instabilities occur for a certain set of parameters they would persist throughout. For this reason, testing the limiting cases give us a good idea about the behaviour of the eigenvalues even if they might not be able to detect the first crossing of the eigenvalue from negative to positive.

Chapter 4

Stability Analysis

The numerical results from Chapter 3 indicate that the real part of the eigenvalues of the linearized system of perturbations remain negative regardless of how we choose the parameters of the hydrodynamic problem. This gives us the intuition to expect perturbations to be damped as time evolves and hence get linear stability of the reference steady state solution. In this chapter, we show that the discrete spectrum of the differential operator defining the linearized equations consists of eigenvalues with negative real part. On the other hand, we use the linearized equations to construct a Lyapunov function and use LaSalle's Invariance Principle to prove the stability of the reference state flow. Since linear stability results are not enough to infer stability of a solution on the non-linear level, we utilize LaSalle's Invariance Principle again and construct a Lyapunov function motivated by Markov chains to prove the stability of the reference solution.

Before starting the stability analysis, in what follows we will introduce notation and some theorems that will be useful when studying certain physical quantities and proving the stability results.

4.1 Miscellaneous definitions and theorems

4.1.1 A Version of Green's Theorem

Since most of the discussions and proofs in this chapter rely heavily on the integration by parts formula in higher dimensions, we recall it in the following remark:

Remark 4.1. *Recall that the product rule for divergence is*

$$\nabla\cdot(\phi\mathbf{v}) = \nabla\phi\cdot\mathbf{v} + \phi\nabla\cdot\mathbf{v}\ .$$

Let Γ *be an open subset of* $\mathbb{R}^n$ *with a piecewise smooth boundary* $\partial\Gamma$*, then*

$$\int_\Gamma \phi\ \nabla\cdot\mathbf{v}\, d\mathbf{x} = \int_\Gamma \nabla\cdot(\phi\mathbf{v})\ d\mathbf{x}\ - \int_\Gamma \mathbf{v}\cdot\nabla\phi\, d\mathbf{x}\ .$$

By the Divergence Theorem, we get

$$\int_\Gamma \nabla\cdot(\phi\mathbf{v})\ d\mathbf{x} = \int_{\partial\Gamma} \phi\ \mathbf{v}\cdot d\mathbf{s}\ ,$$

where $\mathbf{s}$ *is an outward normal to the boundary* $\partial\Gamma$*.*
Therefore, the integration by parts formula can be written as

$$\int_\Gamma \phi\ \nabla\cdot\mathbf{v}\, d\mathbf{x} = \int_{\partial\Gamma} \phi\ \mathbf{v}\cdot d\mathbf{s} - \int_\Gamma \mathbf{v}\cdot\nabla\phi\, d\mathbf{x}\ . \tag{4.1}$$

For simplicity, we will refer to this version of Green's theorem as integration by parts to be understood in the context of Remark 4.1.

4.1.2 Notations for the Spatial Domains

For $\Omega_H = [0, L] \times [0, H]$, let $\partial\,\Omega_H$ denote the boundary of Ω_H consisting of the four curves:

$$C_1 = \{(x, 0) | 0 \leq x \leq L\} \text{ with outward unit normal vector } -\hat{z},$$

$$C_2 = \{(L, z) | 0 \leq z \leq H\} \text{ with outward unit normal vector } \hat{x},$$

$$C_3 = \{(x, H) | 0 \leq x \leq L\} \text{ with outward unit normal vector } \hat{z},$$

$$C_4 = \{(0, z) | 0 \leq z \leq H\} \text{ with outward unit normal vector } -\hat{x},$$

where $\hat{x}$ and $\hat{z}$ are the unit normal vectors in the $x-$ and $z-$direction respectively. We will refer to this notation when using the integration by parts formula given in Remark 4.1.

On the other hand, we will pay special attention to the infinite boundary when using integration by parts on the semi-infinite domain $\Omega_\infty = [0, L] \times [0, \infty]$. To remove any ambiguity, we will state clearly which geometric configuration (Ω_H or Ω_∞) we're considering.

4.1.3 Jensen's Inequality

In what follows, we recall Jensen's inequality as presented in [25]:

Definition 4.2. *A continuous function $f(x)$ is said to be convex on an interval $[a, b]$ if for any two points x_1 and x_2 in $[a, b]$ and any λ such that $0 < \lambda < 1$,*

$$f\Big(\lambda x_1 + (1 - \lambda)\, x_2\Big) \leq \lambda\, f(x_1) + (1 - \lambda)\, f(x_2).$$

Theorem 4.3. *(Jensen's Inequality in Integral Form)*
Let $(\mathcal{X}, \Sigma, \mu)$ be a probability space, such $\mu(\mathcal{X}) = 1$. If f is a real-valued

function that is μ-integrable, and if ϕ is a convex function on the real line, then

$$\phi\left(\int_{\mathcal{X}} f\, d\mu\right) \leq \int_{\mathcal{X}} \phi \circ f\, d\mu\ .$$

Theorem 4.4. *(Jensen's Inequality in Discrete Form)*
If $p_1, p_2, \ldots, p_n$ are positive numbers such that $\sum_{k=1}^{n} p_k = 1$ and f is a real-valued continuous function that is convex, then

$$f\left(\sum_{k=1}^{n} p_k\, x_k\right) \leq \sum_{k=1}^{n} p_k\, f(x_k).$$

4.1.4 Stability of Equilibrium Points

We distinguish between two types of stability of equilibria.

Definition 4.5. *Consider $\dot{x}(t) = f(x(t))$ and let x^* be an equilibrium point as shown in Figure 4.1.*

- *We say that x^* is stable if for all $\epsilon > 0$, there exists $\delta_1 > 0$ such that if $x_0 \in B(x^*, \delta_1)$, then $x(t) \in B(x^*, \epsilon)$ for all $t > 0$.*
- *We say that x^* is asymptotically stable if it is stable and there exists $\delta_2 > 0$ such that if $x_0 \in B(x^*, \delta_2)$, then $x(t) \to x^*$ and $t \to \infty$.*

4.1.5 LaSalle's Invariance Principle

Let $\mathcal{D}$ be a closed subset of a Banach space $\mathcal{B}$ and let $\{\mathcal{U}(t),\, t \geq 0\}$ be a dynamical system on $\mathcal{D}$. In what follows, we will extend some definitions to the infinite dimensional setting:

Definition 4.6. *For $v \in \mathcal{D}$, we define the positive orbit starting from p at $t = 0$ to be the set*

$$\Gamma_+(f) := \{\mathcal{U}(t)\, v \in \mathcal{D},\, t \geq 0\}\ .$$

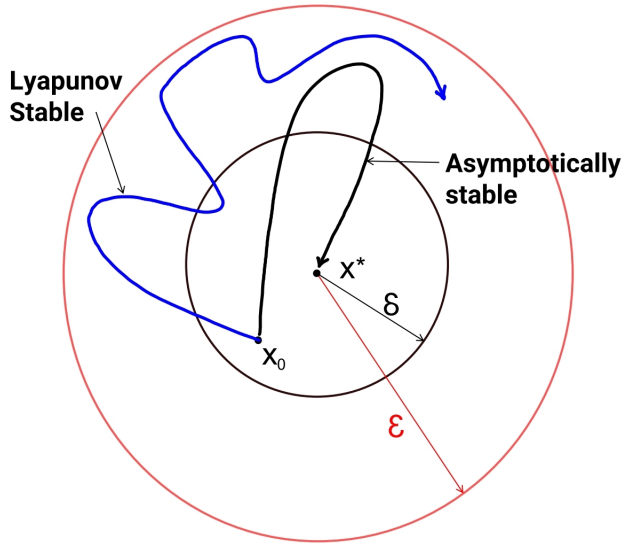

Figure 4.1: Schematic for Lyapunov and asymptotic stability of equilibrium points.

We say that $\phi \in \mathcal{D}$ *is an equilibrium point for* $\{\mathcal{U}(t),\, t \geq 0\}$ *if* $\Gamma_+(\phi) = \phi$.

Definition 4.7. *A set* $\Sigma \subset \mathcal{D}$ *is "positively invariant" for the dynamical system* $\{\mathcal{U}(t),\, t \geq 0\}$ *if*

$$\mathcal{U}(t)\Sigma \subset \Sigma, \quad \text{for any } t \geq 0.$$

Definition 4.8. *A "Lyapunov functional" (or simply Lyapunov function) for the dynamical system* $\{\mathcal{U}(t),\, t \geq 0\}$ *on* $\mathcal{D} \subset \mathcal{B}$ *is a continuous real valued function* $\mathcal{V} : \mathcal{D} \subset \mathcal{B} \to \mathbb{R}$ *such that for all* $v \in \mathcal{D}$,

$$\begin{aligned} &\mathcal{V}(v) \geq 0, \\ &\dot{\mathcal{V}}(v) := \limsup_{t \to 0^+} \frac{1}{t}\Big\{\mathcal{V}\left(\mathcal{U}(t)v\right) - \mathcal{V}(v)\Big\} \leq 0. \end{aligned}$$

At this point, we are in good shape to state LaSalle's Invariance Principle for infinite dimensional systems (see, [28, 67]).

Theorem 4.9. *(LaSalle's Invariance Principle)*

Let $\mathcal{V}$ be a Lyapunov function on $\mathcal{D}$. Define $E \subset \mathcal{D}$ to be the set

$$E := \Big\{ v \in \mathcal{D},\, \dot{\mathcal{V}}(v) = 0 \Big\},$$

and let M be the largest (positively) invariant subset of E. If for $v_0 \in \mathcal{D}$, the orbit $\Gamma_+(v_0)$ is precompact (i.e. lies in a compact subset $\mathcal{C} \subset \mathcal{D}$). Then, every solution starting in $\mathcal{C}$ approaches M as $t \to \infty$, that is,

$$\lim_{t \to +\infty} dist(\mathcal{U}(t)v_0, M) = 0 \ .$$

Remark 4.10. *For dynamical systems generated by evolution equations*

$$\frac{d}{dt} v = \mathcal{A}v + f(v) \ ,$$

where $\mathcal{A}$ is a strongly elliptic operator, bounded orbits are generally precompact (see [68]), and boundedness of orbits frequently follows from the existence of a Lyapunov function such that $\{v \in \mathcal{D},\, \mathcal{V}(v) < k\}$ is a bounded set for a suitable choice of $k > 0$.

4.2 Linear Stability Analysis

Recall that the linearized system of Navier-Stokes equations (2.1)-(2.3) about the steady state solution

$$\bar{\mathbf{u}} = \mathbf{0}, \tag{4.2}$$

$$\bar{T}(z) = T_0, \tag{4.3}$$

$$\bar{n}(z) = \bar{n}(0) \exp\left(\frac{-G}{T_0}\, z\right), \tag{4.4}$$

is given by

$$\partial_t n' = \bar{n}\left[\frac{G}{T_0}\, w' - \nabla\cdot\mathbf{u}'\right], \tag{4.5}$$

$$\bar{n}\ \partial_t u' = -\partial_x\left(\bar{n}\, T' + T_0\, n'\right) + \nu_0\ \nabla^2 u', \tag{4.6}$$

$$\bar{n}\ \partial_t w' = -\partial_z\left(\bar{n}\, T' + T_0\, n'\right) - G\, n' + \nu_0\ \nabla^2 w', \tag{4.7}$$

$$\bar{n}\ \partial_t T' = -\bar{n} T_0\ \nabla\cdot\mathbf{u}' + \kappa_0\ \nabla^2 T', \tag{4.8}$$

with the periodic boundary conditions in the horizontal x-direction given by

$$n'(0,z;t) = n'(L,z;t)\ , \tag{4.9}$$

$$\mathbf{u}'(0,z;t) = \mathbf{u}'(L,z;t)\ , \tag{4.10}$$

$$T'(0,z;t) = T'(L,z;t)\ , \tag{4.11}$$

and the boundary conditions in the vertical direction given by

$$\mathbf{u}'(x,0;t) = \mathbf{0}, \qquad \mathbf{u}'(x,H;t) = 0, \qquad \text{on } \Omega_H, \tag{4.12}$$

$$\mathbf{u}'(x,0;t) = \mathbf{0}, \qquad \lim_{z\to\infty} \mathbf{u}'(x,z;t) = \mathbf{0}, \qquad \text{on } \Omega_\infty, \tag{4.13}$$

$$T'(x,0;t) = 0, \qquad \kappa_0\, \nabla T'(x,z;t)\Big|_{z=H} = 0, \qquad \text{on } \Omega_H, \tag{4.14}$$

$$T'(x,0;t) = 0, \qquad \lim_{z\to\infty} \kappa_0\, \nabla T'(x,z;t) = 0, \qquad \text{on } \Omega_\infty. \tag{4.15}$$

4.2.1 Analysis of the Discrete Spectrum

To study the discrete spectrum of the linear differential operator, we write

$$\begin{aligned} n'(x,z;t) &= \tilde{n}(x,z)\ \mathrm{e}^{\lambda t}, \\ u'(x,z;t) &= \tilde{u}(x,z)\ \mathrm{e}^{\lambda t}, \\ w'(x,z;t) &= \tilde{w}(x,z)\ \mathrm{e}^{\lambda t}, \\ T'(x,z;t) &= \tilde{T}(x,z)\ \mathrm{e}^{\lambda t}, \end{aligned} \tag{4.16}$$

and substitute them into equations (4.5)-(4.8) to get

$$\lambda\ \tilde{n} = \bar{n}\left[\frac{G}{T_0}\ \tilde{w} - \nabla\cdot\tilde{\mathbf{u}}\right], \tag{4.17}$$

$$\lambda\ \bar{n}\ \tilde{u} = -\partial_x\left(\bar{n}\,\tilde{T} + T_0\,\tilde{n}\right) + \nu_0\ \nabla^2\tilde{u}, \tag{4.18}$$

$$\lambda\ \bar{n}\ \tilde{w} = -\partial_z\left(\bar{n}\,\tilde{T} + T_0\,\tilde{n}\right) - G\,\tilde{n} + \nu_0\ \nabla^2\tilde{w}, \tag{4.19}$$

$$\lambda\ \bar{n}\ \tilde{T} = -\bar{n}T_0\ \nabla\cdot\tilde{\mathbf{u}} + \kappa_0\ \nabla^2\tilde{T}, \tag{4.20}$$

so that the boundary conditions would translate to

$$\begin{aligned} &\tilde{n}(0,z) = \tilde{n}(L,z)\ , \\ &\tilde{\mathbf{u}}(0,z) = \tilde{\mathbf{u}}(L,z)\ , \\ &\tilde{T}(0,z) = \tilde{T}(L,z)\ , \\ &\\ &\tilde{\mathbf{u}}(x,0) = \tilde{\mathbf{u}}(x,H) = \mathbf{0}\ , \\ &\tilde{T}(x,0) = \kappa_0\,\partial_z\tilde{T}(x,z)\Big|_{z=H} = 0\ , \qquad \text{on } \Omega_H\ , \\ &\\ &\tilde{\mathbf{u}}(x,0) = \lim_{z\to\infty}\tilde{\mathbf{u}}(x,z) = \mathbf{0}\ , \\ &\tilde{T}(x,0) = \lim_{z\to\infty}\kappa_0\,\partial_z\tilde{T}(x,z) = 0\ , \qquad \text{on } \Omega_\infty\ . \end{aligned} \tag{4.21}$$

In this case, $\left(\tilde{n}, \tilde{u}, \tilde{w}, \tilde{T}\right)$ is an eigenfunction of the linear operator corresponding to the eigenvalue λ and so at least one of $\tilde{n}$, $\tilde{u}$, $\tilde{w}$ and $\tilde{T}$ should be non-zero.

Let $\tilde{n}^*$, $\tilde{u}^*$, $\tilde{w}^*$ and $\tilde{T}^*$ denote the complex conjugate of $\tilde{n}$, $\tilde{u}$, $\tilde{w}$ and $\tilde{T}$, respectively. In what follows, we present the detailed computation for the finite spatial domain Ω_H. The same result can be obtained for the semi-infinite domain Ω_∞ by imposing the decay at infinity boundary conditions on both the velocity and heat flux.

Multiplying (4.18) by $\tilde{u}^*$ and (4.19) by $\tilde{w}^*$, adding the resulting equations and integrating over Ω_H, we get

$$\begin{aligned}\lambda \int_{\Omega_H} \bar{n}\, \left[|\tilde{u}|^2 + |\tilde{w}|^2\right]\, \mathrm{d}\mathbf{x} = &- \int_{\Omega_H} \tilde{\mathbf{u}}^* \cdot \nabla \left(\bar{n}\, \tilde{T} + T_0\, \tilde{n}\right)\, d\mathbf{x} \\ &- G \int_{\Omega_H} \tilde{w}^*\, \tilde{n}\, \mathrm{d}\mathbf{x} \\ &+ \nu_0 \int_{\Omega_H} \left[\tilde{u}^*\, \nabla^2 \tilde{u} + \tilde{w}^*\, \nabla^2 \tilde{w}\right]\, \mathrm{d}\mathbf{x}.\end{aligned} \tag{4.22}$$

1. Using the integration by parts formula (4.1), we have

$$\begin{aligned}\int_{\Omega_H} \tilde{\mathbf{u}}^* \cdot \nabla \left(\bar{n}\, \tilde{T} + T_0\, \tilde{n}\right)\, \mathrm{d}\mathbf{x} = &\int_{\partial\Omega_H} \left(\bar{n}\, \tilde{T} + T_0\, \tilde{n}\right)\, \tilde{\mathbf{u}}^* \cdot \mathrm{d}\mathbf{s} \\ &- \int_{\Omega_H} \left(\bar{n}\, \tilde{T} + T_0\, \tilde{n}\right)\, \nabla \cdot \tilde{\mathbf{u}}^*\, \mathrm{d}\mathbf{x}.\end{aligned} \tag{4.23}$$

   Now, using the geometric construction of Ω_H and the boundary conditions on $\tilde{\mathbf{u}}^*$, we get

$$\begin{aligned}\int_{\partial\Omega_H}\left(\bar{n}\,\tilde{T}+T_0\,\tilde{n}\right)\,\tilde{\mathbf{u}}^*\cdot d\mathbf{s} &= -\int_0^L\left[\bar{n}(0)\,\tilde{T}(x,0)+T_0\,\tilde{n}(x,0)\right]\,\tilde{w}^*(x,0)\,dx\\ &\quad+\int_0^H\left[\bar{n}(z)\,\tilde{T}(L,z)+T_0\,\tilde{n}(L,z)\right]\,\tilde{w}^*(L,z)\,\mathrm{d}z\\ &\quad+\int_0^L\left[\bar{n}(H)\,\tilde{T}(x,H)+T_0\,\tilde{n}(x,H)\right]\,\tilde{w}^*(x,H)\,\mathrm{d}x\\ &\quad-\int_0^H\left[\bar{n}(z)\,\tilde{T}(0,z)+T_0\,\tilde{n}(0,z)\right]\,\tilde{w}^*(0,z)\,\mathrm{d}z\\ &=\int_0^L\left[\bar{n}(H)\,\tilde{T}(x,H)+T_0\,\tilde{n}(x,H)\right]\,\tilde{w}^*(x,H)\,\mathrm{d}x,\end{aligned}$$

which implies that

$$\begin{aligned}\int_{\Omega_H}\tilde{\mathbf{u}}^*\cdot\nabla\left(\bar{n}\,\tilde{T}+T_0\,\tilde{n}\right)\,\mathrm{d}\mathbf{x} = &\int_0^L\left[\bar{n}(H)\,\tilde{T}(x,H)+T_0\,\tilde{n}(x,H)\right]\,\tilde{w}^*(x,H)\,\mathrm{d}x\\ &-\int_{\Omega_H}\left(\bar{n}\,\tilde{T}+T_0\,\tilde{n}\right)\,\nabla\cdot\tilde{\mathbf{u}}^*\,\mathrm{d}\mathbf{x}\ .\end{aligned}$$

Using the no-slip boundary condition $\tilde{w}^*(x,H)=0$, equation (4.23) becomes

$$\int_{\Omega_\infty}\tilde{\mathbf{u}}^*\cdot\nabla\left(\bar{n}\,\tilde{T}+T_0\,\tilde{n}\right)\,\mathrm{d}\mathbf{x}=-\int_{\Omega_H}\left(\bar{n}\,\tilde{T}+T_0\,\tilde{n}\right)\,\nabla\cdot\tilde{\mathbf{u}}^*\,\mathrm{d}\mathbf{x}\ .$$

2. Similarly, we have

$$\begin{aligned}\int_{\Omega_H}\left[\tilde{u}^*\,\nabla^2\tilde{u}+\tilde{w}^*\,\nabla^2\tilde{w}\right]\,\mathrm{d}\mathbf{x} &= -\int_{\Omega_H}\left[\nabla\tilde{u}\cdot\nabla\tilde{u}+\nabla\tilde{w}\cdot\nabla\tilde{w}\right]\,\mathrm{d}\mathbf{x}\\ &= -\int_{\Omega_H}\left[|\nabla\tilde{u}|^2+|\nabla\tilde{w}|^2\right]\,\mathrm{d}\mathbf{x}\ .\end{aligned}$$

Therefore, equation (4.22) can be rewritten as

$$\begin{aligned}\lambda \int_{\Omega_H} \bar{n}\ \left[|\tilde{u}|^2 + |\tilde{w}|^2\right]\ \mathrm{d}\mathbf{x} = \quad & \int_{\Omega_H} \left(\bar{n}\,\tilde{T} + T_0\,\tilde{n}\right)\ \nabla\cdot\tilde{\mathbf{u}}^*\,d\mathbf{x} \\ & - G\int_{\Omega_H} \tilde{w}^*\,\tilde{n}\,\mathrm{d}\mathbf{x} \\ & - \nu_0 \int_{\Omega_H} \left[|\nabla\tilde{u}|^2 + |\nabla\tilde{w}|^2\right]\ \mathrm{d}\mathbf{x}.\end{aligned} \tag{4.24}$$

Now, multiplying (4.17) by $\dfrac{T_0}{\bar{n}}\,\tilde{n}^*$ and integrating over Ω_H, we get

$$\begin{aligned}\lambda \int_{\Omega_H} \frac{T_0}{\bar{n}}\ |\tilde{n}|^2\ \mathrm{d}\mathbf{x} &= \int_{\Omega_H} \left[G\,\tilde{n}^*\,\tilde{w} - T_0\ \tilde{n}^*\,\nabla\cdot\tilde{\mathbf{u}}\right]\ \mathrm{d}\mathbf{x} \\ &= \left(\int_{\Omega_H} \left[G\,\tilde{n}\,\tilde{w}^* - T_0\ \tilde{n}\,\nabla\cdot\tilde{\mathbf{u}}^*\right]\ \mathrm{d}\mathbf{x}\right)^*\end{aligned}$$

and substituting in (4.24), we have

$$\begin{aligned}\lambda \int_{\Omega_H} \bar{n}\ \left[|\tilde{u}|^2 + |\tilde{w}|^2\right]\ \mathrm{d}\mathbf{x} = \quad & \int_{\Omega_H} \bar{n}\,\tilde{T}\,\nabla\cdot\tilde{\mathbf{u}}^*\,d\mathbf{x} - \lambda^* \int_{\Omega_H} \frac{T_0}{\bar{n}}\ |\tilde{n}|^2\ \mathrm{d}\mathbf{x} \\ & - \nu_0 \int_{\Omega_H} \left[|\nabla\tilde{u}|^2 + |\nabla\tilde{w}|^2\right]\ \mathrm{d}\mathbf{x}\ .\end{aligned} \tag{4.25}$$

Finally, multiplying (4.20) by $\dfrac{\tilde{T}^*}{T_0}$ and integrating over Ω_H, we get

$$\lambda \int_{\Omega_H} \frac{\bar{n}}{T_0}\ |\tilde{T}|^2\mathrm{d}\mathbf{x} = \int_{\Omega_H} \left[-\bar{n}\,\tilde{T}^*\ \nabla\cdot\tilde{\mathbf{u}} + \frac{\kappa_0}{T_0}\ \tilde{T}^*\ \nabla^2\tilde{T}\right]\mathrm{d}\mathbf{x}\ . \tag{4.26}$$

Using integration by parts , we have

$$\int_{\Omega_H} \tilde{T}^*\ \nabla^2\tilde{T}\mathrm{d}\mathbf{x} = \int_{\partial\Omega_H} \tilde{T}^*\ \nabla\tilde{T}\cdot\mathrm{d}\mathbf{s} - \int_{\Omega_H} \nabla\tilde{T}\cdot\nabla\tilde{T}\,\mathrm{d}\mathbf{x}\ .$$

Employing the boundary conditions on $\tilde{T}$, we have

$$\begin{aligned}
\int_{\partial\Omega_H} \tilde{T}^*\ \nabla\tilde{T}\cdot d\mathbf{s} &= -\int_0^L \tilde{T}^*(x,0)\ \partial_z\tilde{T}(x,z)|_{z=0}\,\mathrm{d}x \\
&\quad + \int_0^H \tilde{T}^*(L,z)\ \partial_x\tilde{T}(x,z)|_{x=L}\,\mathrm{d}z \\
&\quad + \int_0^L \tilde{T}^*(x,H)\ \partial_z\tilde{T}(x,z)|_{z=H}\,\mathrm{d}x \\
&\quad - \int_0^H \tilde{T}^*(0,z)\ \partial_x\tilde{T}(x,z)|_{x=0}\,\mathrm{d}z \\
&= -\int_0^L \tilde{T}^*(x,0)\ \partial_z\tilde{T}(x,z)|_{z=0}\,\mathrm{d}x \\
&\quad + \int_0^L \tilde{T}^*(x,H)\ \partial_z\tilde{T}(x,z)|_{z=H}\,\mathrm{d}x \\
&= 0.
\end{aligned}$$

Therefore,

$$\int_{\Omega_H} \tilde{T}^*\ \nabla^2\tilde{T}\mathrm{d}\mathbf{x} = -\int_{\Omega_H} \nabla\tilde{T}\cdot\nabla\tilde{T}\,\mathrm{d}\mathbf{x} = -\int_{\Omega_H} |\nabla\tilde{T}|^2\,\mathrm{d}\mathbf{x}\ ,$$

and equation (4.26) becomes

$$\begin{aligned}
\lambda\int_{\Omega_H}\frac{\bar{n}}{T_0}\ |\tilde{T}|^2\mathrm{d}\mathbf{x} &= -\int_{\Omega_H}\left[\bar{n}\,\tilde{T}^*\ \nabla\cdot\tilde{\mathbf{u}} + \frac{\kappa_0}{T_0}\ |\nabla\tilde{T}|^2\right]\mathrm{d}\mathbf{x} \\
&= -\left(\int_{\Omega_H}\left[\bar{n}\,\tilde{T}\ \nabla\cdot\tilde{\mathbf{u}}^* + \frac{\kappa_0}{T_0}\ |\nabla\tilde{T}|^2\right]\mathrm{d}\mathbf{x}\right)^*.
\end{aligned} \tag{4.27}$$

Substituting in (4.25), we get

$$\begin{aligned}
\lambda\ \int_{\Omega_H}\bar{n}\ \left[|\tilde{u}|^2+|\tilde{w}|^2\right]\ \mathrm{d}\mathbf{x} &= -\lambda^*\int_{\Omega_H}\left[\frac{\bar{n}}{T_0}\ |\tilde{T}|^2 + \frac{T_0}{\bar{n}}\ |\tilde{n}|^2\right]\mathrm{d}\mathbf{x} \\
&\quad - \int_{\Omega_H}\frac{\kappa_0}{T_0}\ |\nabla\tilde{T}|^2\,\mathrm{d}\mathbf{x} \\
&\quad - \nu_0\int_{\Omega_H}\left[|\nabla\tilde{u}|^2+|\nabla\tilde{w}|^2\right]\ \mathrm{d}\mathbf{x}\ .
\end{aligned} \tag{4.28}$$

Separating the real and imaginary parts, we get

$$\mathsf{Re}\,\lambda \;= -\frac{\int_{\Omega_H}\left\{\frac{\kappa_0}{T_0}\;|\nabla\tilde{T}|^2+\nu_0\;(|\nabla\tilde{u}|^2+|\nabla\tilde{w}|^2)\right\}\,\mathrm{d}\mathbf{x}}{\int_{\Omega_H}\left\{\bar{n}\;\left[|\tilde{u}|^2+|\tilde{w}|^2\right]\;+\frac{\bar{n}}{T_0}\;|\tilde{T}|^2+\frac{T_0}{\bar{n}}\;|\tilde{n}|^2\right\}\,\mathrm{d}\mathbf{x}}\;, \tag{4.29}$$

$$\mathsf{Im}\lambda\;\int_{\Omega_H}\left\{\bar{n}\;\left[|\tilde{u}|^2+|\tilde{w}|^2\right]\;-\frac{\bar{n}}{T_0}\;|\tilde{T}|^2-\frac{T_0}{\bar{n}}\;|\tilde{n}|^2\right\}\,\mathrm{d}\mathbf{x}=0\;. \tag{4.30}$$

This implies that the eigenvalue λ is not necessarily real however its real part is always negative and hence is in good agreement with the numerical results obtained in Chapter 3.

4.2.2 Proof of Linear Stability

Using spectral theory, we show that the discrete spectrum of the linear operator consists of eigenvalues with negative real part. Although this is consistent with the numerical results, it is insufficient to deduce linear stability of solutions because this approach gives information about the discrete part of the spectrum only. To bypass this difficulty, we construct a Lyapunov function that decreases over solutions of the linearized system and use LaSalle's Invariance Principle to deduce linear stability.

Since there is no systematic way for constructing Lyapunov functions, it is important that we show all the steps that led to this construction rather than just giving the final result. Throughout the following discussion, we will be referring to the linearized equations (4.5)-(4.8) with the boundary conditions (4.9)-(4.15).

As a first attempt, for $\Omega = \Omega_\infty$ or Ω_H, consider the function $\tilde{\mathcal{V}}$ given by

$$\tilde{\mathcal{V}}(u', w') := \frac{1}{2} \int_\Omega \bar{n} \left[u'^{\,2} + w'^{\,2} \right] d\mathbf{x}, \tag{4.31}$$

so that

$$\tilde{\mathcal{V}}(u', w') \geq 0 \quad \text{for all } u' \text{ and } w'. \tag{4.32}$$

In order for $\tilde{\mathcal{V}}$ to define a Lyapunov function, this function should decrease over solutions of the linearized system of equation. For this reason, we investigate the rate of change of $\tilde{\mathcal{V}}$ given by

$$\frac{\mathrm{d}\tilde{\mathcal{V}}}{\mathrm{d}t}(u', w') = \int_\Omega \bar{n} \left[u' \, \partial_t u' + w' \, \partial_t w' \right] d\mathbf{x}. \tag{4.33}$$

At this point, we will show the computation in the case of the finite domain Ω_H. Imposing the decay at infinity boundary conditions when dealing with the semi-infinite domain Ω_∞ will yield the same results.

Using equations (4.6) and (4.7), we can rewrite this as

$$\begin{aligned} \frac{\mathrm{d}\tilde{\mathcal{V}}}{\mathrm{d}t}(u', w') = &- \int_{\Omega_H} \mathbf{u}' \cdot \nabla \left(\bar{n} \, T' + T_0 \, n' \right) \, \mathrm{d}\mathbf{x} \\ &- \int_{\Omega_H} G \, w' \, n' \, \mathrm{d}\mathbf{x} \\ &+ \nu_0 \int_{\Omega_H} \left[u' \, \nabla^2 u' + w' \, \nabla^2 w' \right] \, \mathrm{d}\mathbf{x}. \end{aligned} \tag{4.34}$$

1. Using integration by parts, we have

$$\int_{\Omega_H} u' \, \nabla^2 u' \, \mathrm{d}\mathbf{x} = \int_{\partial\Omega_H} u' \, \nabla u' \cdot \mathrm{d}\mathbf{s} - \int_{\Omega_H} \nabla u' \cdot \nabla u' \, \mathrm{d}\mathbf{x}, \tag{4.35}$$

where using the boundary conditions on u', we get

$$\begin{aligned}
\int_{\partial\Omega_H} u' \, \nabla u' \cdot \mathrm{d}\mathbf{s} &= -\int_0^L u'(x,0)\, \partial_z u'(x,z)|_{z=0} \, \mathrm{d}x \\
&\quad + \int_0^H u'(L,z)\, \partial_x u'(x,z)|_{x=L} \, \mathrm{d}z \\
&\quad + \int_0^L u'(x,H)\, \partial_z u'(x,z)|_{z=H} \, \mathrm{d}x \\
&\quad - \int_0^H u'(0,z)\, \partial_x u'(x,z)|_{x=0} \, \mathrm{d}z \\
&= -\int_0^L u'(x,0)\, \partial_z u'(x,z)|_{z=0} \, \mathrm{d}x \\
&\quad - \int_0^H u'(0,z)\, \partial_x u'(x,z)|_{x=0} \, \mathrm{d}z \\
&= 0 \; .
\end{aligned}$$

Therefore, we can rewrite (4.35) as

$$\int_{\Omega_H} u' \, \nabla^2 u' \, \mathrm{d}\mathbf{x} = -\int_{\Omega_H} \nabla u' \cdot \nabla u' \; \mathrm{d}\mathbf{x} = -\int_{\Omega_H} |\nabla u'|^2 \; \mathrm{d}\mathbf{x} \; . \tag{4.36}$$

Similarly, since w' satisfies the same boundary conditions that u' satisfies, we have

$$\int_{\Omega_H} w' \, \nabla^2 w' \, \mathrm{d}\mathbf{x} = -\int_{\Omega_H} |\nabla w'|^2 \; \mathrm{d}\mathbf{x} \; . \tag{4.37}$$

2. Also, using integration by parts and using the boundary conditions on u', we can write

$$\begin{aligned}
\int_{\Omega_H} \mathbf{u}' \cdot \nabla \left(\bar{n}\, T' + T_0\, n' \right) \, \mathrm{d}\mathbf{x} &= -\int_{\Omega_H} \left(\bar{n}\, T' + T_0\, n' \right) \, \nabla \cdot \mathbf{u}' \, \mathrm{d}\mathbf{x} \\
&\quad - \int_{\Omega_H} \left(\bar{n}\, T' + T_0\, n' \right) \, \nabla \cdot \mathbf{u}' \, \mathrm{d}\mathbf{x} \; .
\end{aligned} \tag{4.38}$$

Substituting (4.36), (4.37) and (4.38) into (4.34), we get an expression for the rate of change of the function $\tilde{\mathcal{V}}$

$$\begin{aligned}\frac{\mathrm{d}\tilde{\mathcal{V}}}{\mathrm{d}t}(u',w') = &-\int_{\Omega_H} n' \ [G\,w' - T_0\ \nabla\cdot\mathbf{u}']\ \mathrm{d}\mathbf{x} \\ &+\int_{\Omega_H} \bar{n}\,T'\ \nabla\cdot\mathbf{u}'\,\mathrm{d}\mathbf{x} \\ &-\nu_0\int_{\Omega_H}\left[|\nabla u'|^2+|\nabla w'|^2\right]\ \mathrm{d}\mathbf{x}\ .\end{aligned} \tag{4.39}$$

Let's use equations (4.5)-(4.8) to rewrite (4.39) in terms of n' and T' and their time derivatives.

Multiplying (4.5) by $\dfrac{T_0}{\bar{n}}\,n'$ and integrating over Ω_H, we have

$$\int_{\Omega_H}\frac{T_0}{\bar{n}}\,n'\,\partial_t n'\,\mathrm{d}\mathbf{x} = \int_{\Omega_H} n'\,[G\,w' - T_0\,\nabla\cdot\mathbf{u}']\ \mathrm{d}\mathbf{x}\ . \tag{4.40}$$

On the other hand, multiplying (4.8) by $\dfrac{T'}{T_0}$ and integrating over Ω_H, we get

$$\int_{\Omega_H}\frac{\bar{n}}{T_0}\,T'\,\partial_t T'\,\mathrm{d}\mathbf{x} = -\int_{\Omega_H}\bar{n}\,T'\ \nabla\cdot\mathbf{u}'\,\mathrm{d}\mathbf{x} + \frac{\kappa_0}{T_0}\int_{\Omega_H} T'\ \nabla^2 T'\,\mathrm{d}\mathbf{x}\ . \tag{4.41}$$

By integration by parts, we write

$$\int_{\Omega_H} T'\ \nabla^2 T'\,\mathrm{d}\mathbf{x} = \int_{\partial\Omega_H} T'\ \nabla T'\cdot\mathrm{d}\mathbf{s} - \int_{\Omega_H}|\nabla T'|^2\,\mathrm{d}\mathbf{x}\ ,$$

where

$$\begin{aligned}\int_{\partial\Omega_H} T'\ \nabla T'\cdot\mathrm{d}\mathbf{s} = &-\int_0^L T'(x,0)\,\partial_z T'(x,z)|_{z=0}\,\mathrm{d}x \\ &+\int_0^H T'(L,z)\,\partial_x T'(x,z)|_{x=L}\,\mathrm{d}z \\ &+\int_0^L T'(x,H)\,\partial_z T'(x,z)|_{z=H}\,\mathrm{d}x \\ &-\int_0^H T'(0,z)\,\partial_x T'(x,z)|_{x=0}\,\mathrm{d}z\ .\end{aligned}$$

Using the periodic boundary conditions on T' and $T'(x,0)=0$, we have

$$\int_{\partial\Omega_H} T'\ \nabla T'\cdot d\mathbf{s} = -\int_0^H T'(0,z)\,\partial_x T'(x,z)|_{x=0}\,dz\ .$$

But $\partial_z T'(x,z)\Big|_{z=H}=0$ so that $\displaystyle\int_{\partial\Omega_H} T'\ \nabla T'\cdot d\mathbf{s}=0$ and hence

$$\int_{\Omega_H} T'\ \nabla^2 T'\,\mathrm{d}\mathbf{x} = -\int_{\Omega_H}|\nabla T'|^2\,\mathrm{d}\mathbf{x}\ .$$

Therefore, we can rewrite (4.41) as

$$\int_{\Omega_H}\frac{\bar n}{T_0}\,T'\,\partial_t T'\,\mathrm{d}\mathbf{x} = -\int_{\Omega_H}\bar n\,T'\ \nabla\cdot\mathbf{u}'\,\mathrm{d}\mathbf{x} - \frac{\kappa_0}{T_0}\int_{\Omega_H}|\nabla T'|^2\,\mathrm{d}\mathbf{x}\ . \tag{4.42}$$

Substituting (4.40) and (4.42) (and their respective counterparts obtained for Ω_∞ by imposing the decay at infnity boundary conditions) into equation (4.39), we get for $\Omega=\Omega_H$ or Ω_∞

$$\begin{aligned}\frac{\mathrm{d}\tilde{\mathcal{V}}}{\mathrm{d}t}(u',w') = &-\int_\Omega\frac{T_0}{\bar n}\,n'\,\partial_t n'\,\mathrm{d}\mathbf{x}\\ &-\int_\Omega\frac{\bar n}{T_0}\,T'\,\partial_t T'\,\mathrm{d}\mathbf{x} - \frac{\kappa_0}{T_0}\int_\Omega|\nabla T'|^2\,\mathrm{d}\mathbf{x}\\ &-\nu_0\int_\Omega\left[|\nabla u'|^2+|\nabla w'|^2\right]\,\mathrm{d}\mathbf{x}\ .\end{aligned} \tag{4.43}$$

Although we cannot conclude from (4.43) that $\dfrac{\mathrm{d}\tilde{\mathcal{V}}}{\mathrm{d}t}(u',w')\le 0$, this gives us a way to construct a Lyapunov function given in the theorem below.

Theorem 4.11. *For the perturbations n', u', w' and T' defined on $\Omega=\Omega_H$ or Ω_∞, the functional*

$$\mathcal{V}(n',u',w',T') = \frac{1}{2}\int_\Omega\left\{\bar n\left(u'^{\,2}+w'^{\,2}\right)+\frac{T_0}{\bar n}\,n'^{\,2}+\frac{\bar n}{T_0}\,T'^{\,2}\right\}\mathrm{d}\mathbf{x}$$

defines a Lyapunov function and hence proves the linear stability of the steady state solution (2.18)-(2.20).

Proof. Consider the functional

$$\mathcal{V} = \frac{1}{2}\int_\Omega \left\{ \bar{n}\left(u'^{\,2} + w'^{\,2}\right) + \frac{T_0}{\bar{n}}\, n'^{\,2} + \frac{\bar{n}}{T_0}\, T'^{\,2} \right\} \mathrm{d}\mathbf{x} \ . \tag{4.44}$$

By construction, we have

$$\mathcal{V}(n', u', w', T') \geq 0 \qquad \text{for all perturbations } n',\ u',\ w' \text{ and } T'. \tag{4.45}$$

Thus, it remains to check whether $\mathcal{V}$ decreases over solutions of the linearized system (4.5)-(4.8). To do this, consider the rate of change of $\mathcal{V}$ given by

$$\frac{d\mathcal{V}}{dt}(n', u', w', T') = \int_\Omega \left\{ \bar{n}\left(u'\,\partial_t u' + w'\,\partial_t w'\right) + \frac{T_0}{\bar{n}}\, n'\,\partial_t n' + \frac{\bar{n}}{T_0}\, T'\,\partial_t T' \right\} \mathrm{d}\mathbf{x}$$

which can be written in terms of $\dfrac{\mathrm{d}\tilde{\mathcal{V}}}{\mathrm{d}t}$ as

$$\frac{\mathrm{d}\mathcal{V}}{\mathrm{d}t}(n', u', w', T') = \frac{\mathrm{d}\tilde{\mathcal{V}}}{\mathrm{d}t}(u, w') + \int_\Omega \left\{ \frac{T_0}{\bar{n}}\, n'\,\partial_t n' + \frac{\bar{n}}{T_0}\, T'\,\partial_t T' \right\} \mathrm{d}\mathbf{x} \ . \tag{4.46}$$

But by (4.43), we have

$$\frac{\mathrm{d}\tilde{\mathcal{V}}}{\mathrm{d}t} + \int_{\Omega_\infty} \left(\frac{T_0}{\bar{n}}\, n'\,\partial_t n' + \frac{\bar{n}}{T_0}\, T'\,\partial_t T' \right) \mathrm{d}\mathbf{x} = -\int_\Omega \left\{ \nu_0 \left(|\nabla u'|^2 + |\nabla w'|^2 \right) + \frac{\kappa_0}{T_0} |\nabla T'|^2 \right\} \mathrm{d}\mathbf{x},$$

which implies that

$$\frac{\mathrm{d}\mathcal{V}}{\mathrm{d}t}(n', u', w', T') = -\int_\Omega \left\{ \nu_0 \left(|\nabla u'|^2 + |\nabla w'|^2 \right) + \frac{\kappa_0}{T_0} |\nabla T'|^2 \right\} \mathrm{d}\mathbf{x} \ \leq 0. \tag{4.47}$$

It is easy to see that for $\mathbf{u}' = \bar{\mathbf{u}} = \mathbf{0}$, $T' = \bar{T} = T_0$ and $n' = \bar{n}$, then

$$\frac{\mathrm{d}\mathcal{V}}{\mathrm{d}t}(\bar{n}, \bar{u}, \bar{w}, \bar{T}) = 0 \ .$$

On the other hand, if $\dfrac{\mathrm{d}\mathcal{V}}{\mathrm{d}t}(n', u', w', T') = 0$, then by (4.47), we have

$$\nabla u' = \nabla w' = \mathbf{0} \quad \text{and} \quad \nabla T' = \mathbf{0} \ .$$

Using the boundary conditions $u'(x, 0; t) = w'(x, 0; t) = 0$ and $u'(x, H, t) = w'(x, H; t) = 0$ or the decay at infinity boundary condition, we get

$$u'(x, z; t) = w'(x, z; t) = 0 \quad \text{on } \Omega = \Omega_H \text{ or } \Omega_\infty \ .$$

Similarly, using the boundary condition $T'(x, 0; t) = 0$ and $\kappa_0 \nabla T'(x, z; t)\Big|_{z=H} = 0$ or the decay at infinity of the heat flux, we get

$$T'(x, z; t) = 0 \quad \text{on } \Omega = \Omega_H \text{ or } \Omega_\infty \ .$$

Substituting $u'(x, z; t) = w'(x, z; t) = 0$ and $T'(x, z; t) = 0$ into (4.5)-(4.8), we get

$$\partial_x n' = 0 \quad \text{and} \quad T_0 \, \partial_z n' = -G \, n',$$

whose solution is $n'(x, z; t) \equiv n'(z) = n'(0) \exp\left(-\dfrac{G}{T_0} \, z\right)$.
But by (2.4),

$$\int_\Omega n(\mathbf{x}, t) \, \mathrm{d}\mathbf{x} = \int_\Omega \bar{n}(z) \, \mathrm{d}\mathbf{x} = N \equiv Constant,$$

so that $\displaystyle\int_\Omega n'(\mathbf{x}, t) \, \mathrm{d}\mathbf{x} = 0$ which forces $n'(x, z; t) = 0$.

This implies that

$$\Big\{ (n', u', w', T') \;\Big|\; \frac{\mathrm{d}\mathcal{V}}{\mathrm{d}t}(n', u', w', T') = 0 \Big\} = \Big\{ (0,0,0,0) \Big\},$$

which is invariant under the dynamics ($(0,0,0,0)$ is an equilibrium point) and so by LaSalle's Invariance Principle, all perturbations (n', u', w', T') should approach $(0,0,0,0)$ as $t \to \infty$. This proves the linear stability of the reference steady state solution (2.18)- (2.20). □

4.3 Non-linear Stability Analysis

Although linear stability results are important, unfortunately they are not enough to infer stability of solutions in the non-linear case. To bypass this, we have to construct a Lyapunov function that decreases over solutions of the non-linear system and hence deduce global stability of the reference steady state solution using LaSalle's Invariance Principle.

4.3.1 Motivation Behind the Construction of Lyapunov Function

In studying the dynamics of a fluid in a vessel, we can divide the container into cells small enough that the velocity does not change over each of these cells. Thus, we can think of the following set-up:

Divide the domain into small cells so that the position of each particle is pinned down and we know the average velocity over each cell but we do not know the velocity of each of the individual particles in the cell. The question then becomes: Knowing only the average and variance, what is the least

biased velocity distribution of the molecules that results in the most evenly distributed energy?

Let $\rho(V)$ be the density of the distribution. Since entropy gives a measure of the number of arrangements the molecules of the system can have, the statement of the problem can be stated as follows:

Given

$$\mathbb{E}[V] = \begin{pmatrix} u \\ w \end{pmatrix}, \quad V \in \mathbb{R}^d,$$
$$\mathbb{E}\left[\frac{1}{2}\left|V - \begin{pmatrix} u \\ w \end{pmatrix}\right|^2\right] = \frac{d}{2}T, \quad V \in \mathbb{R}^d,$$

find the density $\rho(V)$ that minimizes the entropy

$$\mathcal{J}[\rho(V)] = -\int \rho(V)\, \log \rho(V)\, \mathrm{d}V$$

subject to the constraints

$$\rho(V) \geq 0, \tag{4.48}$$
$$\mathcal{I}_1[\rho(V)] = \int \rho(V)\, \mathrm{d}V = 1, \tag{4.49}$$
$$\mathcal{I}_2[\rho(V)] = \int \rho(V)\, V\, \mathrm{d}V = \begin{pmatrix} u \\ w \end{pmatrix}, \tag{4.50}$$
$$\mathcal{I}_3[\rho(V)] = \int \rho(V)\, \frac{1}{2}\left|V - \begin{pmatrix} u \\ w \end{pmatrix}\right|^2 \mathrm{d}V = \frac{d}{2}T. \tag{4.51}$$

At this point, write $\hat{\rho} = \rho + \epsilon\,\eta$, where $\hat{\rho}$ satisfies the constraints. Then,

$$\Psi(\epsilon) =: \mathcal{J}[\hat{\rho}] = -\int \hat{\rho}\, \log \hat{\rho}\, \mathrm{d}V = -\int (\rho + \epsilon\,\eta)\, \log(\rho + \epsilon\,\eta)\, \mathrm{d}V,$$
$$\Phi_1(\epsilon) =: \mathcal{I}_1[\hat{\rho}] = \int (\rho + \epsilon\,\eta)\, \mathrm{d}V = 1,$$
$$\Phi_2(\epsilon) =: \mathcal{I}_2[\hat{\rho}] = \int (\rho + \epsilon\,\eta)\, V\, \mathrm{d}V = \begin{pmatrix} u \\ w \end{pmatrix},$$
$$\Phi_3(\epsilon) =: \mathcal{I}_3[\hat{\rho}] = \int (\rho + \epsilon\, V)\, \frac{1}{2}\left|V - \begin{pmatrix} u \\ w \end{pmatrix}\right|^2 \mathrm{d}V = \frac{d}{2}T.$$

Using Lagrange multipliers, we need to solve

$$\partial_\epsilon \Psi(\epsilon) = \mu_1\, \partial_\epsilon(\Phi_1(\epsilon) - 1) + \mu_2\, \partial_\epsilon \left(\Phi_2(\epsilon) - \begin{pmatrix} u \\ w \end{pmatrix} \right) + \mu_3\, \partial_\epsilon \left(\Phi_3(\epsilon) - \frac{d}{2}\, T \right),$$

that is

$$\partial_\epsilon \Psi(\epsilon) - \mu_1\, \partial_\epsilon \Phi_1(\epsilon) - \mu_2\, \partial_\epsilon \Phi_2(\epsilon) - \mu_3\, \partial_\epsilon \Phi_3(\epsilon) = 0. \tag{4.52}$$

At $\epsilon = 0$, $\hat{\rho} = \rho$ is an extremal, so we have to evaluate the partial derivatives at $\epsilon = 0$. But

$$\begin{aligned}
\partial_\epsilon \Psi(\epsilon) &= -\int \left[\eta\, \log(\rho + \epsilon\, \eta) + \eta\right]\, dV, \\
\partial_\epsilon \Phi_1(\epsilon) &= \int \eta\, dV, \\
\partial_\epsilon \Phi_2(\epsilon) &= \int \eta\, V\, dV, \\
\partial_\epsilon \Phi_3(\epsilon) &= \int \eta\, \frac{1}{2} \left| V - \begin{pmatrix} u \\ w \end{pmatrix} \right|^2 \mathrm{d}V,
\end{aligned}$$

so that evaluating (4.52) at $\epsilon = 0$ gives

$$\int \eta \left[\log \rho(V) + 1 + \mu_1 + \mu_2\, V + \mu_3\, \frac{1}{2} \left| V - \begin{pmatrix} u \\ w \end{pmatrix} \right|^2 \right] \mathrm{d}V = 0.$$

Since this equation is true for every arbitrary η, we get

$$\log \rho(V) = -1 - \mu_1 - \mu_2\, V - \mu_3\, \frac{1}{2} \left| V - \begin{pmatrix} u \\ w \end{pmatrix} \right|^2,$$

and so

$$\rho(V) = \exp \left\{ -(1 + \mu_1) - \mu_2\, V - \mu_3\, \frac{1}{2} \left| V - \begin{pmatrix} u \\ w \end{pmatrix} \right|^2 \right\} \tag{4.53}$$

for which μ_1, μ_2 and μ_3 can be obtained by using the constraints (4.48)-(4.51).

1. Note that the constraint (4.48) is trivially satisfied by the construction of $\rho(V)$.

2. Using the constraint (4.49), we have

$$\mathrm{e}^{-(1+\mu_1)} \int \exp\left\{-\mu_2 V - \mu_3 \frac{1}{2}\left|V - \begin{pmatrix} u \\ w \end{pmatrix}\right|^2\right\} \mathrm{d}V = 1. \tag{4.54}$$

3. Note that by change of variables and using (4.54), we can write

$$\begin{aligned}\int V\,\rho(V)\,dV &= e^{-(1+\mu_1)} \int V\, \exp\left\{-\mu_2 V - \mu_3 - \frac{1}{2}\left|V - \begin{pmatrix} u \\ w \end{pmatrix}\right|^2\right\} \mathrm{d}V \\ &= \begin{pmatrix} u \\ w \end{pmatrix} + e^{-(1+\mu_1)-\mu_2 \begin{pmatrix} u \\ w \end{pmatrix}} \int V \exp\left\{-\mu_2 V - \mu_3 \frac{1}{2}|V|^2\right\} \mathrm{d}V\ .\end{aligned}$$

Imposing (4.50), we have

$$\mathrm{e}^{-(1+\mu_1)-\mu_2 \begin{pmatrix} u \\ w \end{pmatrix}} \int V \exp\left\{-\mu_2 V - \mu_3 \frac{1}{2}|V|^2\right\} \mathrm{d}V = 0. \tag{4.55}$$

Similarly as in the 1-D case, setting $\mu_2 = 0$ would give us

$$\mathrm{e}^{-(1+\mu_1)} \int V \exp\left\{-\mu_3 \frac{1}{2}|V|^2\right\} \mathrm{d}V = 0,$$

so that the new expression for $\rho(V)$ becomes

$$\rho(V) = \mathrm{e}^{-(1+\mu_1)} \exp\left\{-\mu_3 \frac{1}{2}\left|V - \begin{pmatrix} u \\ w \end{pmatrix}\right|^2\right\}.$$

Moreover, using the properties of Gaussians and their probability density functions together with (4.49), we get a relation between μ_1 and μ_3 given by $\mathrm{e}^{-(1+\mu_1)} = \sqrt{\dfrac{2\pi}{\mu_3}}$,

so that the new expression for $\rho(V)$ would depend on μ_3 only as follows:

$$\rho(V) = \sqrt{\frac{\mu_3}{2\pi}} \exp\left\{-\mu_3 \frac{1}{2} \left|V - \begin{pmatrix} u \\ w \end{pmatrix}\right|^2\right\}. \tag{4.56}$$

4. Finally, (4.50) requires that

$$\int \rho(V) \frac{1}{2} \left|V - \begin{pmatrix} u \\ w \end{pmatrix}\right|^2 \mathrm{d}V = \frac{d}{2} T,$$

where the integral represents the variance of $\rho(V)$ and hence equation (4.56) can be written as

$$\rho(V) = \frac{1}{\sqrt{2\pi T}^{\,d}} \exp\left\{-\frac{1}{2T} \left|V - \begin{pmatrix} u \\ w \end{pmatrix}\right|^2\right\}. \tag{4.57}$$

The density $\rho(V)$ obtained in (4.57) depends on the position of the cell, that is,

$$\rho_q(V) = \frac{1}{\sqrt{2\pi T}^{\,d}} \exp\left\{-\frac{1}{2T} \left|V - \begin{pmatrix} u \\ w \end{pmatrix}\right|^2\right\},$$

so that globally the molecular distribution function that is the least biased is given by

$$\rho(q, V) = \frac{n}{N} \frac{1}{\sqrt{2\pi T}^{\,d}} \exp\left\{-\frac{1}{2T} \left|V - \begin{pmatrix} u \\ w \end{pmatrix}\right|^2\right\}, \tag{4.58}$$

where $n(q)$ is the particle count per unit volume and $N = \int n(q)\,\mathrm{d}q$ is the total number of particles in the vessel.

To facilitate the construction of the Lyapunov function, we introduce the definition of the relative entropy (known as KullbackLeibler divergence) of probability distributions (see [52, 56, 57]) and relate it to Markov chains.

Definition 4.12. ***Relative Entropy***

Let $P(x)$ and $Q(x)$ be two probability distributions of the random variables X and Y with probability densities $p(x)$ and $q(x)$ respectively. Then, the relative entropy of P with respect to Q, also called Kullback - Leibler divergence, is defined to be the integral

$$\mathcal{H}(P \,\|\, Q) = \int_{-\infty}^{\infty} p(x) \, \log\left(\frac{p(x)}{q(x)}\right) \, \mathrm{d}x. \tag{4.59}$$

More generally, if P and Q are probability measures over a set $\mathcal{X}$, and P is absolutely continuous with respect to Q, then the relative entropy of P with respect to Q is defined as

$$\mathcal{H}(P \,\|\, Q) = \int_{\mathcal{X}} \log h \, \mathrm{d}P = \int_{\mathcal{X}} h \, \log h \, \mathrm{d}Q, \tag{4.60}$$

where $h = \dfrac{\mathrm{d}P}{\mathrm{d}Q}$ is the Radon-Nikodym derivative of P with respect to Q and provided that the expression on the right-hand side exists.

In the case when the random variables X and Y take on only a finite of different values $x_1, x_2, \ldots, x_m$ and $y_1, y_2, \ldots, y_m$ respectively and we put $Pr\{X = x_k\} = p_k$ and $Pr\{Y = y_k\} = q_k$ for $k = 1, 2, \ldots, m$, then(4.60) *reduces to*

$$\mathcal{H}(P \,\|\, Q) = \sum_{k=1}^{m} p_k \, \log\left(\frac{p_k}{q_k}\right). \tag{4.61}$$

Remark 4.13. *The relative entropy has many useful properties, in particular,*

$$\mathcal{H}(P \,\|\, Q) \geq 0,$$

$$\mathcal{H}(P \,\|\, Q) = 0 \iff P \text{ and } Q \text{ are identical.}$$

Because the relative entropy is non-negative and measures the difference between two distributions, it is often conceptualized as measuring some sort of distance between these distributions. However, it is not a true distance measure because it is not symmetric: $\mathcal{H}(P \,\|\, Q) \neq \mathcal{H}(Q \,\|\, P)$ *in general.*

Proof. We will prove these results for the case when P is absolutely continous with respect to Q.

By (4.60),

$$\mathcal{H}(P \,\|\, Q) = \int_{\mathcal{X}} h \, \log h \, \mathrm{d}Q,$$

where $h = \dfrac{\mathrm{d}P}{\mathrm{d}Q}$.

Since $\Psi(s) = s \, \log s$ is convex, then by Jensen's inequality

$$\begin{aligned} \mathcal{H}(P \,\|\, Q) = \mathbb{E}_Q \left[\Psi(h)\right] &\geq \Psi\Big(\mathbb{E}_Q \left[h\right]\Big) \\ &= \Psi\left(\int_{\mathcal{X}} h \, \mathrm{d}Q\right) \\ &= \Psi\left(\int_{\mathcal{X}} \mathrm{d}P\right) \\ &= \Psi\left(1\right) = 0 \ . \end{aligned}$$

It follows from this that $\mathcal{H}(P \,\|\, Q) = 0 \iff$ P and Q are identical. □

Remark 4.14. *Let* $(X_n)_{n\geq 0}$ *be a discrete time Markov chain with stationary distribution* π*. Then, the relative entropy* $\mathcal{H}(X_n \,\|\pi)$ *monotonically decreases as* n *increases.*

Proof. Let p_{jk} for j, $k = 1, 2, \ldots, M$ denote the transition probability in one step and suppose that X_n has probability distibution $\mu^{(n)}$. We want to show that

$$\mathcal{H}(X_{n+1} \,\|\, \pi) \leq \mathcal{H}(X_n \,\|\, \pi), \quad \text{for all } n \geq 0.$$

By (4.61),

$$\mathcal{H}(X_{n+1} \,\|\, \pi) = \sum_{k=1}^{M} \mu_k^{(n+1)} \, \log\left(\frac{\mu_k^{(n+1)}}{\pi_k}\right) = \sum_{k=1}^{M} \pi_k \, h_k^{(n+1)} \, \log\left(h_k^{(n+1)}\right),$$

where $h_k^{(n+1)} = \dfrac{\mu_k^{(n+1)}}{\pi_k}$. But $\mu_k^{(n+1)} = \displaystyle\sum_{j=1}^{M} \mu_j^{(n)} \, p_{jk}$ and so using the notation $h_k^{(n)} = \dfrac{\mu_k^{(n)}}{\pi_k}$, we have

$$\begin{aligned} h_k^{(n+1)} &= \frac{1}{\pi_k} \, \mu_k^{(n+1)} = \frac{1}{\pi_k} \sum_{j=1}^{M} \mu_j^{(n)} \, p_{jk} \\ &= \frac{1}{\pi_k} \sum_{j=1}^{M} \pi_j \, h_j^{(n)} \, p_{jk} = \sum_{j=1}^{M} \frac{\pi_j}{\pi_k} \, p_{jk} \, h_j^{(n)} := \sum_{j=1}^{M} Q_{kj} \, h_j^{(n)}, \end{aligned}$$

where $\quad Q_{kj} = \dfrac{\pi_j}{\pi_k} \, p_{jk}$ and so $h^{(n+1)} = Q \, h^{(n)}$.

Note that by the definition of Q_{kj}, we have

$$\sum_{j=1}^{M} Q_{kj} = \sum_{j=1}^{M} \frac{\pi_j}{\pi_k} \, p_{jk} = \frac{1}{\pi_k} \sum_{j=1}^{M} \pi_j \, p_{jk} = 1 \; .$$

So, by the convexity of the function $\Psi(s) = s \, \log s$ and Jensen's inequality, we have

$$\Psi(h_k^{(n+1)}) = \Psi\left(\sum_{j=1}^{M} Q_{kj} \, h_j^{(n)}\right) \leq \sum_{j=1}^{M} Q_{kj} \, \Psi(h_j^{(n)}),$$

and so $\Psi(h^{(n+1)}) \leq Q \, \Psi(h^{(n)}$. This implies that

$$\begin{aligned} \mathcal{H}\left(X_{n+1} \,\|\, \pi\right) = \mathbb{E}_\pi\left[\Psi(h^{(n)})\right] &= \mathbb{E}_\pi\left[\Psi\left(Q \, h^{(n)}\right)\right] \leq \mathbb{E}_\pi\left[Q \, \Psi\left(h^{(n)}\right)\right] \\ &= \sum_{k=1}^{M} \pi_k \sum_{j=1}^{M} Q_{kj} \, \Psi\left(h_j^{(n)}\right) \\ &= \sum_{j=1}^{M} \pi_k \sum_{j=1}^{M} \frac{\pi_j}{\pi_k} \, p_{jk} \, \Psi\left(h_j^{(n)}\right) \\ &= \sum_{j=1}^{M} \left[\pi_j \, \Psi\left(h_j^{(n)}\right) \sum_{k=1}^{M} p_{jk}\right] = \sum_{j=1}^{M} \left[\pi_j \, \Psi\left(h_j^{(n)}\right)\right] \\ &= \mathbb{E}_\pi\left[\Psi\left(h^{(n)}\right)\right] = \mathcal{H}(X_n \,\|\, \pi), \end{aligned}$$

and $\mathcal{H}(X_n \,\|\, \pi)$ is a decreasing function. $\square$

The above discussion suggests that if we assume that the molecules evolve according to a Markov chain (although this might not be quite true because it does not take into account the intermolecular collision), then a good candidate for a Lyapunov function is

$$\mathcal{E}(n, u, w, T) = \int_\Omega \mathcal{H}(\rho_t \,\|\, \bar{\rho})\, \mathrm{d}\mathbf{x}, \tag{4.62}$$

where

$$\rho_t(q, V) = \frac{n}{N} \frac{1}{2\pi T} \exp\left(-\frac{1}{2T} \left| V - \begin{pmatrix} u \\ w \end{pmatrix} \right|^2 \right), \tag{4.63}$$

and

$$\bar{\rho}(q, V) = \frac{\bar{n}}{N} \frac{1}{2\pi T_0} \exp\left(-\frac{1}{2T_0} \, |V|^2 \right). \tag{4.64}$$

At this point, it is useful to derive the relative entropy of two Gaussian random variables. So, consider two Gaussian random variables Z_1 and Z_2 with probability densities $f_1(V)$ and $f_2(V)$ given by

$$f_1(V) = \frac{n_1}{N} \frac{1}{\sqrt{2\pi\sigma_1^2}^{\,d}} \exp\left(-\frac{1}{2\sigma_1^2} \left| V - \begin{pmatrix} u_1 \\ w_1 \end{pmatrix} \right|^2 \right),$$

$$f_2(V) = \frac{n_2}{N} \frac{1}{\sqrt{2\pi\sigma_2^2}^{\,d}} \exp\left(-\frac{1}{2\sigma_2^2} \left| V - \begin{pmatrix} u_2 \\ w_2 \end{pmatrix} \right|^2 \right).$$

Then,

$$\begin{aligned}
\mathcal{H}(f_1 \,||\, f_2) &= \int \log\left(\frac{f_1(V)}{f_2(V)} \right) f_1(V)\, \mathrm{d}V \\
&= \int \frac{n_1}{N} \frac{1}{\sqrt{2\pi\sigma_1^2}^{\,d}} \exp\left(\frac{-\left| V - \begin{pmatrix} u_1 \\ w_1 \end{pmatrix} \right|^2}{2\sigma_1^2} \right) \left[\log\left(\frac{n_1}{n_2} \right) + \frac{d}{2} \log\left(\frac{\sigma_2^2}{\sigma_1^2} \right) \right] \mathrm{d}V \\
&+ \int \frac{n_1}{N} \frac{1}{\sqrt{2\pi\sigma_1^2}^{\,d}} \exp\left(-\frac{1}{2\sigma_1^2} \left| V - \begin{pmatrix} u_1 \\ w_1 \end{pmatrix} \right|^2 \right) \frac{1}{2\sigma_2^2} \left| V - \begin{pmatrix} u_2 \\ w_2 \end{pmatrix} \right|^2 \mathrm{d}V \\
&- \int \frac{n_1}{N} \frac{1}{\sqrt{2\pi\sigma_1^2}^{\,d}} \exp\left(-\frac{1}{2\sigma_1^2} \left| V - \begin{pmatrix} u_1 \\ w_1 \end{pmatrix} \right|^2 \right) \frac{1}{2\sigma_1^2} \left| V - \begin{pmatrix} u_1 \\ w_1 \end{pmatrix} \right|^2 \mathrm{d}V.
\end{aligned}$$

Using the properties of Gaussian random variables,

$$\text{First Integral } = \frac{n_1}{N}\left[\log\left(\frac{n_1}{n_2}\right) + \frac{d}{2}\,\log\left(\frac{\sigma_2^2}{\sigma_1^2}\right)\right], \tag{4.65}$$

$$\text{Third Integral } = \frac{1}{2\sigma_1^2}\,\frac{n_1}{N}\,d\,\sigma_1^2 = \frac{d}{2}\frac{n_1}{N}. \tag{4.66}$$

For the second integral, we write

$$\left|V - \begin{pmatrix} u_2 \\ w_2 \end{pmatrix}\right|^2 = \left|V - \begin{pmatrix} u_1 \\ w_1 \end{pmatrix}\right|^2 + 2\left(V - \begin{pmatrix} u_1 \\ w_1 \end{pmatrix}\right)\cdot\begin{pmatrix} u_1 - u_2 \\ w_1 - w_2 \end{pmatrix} + \left|\begin{pmatrix} u_1 - u_2 \\ w_1 - w_2 \end{pmatrix}\right|^2,$$

and use change of variables to get

$$\text{Second Integral } = \frac{d}{2}\,\frac{n_1}{N}\,\frac{\sigma_1^2}{\sigma_2^2} + \frac{1}{2\sigma_2^2}\,\frac{n_1}{N}\,\left|\begin{pmatrix} u_1 - u_2 \\ w_1 - w_2 \end{pmatrix}\right|^2. \tag{4.67}$$

Substituting (4.65)-(4.67), we get the final expression for $\mathcal{H}(\eta_1\,||\eta_2)$ given by

$$\begin{aligned}\mathcal{H}(\eta_1\,\|\eta_2) = \frac{n_1}{N}\left\{\log\left(\frac{n_1}{n_2}\right) + \frac{d}{2}\left[\frac{\sigma_1^2}{\sigma_2^2} - 1 - \log\left(\frac{\sigma_1^2}{\sigma_2^2}\right)\right]\right\} \\ + \frac{n_1}{N}\frac{1}{2\sigma_2^2}\left|\begin{pmatrix} u_1 - u_2 \\ w_1 - w_2 \end{pmatrix}\right|^2.\end{aligned} \tag{4.68}$$

Now, for the expressions of $\rho_t(q, V)$ and $\bar{\rho}(q, V)$ given by (4.63) and (4.64) and for $d = 2$, we get

$$\mathcal{H}(\rho_t\,\|\,\bar{\rho}) = \frac{n}{N}\,\left\{\log\left(\frac{n}{\bar{n}}\right) + \Psi\left(\frac{T}{T_0}\right) + \frac{1}{2\,T_0}\left(u^2 + w^2\right)\right\} \tag{4.69}$$

where $\Psi(s) = s - 1 - \log(s)$.

4.3.2 Proof of Stability of Steady State Solution

Using the expression for the stress tensor Π_{ij} and still assuming (for simplicity) that κ and ν are constant, we can rewrite the non-linear Navier-Stokes equations (2.1)-(2.3) as

$$\partial_t n = -\nabla\cdot(n\,\mathbf{u}), \tag{4.70}$$

$$n\,\partial_t u = -n\,\mathbf{u}\cdot\nabla u - \partial_x(n\,T) + \nu_0\,\nabla^2 u, \tag{4.71}$$

$$n\,\partial_t w = -n\,\mathbf{u}\cdot\nabla w - \partial_z(nT) - G\,n + \nu_0\nabla^2 w, \tag{4.72}$$

$$\begin{aligned} n\,\partial_t T = &-n\,\mathbf{u}\cdot\nabla T - (nT)\,\nabla\cdot\mathbf{u} + \kappa_0\,\nabla^2 T \\ &+ \nu_0\left(|\nabla u|^2 + |\nabla w|^2\right) - 2\nu_0\left[(\partial_x u)(\partial_z w) - (\partial_x w)(\partial_z u)\right], \end{aligned} \tag{4.73}$$

with the periodic boundary conditions in the horizontal x-direction given by

$$\begin{aligned} n(0,z;t) &= n(L,z;t), \\ \mathbf{u}(0,z;t) &= \mathbf{u}(L,z;t), \\ T(0,z;t) &= T(L,z;t), \end{aligned} \tag{4.74}$$

and the boundary conditions in the vertical direction given by

$$\begin{aligned} &\mathbf{u}(x,0;t) = \mathbf{0}, \quad \mathbf{u}'(x,H;t) = \mathbf{0}, \\ &T'(x,0;t) = T_0, \quad \kappa_0\,\nabla T'(x,z;t)\Big|_{z=H} = \mathbf{0}, \end{aligned} \qquad \text{on } \Omega_H$$

$$\begin{aligned} &\mathbf{u}'(x,0;t) = \mathbf{0}, \quad \lim_{z\to\infty}\mathbf{u}'(x,z;t) = \mathbf{0}, \\ &T'(x,0;t) = 0, \quad \lim_{z\to\infty}\kappa_0\,\nabla T'(x,z;t) = \mathbf{0}. \end{aligned} \qquad \text{on } \Omega_\infty \tag{4.75}$$

Recall that the steady state solution is given by

$$\bar{\mathbf{u}} = \mathbf{0} \ , \tag{4.76}$$

$$\bar{T}(z) = T_0 \ , \tag{4.77}$$

$$\bar{n}(z) = \bar{n}(0) \ \exp\left(-\frac{G}{T_0}\, z\right), \tag{4.78}$$

so that both n and $\bar{n}$ satisfy for $\Omega = \Omega_H$ or Ω_∞

$$\int_\Omega n(\mathbf{x}, t)\, \mathrm{d}\mathbf{x} = N = \int_\Omega \bar{n}(z)\, \mathrm{d}\mathbf{x} \ . \tag{4.79}$$

Theorem 4.15. *The functional*

$$\mathcal{E}(n, u, w, T) := \int_\Omega \frac{n}{N} \left[\log\left(\frac{n}{\bar{n}}\right) + \Psi\left(\frac{T}{T_0}\right) + \frac{1}{2\,T_0}\,(u^2 + w^2)\right] d\mathbf{x},$$

where

$$\Psi\left(\frac{T}{T_0}\right) = \frac{T}{T_0} - 1 - \log\left(\frac{T}{T_0}\right)$$

defines a Lyapunov function for the non-linear system (4.70)-(4.73) *on* $\Omega = \Omega_H$ *or* Ω_∞ *and hence we prove stability of the steady state solution* (4.76)-(4.78).

Proof. To show that the function $\mathcal{E}(n, u, w, T)$ is a Lyapunov function, we need to show that for $\Omega = \Omega_H$ or Ω_∞

I. $\mathcal{E}(n, u, w, T)$ is non-negative; that is,

$$\mathcal{E}(n, u, w, T) \geq 0 \quad \text{for all } n, u, w, \text{ and } T.$$

II. $\mathcal{E}(n, u, w, T)$ decreases over solutions of the non-linear system (4.70)-(4.73); that is, for all $n, u, w,$ and T satisfying (4.70)-(4.73), we have

$$\frac{d\mathcal{E}}{dt}(n, u, w, T) \leq 0.$$

I. **Checking Non-negativity:**

1. Note first that the function $\Psi(\alpha) = \alpha - 1 - \log(\alpha)$ has a global minimum at $\alpha = 1$ and so

$$\Psi(\alpha) \geq \Psi(1) = 0 \quad \text{for all } \alpha > 0.$$

2. Consider now the integral

$$\int_\Omega \frac{n}{N} \log\left(\frac{n}{\bar{n}}\right) \mathrm{d}\mathbf{x} = \int_\Omega \frac{\bar{n}}{N} \frac{n}{\bar{n}} \log\left(\frac{n}{\bar{n}}\right) \mathrm{d}\mathbf{x} = \int_\Omega \frac{\bar{n}}{N} \Phi\Big(\frac{n}{\bar{n}}\Big) \mathrm{d}\mathbf{x},$$

where $\Phi(\alpha) = \alpha \log(\alpha)$ and note that by (4.79)

$$\int_\Omega \frac{\bar{n}}{N} \mathrm{d}\mathbf{x} = 1 \quad \text{so that } \mathrm{d}\pi = \frac{\bar{n}}{N} \mathrm{d}\mathbf{x} \text{ is a probability measure on } \Omega.$$

Since $H(\alpha)$ is convex and $\mathrm{d}\pi$ is a probability measure we can apply Jensen's inequality together with (4.79) to get

$$\int_\Omega \Phi\Big(\frac{n}{\bar{n}}\Big) \frac{n}{\bar{n}} \mathrm{d}\mathbf{x} \geq \Phi\bigg(\int_\Omega \frac{n}{\bar{n}} \frac{\bar{n}}{N} \mathrm{d}\mathbf{x}\bigg) = \Phi\bigg(\int_\Omega \frac{n}{N} \mathrm{d}\mathbf{x}\bigg) = \Phi(1) = 0.$$

Hence, for all $n, u, w,$ and T,

$$\mathcal{E}(n, u, w, T) := \int_\Omega \frac{n}{N} \left[\log\left(\frac{n}{\bar{n}}\right) + \Psi\left(\frac{T}{T_0}\right) + \frac{1}{2\,T_0}\,(u^2 + w^2)\right] \mathrm{d}\mathbf{x} \geq 0,$$

and so the non-negativity condition of $\mathcal{E}(n, u, w, T)$ is proved.

II. **Checking the Rate of Change:**

Taking the time derivative of $\mathcal{E}(n,u,w,T)$ and using the definition of $\Psi(\alpha)$, we can write the rate of change as

$$\begin{aligned}\frac{\mathrm{d}\mathcal{E}}{\mathrm{d}t} = &\int_\Omega \frac{\partial_t n}{N}\left[\log\left(\frac{n}{\bar{n}}\right)+\frac{T}{T_0}-\log\left(\frac{T}{T_0}\right)+\frac{1}{2\,T_0}\,\left(u^2+w^2\right)\right]d\mathbf{x}\\ &+\frac{1}{N\,T_0}\int_{\Omega_\infty}\left[\left(1-\frac{T_0}{T}\right)n\,\partial_t T+u\;n\,\partial_t u+w\;n\,\partial_t w\right]\mathrm{d}\mathbf{x}.\end{aligned} \tag{4.80}$$

Since most of the steps in this computation are very similar to those done in the case of linear stability, we will go quickly over the steps that use the same conditions and give more details whenever needed.

1. Using (4.70), integration by parts and the boundary conditions (4.74)-(4.75) on $\mathbf{u}$, we can rewrite the first integral as

$$\begin{aligned}&\int_\Omega \frac{\partial_t n}{N}\left[\log\left(\frac{n}{\bar{n}}\right)+\frac{T}{T_0}-\log\left(\frac{T}{T_0}\right)+\frac{1}{2T_0}\,\left(u^2+w^2\right)\right]\mathrm{d}\mathbf{x}\\ &=-\int_\Omega \frac{\nabla\cdot(n\,\mathbf{u})}{N}\left[\log\left(\frac{n}{\bar{n}}\right)+\frac{T}{T_0}-\log\left(\frac{T}{T_0}\right)+\frac{1}{2T_0}\,\left(u^2+w^2\right)\right]\mathrm{d}\mathbf{x}\\ &=\frac{1}{N}\int_\Omega (n\,\mathbf{u})\cdot\nabla\left[\log\left(\frac{n}{\bar{n}}\right)+\frac{T}{T_0}-\log\left(\frac{T}{T_0}\right)+\frac{1}{2\,T_0}\,\left(u^2+w^2\right)\right]\mathrm{d}\mathbf{x}\\ &=\frac{1}{N}\int_\Omega\left[\mathbf{u}\cdot\nabla n+\frac{G}{T_0}\,n\,w\right]d\mathbf{x}+\frac{1}{NT_0}\int_{\Omega_\infty} n\,\mathbf{u}\cdot\left(1-\frac{T_0}{T}\right)\nabla T\,\mathrm{d}\mathbf{x}\\ &\quad+\frac{1}{2\,NT_0}\int_\Omega n\,\mathbf{u}\cdot\nabla\left(u^2+w^2\right)\mathrm{d}\mathbf{x}.\end{aligned}$$

2. Multiplying (4.71) by u and (4.72) by w and adding we get

$$\begin{aligned} u\ n\,\partial_t u + w\ n\,\partial_t w &= -n\ \mathbf{u}\cdot u\,\nabla u - n\ \mathbf{u}\cdot w\,\nabla w \\ &\quad - \left[u\,\partial_x(n\,T) + w\,\partial_z(nT)\right] - G\,n\,w + \nu_0\left[u\,\nabla^2 u + w\,\nabla^2 w\right] \\ &= -\frac{1}{2}\,n\ \mathbf{u}\cdot\nabla(u^2+w^2) - \mathbf{u}\cdot\nabla(n\,T) - G\,n\,w \\ &\quad + \nu_0\left[u\nabla^2 u + w\,\nabla^2 w\right]. \end{aligned}$$

Moreover, using integration by parts and utilizing the boundary conditions, we have

$$\int_\Omega \mathbf{u}\cdot\nabla(n\,T)\ \mathrm{d}\mathbf{x} = -\int_\Omega (n\ T)\ \nabla\cdot\mathbf{u}\ \mathrm{d}\mathbf{x},$$

$$\int_\Omega \left(u\,\nabla^2 u + w\,\nabla^2 w\right)\ \mathrm{d}\mathbf{x} = -\int_\Omega \left(|\nabla u|^2 + |\nabla w|^2\right)\ \mathrm{d}\mathbf{x},$$

so that we can write

$$\begin{aligned} \frac{1}{NT_0}\int_\Omega (u\ n\,\partial_t u + w\ n\,\partial_t w)\ \mathrm{d}\mathbf{x} &= -\frac{1}{2\,N\,T_0}\int_\Omega n\,\mathbf{u}\cdot\nabla(u^2+w^2)\,\mathrm{d}\mathbf{x} \\ &\quad + \frac{1}{NT_0}\int_\Omega (n\,T)\,\nabla\cdot\mathbf{u}\,\mathrm{d}\mathbf{x} \\ &\quad - \frac{1}{NT_0}\int_\Omega G\,n\,w\,\mathrm{d}\mathbf{x} \\ &\quad - \frac{\nu_0}{NT_0}\int_\Omega \left(|\nabla u|^2 + |\nabla w|^2\right)\ \mathrm{d}\mathbf{x}. \end{aligned}$$

3. Finally, multiplying (4.73) by $\left(1-\frac{T_0}{T}\right)$, we get

$$\begin{aligned}\frac{1}{NT_0}\int_\Omega \left(1-\frac{T_0}{T}\right) n\,\partial_t T\,d\mathbf{x} = &-\frac{1}{NT_0}\int_\Omega n\,\mathbf{u}\cdot\left(1-\frac{T_0}{T}\right)\nabla T\,\mathrm{d}\mathbf{x}\\ &-\frac{1}{NT_0}\int_\Omega (n\,T)\,\nabla\cdot\mathbf{u}\;\mathrm{d}\mathbf{x}\\ &+\frac{\nu_0}{NT_0}\int_\Omega \left(|\nabla u|^2+|\nabla w|^2\right)\mathrm{d}\mathbf{x}\\ &-\frac{\nu_0}{N}\int_\Omega \frac{1}{T}\left(|\nabla u|^2+|\nabla w|^2\right)\mathrm{d}\mathbf{x}\\ &+\frac{1}{N}\int_\Omega n\,\nabla\cdot\mathbf{u}\;\mathrm{d}\mathbf{x}\\ &+\frac{\kappa_0}{NT_0}\int_\Omega \left(1-\frac{T_0}{T}\right)\nabla^2 T\,\mathrm{d}\mathbf{x}\\ &-\frac{2\nu_0}{NT_0}\int_\Omega \left[(\partial_x u)(\partial_z w)-(\partial_x w)(\partial_z u)\right]\mathrm{d}\mathbf{x}\\ &+\frac{2\nu_0}{N}\int_\Omega \frac{1}{T}\left[(\partial_x u)(\partial_z w)-(\partial_x w)(\partial_z u)\right]\mathrm{d}\mathbf{x}.\end{aligned}$$

Using integration by parts, the periodic boundary conditions on both n and $\mathbf{u}$ and the conditions $\mathbf{u}(x,0;t)=\mathbf{u}(x,H;t)=0$ or the decay at infinity conditions, we get

$$\frac{1}{N}\int_\Omega n\,\nabla\cdot\mathbf{u}\;\mathrm{d}\mathbf{x} = -\frac{1}{N}\int_\Omega \mathbf{u}\cdot\nabla n\,\mathrm{d}\mathbf{x}.$$

Similarly, using the periodic boundary conditions on $\mathbf{u}$, the no-slip boundary conditions on $z=0$ and the no-slip boundary condition at $z=H$ or the decay at infinity conditions, we get

$$\int_\Omega (\partial_x u)\,(\partial_z w)\ \mathrm{d}\mathbf{x} = \int_\Omega (\partial_z u)\,(\partial_x w)\ \mathrm{d}\mathbf{x},$$

and

$$-\frac{2\nu_0}{NT_0}\int_\Omega [(\partial_x u)(\partial_z w) - (\partial_x w)(\partial_z u)]\,\mathrm{d}\mathbf{x} = 0.$$

Note that since $T(x,0;t) = T_0$, then

$$\left(1 - \frac{T_0}{T}\right)\Big|_{z=0} = 0.$$

Hence, using integration by parts, the periodic boundary conditions on T and the zero heat flux condition on $z = H$ or the decay at infinity of the heat flux, we can write

$$\begin{aligned}\int_\Omega \left(1 - \frac{T_0}{T}\right)\nabla^2 T\,\mathrm{d}\mathbf{x} &= -\int_\Omega \nabla\left(1 - \frac{T_0}{T}\right)\cdot\nabla T\,\mathrm{d}\mathbf{x}\\ &= -T_0\int_\Omega \frac{1}{T^2}\,\nabla T\cdot\nabla T\,\mathrm{d}\mathbf{x}\\ &= -T_0\int_\Omega \frac{1}{T^2}\,|\nabla T|^2\ \mathrm{d}\mathbf{x},\end{aligned}$$

and so,

$$\frac{\kappa_0}{NT_0}\int_\Omega \left(1 - \frac{T_0}{T}\right)\nabla^2 T\,\mathrm{d}\mathbf{x} = -\frac{\kappa_0}{N}\int_\Omega \frac{1}{T^2}\,|\nabla T|^2\ \mathrm{d}\mathbf{x}.$$

Therefore,

$$\begin{aligned}\frac{1}{N\,T_0}\int_\Omega \left(1-\frac{T_0}{T}\right) n\,\partial_t T\,\mathrm{d}\mathbf{x} = &-\frac{1}{N\,T_0}\int_\Omega n\,\mathbf{u}\cdot\left(1-\frac{T_0}{T}\right)\nabla T\,\mathrm{d}\mathbf{x}\\ &-\frac{1}{N\,T_0}\int_\Omega (n\,T)\,\nabla\cdot\mathbf{u}\;\mathrm{d}\mathbf{x}\\ &+\frac{\nu_0}{N\,T_0}\int_\Omega \left(|\nabla u|^2+|\nabla w|^2\right)\mathrm{d}\mathbf{x}\\ &-\frac{\nu_0}{N}\int_\Omega \frac{1}{T}\;\left(|\nabla u|^2+|\nabla w|^2\right)\mathrm{d}\mathbf{x}\\ &-\frac{1}{N}\int_\Omega \mathbf{u}\cdot\nabla n\,\mathrm{d}\mathbf{x}\\ &-\frac{\kappa_0}{N}\int_\Omega \frac{1}{T^2}\;|\nabla T|^2\;\mathrm{d}\mathbf{x}\\ &+\frac{2\nu_0}{N}\int_\Omega \frac{1}{T}\;\left[(\partial_x u)(\partial_z w)-(\partial_x w)(\partial_z u)\right]\mathrm{d}\mathbf{x}.\end{aligned}$$

Putting all these steps together, we get a simplified expression for the rate of change given by

$$\begin{aligned}\frac{\mathrm{d}\mathcal{E}}{\mathrm{d}t}(n,u,w,T) = &-\frac{\nu_0}{N}\int_\Omega \frac{1}{T}\;\left(|\nabla u|^2+|\nabla w|^2\right)\mathrm{d}\mathbf{x}\\ &-\frac{\kappa_0}{N}\int_\Omega \frac{1}{T^2}\;|\nabla T|^2\;\mathrm{d}\mathbf{x}\\ &+\frac{2\nu_0}{N}\int_\Omega \frac{1}{T}\;\left[(\partial_x u)(\partial_z w)-(\partial_x w)(\partial_z u)\right]\mathrm{d}\mathbf{x}\;.\end{aligned}$$

But

$$
\begin{aligned}
&|\nabla u|^2 + |\nabla w|^2 - 2(\partial_x u)(\partial_z w) + 2(\partial_x w)(\partial_z u) \\
&= \left[(\partial_x u)^2 + (\partial_z u)^2\right] + \left[(\partial_x w)^2 + (\partial_z w)^2\right] - 2(\partial_x u)(\partial_z w) + 2(\partial_x w)(\partial_z u) \\
&= \left[(\partial_x u)^2 - 2(\partial_x u)(\partial_z w) + (\partial_z w)^2\right] + \left[(\partial_x w)^2 + 2(\partial_x w)(\partial_z u) + (\partial_z u)^2\right] \\
&= \left[\partial_x u - \partial_z w\right]^2 + \left[\partial_x w + \partial_z u\right]^2 .
\end{aligned}
$$

This implies that the rate of change of $\mathcal{E}(n, u, w, T)$ can be written as

$$
\begin{aligned}
\frac{\mathrm{d}\mathcal{E}}{\mathrm{d}t}(n, u, w, T) = &- \frac{\nu_0}{N} \int_\Omega \frac{1}{T} \left[(\partial_x u - \partial_z w)^2 + (\partial_x w + \partial_z u)^2\right] \mathrm{d}\mathbf{x} \\
&- \frac{\kappa_0}{N} \int_\Omega \frac{1}{T^2} |\nabla T|^2 \, \mathrm{d}\mathbf{x}.
\end{aligned} \tag{4.81}
$$

Since $T(\mathbf{x}, t) \geq 0$ is the temperature of the fluid, then from (4.81) we conclude that for all $n, u, w,$ and T satisfying (4.70)-(4.73), we have

$$
\frac{d\mathcal{E}}{dt}(n, u, w, T) \leq 0 \quad \text{for all } n, u, w \text{ and } T.
$$

So far, we proved that $\mathcal{E}(n, u, w, T)$ is a Lyapunov function for the non-linear system (4.70)-(4.73). In order to apply LaSalle's Invariance Principle, we still need to show that

$$
\left\{ (n, u, w, T) \,\middle|\, \frac{\mathrm{d}\mathcal{E}}{\mathrm{d}t}(n, u, w, T) = 0 \right\} = \left\{ \left(\bar{n}, \bar{u}, \bar{w}, \bar{T}\right) \right\}.
$$

Since this set is invariant under the dynamics $\left(\left(\bar{n}, \bar{u}, \bar{w}, \bar{T}\right) \text{ is a fixed point}\right)$, applying LaSalle's Invariant Principle on this set would then allow us to con-

clude that all solutions starting in a compact neighbourhood of $\left(\bar{n}, \bar{u}, \bar{w}, \bar{T}\right)$ approach this fixed points and hence prove the stability of the steady state solution.

To prove the claim, first note that since the reference steady state solution satisfies equations (4.70)-(4.73), then

$$\frac{\mathrm{d}\mathcal{E}}{\mathrm{d}t}(\bar{n}, \bar{u}, \bar{w}, \bar{T}) = 0,$$

and it remains to show that the only place where $\dfrac{\mathrm{d}\mathcal{E}}{\mathrm{d}t}(n, u, w, T) = 0$ is at the reference solution.
Setting $\dfrac{\mathrm{d}\mathcal{E}}{\mathrm{d}t}(n, u, w, T) = 0$, we get

$$\partial_x u - \partial_z w = 0, \tag{4.82}$$

$$\partial_x w + \partial_z u = 0, \tag{4.83}$$

$$\nabla T = \mathbf{0}, \tag{4.84}$$

with $\mathbf{u}$ and T satisfying the boundary conditions (4.74)-(4.75).

(i) From (4.84) and imposing the boundary conditions, it is easy to see that $T(x, z; t) = T_0$.

(ii) Differentiating (4.82) with respect to x and (4.83) with respect to z and adding, we get

$$\partial_x^2 u + \partial_z^2 u = 0 \ ,$$

$$u(0, z; t) = u(L, z; t) \ ,$$

$$u(x, 0; t) = 0 \ ,$$

$$u(x, H; t) = 0 \ , \quad \text{or} \quad \lim_{z \to \infty} u(x, z; t) = 0 \ .$$

Writing

$$u = V_1(z,t)\,\cos\left(\frac{2\pi\,x}{L}\right) + V_2(z,t)\,\sin\left(\frac{2\pi\,x}{L}\right),$$

then the periodic boundary condition is trivially satisfied and by substitution, we get the 2nd order system in V_1 and V_2, given by

$$-\left(\frac{2\pi}{L}\right)^2 V_1 + \partial_z^2 V_1 = 0,$$
$$-\left(\frac{2\pi}{L}\right)^2 V_2 + \partial_z^2 V_2 = 0,$$

with the boundary conditions

$$V_1(0,t) = V_2(0,t) = 0,$$
$$V_1(H,t) = V_2(H,t) = 0 \text{ or } \lim_{z\to\infty} V_1(z,t) = \lim_{z\to\infty} V_2(z,t) = 0.$$

At this point, it is an easy computation to show that the only solutions to this system are

$$V_1(z,t) = V_2(z,t) = 0 \quad \text{and so} \quad u(x,z;t) \equiv 0.$$

But this implies that $\partial_x w = \partial_z w = 0$ with the boundary conditions (4.74)-(4.75) and so $w(x,z;t) \equiv 0$.

Hence, we have $\mathbf{u}(\mathbf{x},t) \equiv \mathbf{0} := \bar{\mathbf{u}}$ and $T(\mathbf{x},t) = T_0 := \bar{T}$. Substituting these solutions in equations (4.70)-(4.73), we get that n is independent of x and t and satisfies

$$T_0\,\frac{\mathrm{d}n}{\mathrm{d}z} = -G\,n,$$

whose solution is $n(z) = n(0)\exp\left(-\dfrac{G}{T_0}\,z\right) := \bar{n}(z)$.

This discussion shows that $\dfrac{\mathrm{d}\mathcal{E}}{\mathrm{d}t}(n,u,w,T)=0 \iff (n,u,w,T)=(\bar{n},\bar{u},\bar{w},\bar{T})$, thus proving the claim. □

Remark 4.16. *For $n=\bar{n}+n'$, $u=0+u'$, $w=0+w'$, and $T=T_0+T'$, we get*

$$\mathcal{E}(n,u,w,T)=\frac{1}{2\,N\,T_0}\,\mathcal{V}(n',u',w,T')+\textit{ Higher order terms,}$$

where $\mathcal{V}(n',u',w,T')$ is the Lyapunov function in the linear case.

Proof. For $n=\bar{n}+n'$, $u=0+u'$, $w=0+w'$, and $T=T_0+T'$, we can write for $\Omega=\Omega_H$ or Ω_∞

$$\begin{aligned}\mathcal{E}(n,u,w,T)=&\int_\Omega\left(\frac{\bar{n}+n'}{N}\right)\left[\log\left(1+\frac{n'}{\bar{n}}\right)+\Psi\left(1+\frac{T'}{T_0}\right)\right]\,d\mathbf{x}\\&+\int_\Omega\left(\frac{\bar{n}+n'}{N}\right)\left[\frac{1}{2\,T_0}\,\left(u'^{\,2}+w'^{\,2}\right)\right]\,d\mathbf{x}.\end{aligned}$$

But by Taylor series expansion, and for small perturbations n' and T', we can write

$$\begin{aligned}\log\left(1+\frac{n'}{\bar{n}}\right)&=\frac{n'}{\bar{n}}-\frac{1}{2}\left(\frac{n'}{\bar{n}}\right)^2+\frac{1}{3}\left(\frac{n'}{\bar{n}}\right)^3+\dots\\\Psi\left(1+\frac{T'}{T_0}\right)&=\frac{T'}{T_0}-\log\left(1+\frac{T'}{T_0}\right)=\frac{1}{2}\left(\frac{T'}{T_0}\right)^2-\frac{1}{3}\left(\frac{T'}{T_0}\right)^3+\dots,\end{aligned}$$

so that

$$\begin{aligned}\mathcal{E}(n,u,w,T)=\;&\frac{1}{2\,N\,T_0}\int_\Omega\left[\frac{T_0}{\bar{n}}\,n'^{\,2}+\frac{\bar{n}}{T_0}T'^{\,2}+\bar{n}\left(u'^{\,2}+w'^{\,2}\right)\right]\,d\mathbf{x}+\int_{\Omega_\infty}\frac{n'}{N}\,d\mathbf{x}\\&+\;\text{Higher order terms.}\end{aligned}$$

But using (4.79), we have

$$\int_\Omega\frac{n'}{N}\,d\mathbf{x}=\frac{1}{N}\int_\Omega n\,d\mathbf{x}-\frac{1}{N}\int_\Omega\bar{n}\,d\mathbf{x}=1-1=0,$$

and so if $n = \bar{n} + n'$, $u = 0 + u'$, $w = 0 + w'$, and $T = T_0 + T'$, we have

$$\mathcal{E}(n, u, w, T) = \frac{1}{2\,N\,T_0}\,\mathcal{V}(n', u', w', T') + \text{Higher order terms.}$$

□

Part II

Flow Dynamics in a Stratified Fluid in a Channel

Chapter 5

Problem Formulation

5.1 Introduction and Literature Review

5.1.1 Motivation

Natural convection in rectangular cavities with unequally heated sidewalls is a problem of fundamental interest to fluid mechanics and heat transfer, with many geophysical and industrial applications. For example, it is well known that convection in narrow vertical tubes of various heat engineering equipment influences its operating features. In particular, in heat pipes, a slug regime of boiling appears in the case of natural convection lowering, which reduces the heat transfer and decreases the thermosyphon efficiency [64]. As a consequence, it is required to reveal the dependency of natural convection intensity on the inner diameter of the pipes and the way of heating.

The fact that air is a good insulator has been appreciated and utilized in the construction of buildings for many years. For instance, in the construction of residential units, it is common practice to build walls consisting of two thick-

nesses of brick separated by an unventilated air gap of a few inches. Engineers have therefore been interested in studying how much heat is transferred across the air gap, and how the rate at which heat is transferred depends on the distance and the temperature difference between the two vertical walls. Moreover, fluid adjacent to a heated wall undergoes motion as a result of variations in the buoyancy force caused by temperature gradients in the fluid. Rather than studying the rate of transfer of heat across the cavity, geophysicists have been more concerned with discovering the motion of the fluid and the temperature distribution within. The evident interest in the problem has led to theoretical and experimental studies of the role played by buoyancy forces in a variety of circumstances and to one of the earliest formulations of the problem in the two-dimensional form [5].

Another interesting application of natural convection that has attracted increasing research attention in recent years is the adoption of solar chimneys for building ventilation as an energy-efficient means of delivering fresh air to the occupants (see, for example, [49, 55, 73, 26, 35]). A solar chimney may be described as an asymmetrically heated air channel with air flow constrained between two vertical walls (glazing and absorber). The air movement is due to the buoyancy force generated by solar heating such that hot air rises and exits from the top of the chimney cavity, drawing cooler air into the building in a continuous fashion [4].

5.1.2 One-Dimensional Flows in Plane Geometries

Due to its significance for a variety of engineering and industrial applications, the natural convection flow of a viscous fluid along a vertical plate has been studied extensively in the literature. In the case where the plate is doubly-infinite, the equations of motion and thermodynamic energy reduce to one-dimensional forms, and the problem becomes analytically tractable. Solutions by the method of Laplace transforms have been obtained for a variety of plate boundary conditions [31, 24, 14], assuming the fluid is unstratified. These exact solutions provide rare analytical descriptions of transient natural convection flows and are potentially valuable as a means of validating numerical convection models.

Since thermally stratified media often occur in nature, of particular interest is the case when there exists a prevailing vertical stratification in addition to a temperature contrast in the horizontal direction between two vertical sidewalls. Steady-state solutions for these flows were obtained by several researchers [5, 18, 22, 7]. The analytical procedure was focused on an exact solution of the Boussinesq equation in an infinite vertical layer. By examining the asymptotic structure of the base flow for large Rayleigh numbers, it was shown that the mass flux is carried by the boundary layer on the vertical wall. The dynamical significance of this layer, referred to as the buoyancy layer, has been asserted in a wide variety of strongly stratified fluid systems. A large part of the literature on natural convection in an enclosure has been concerned with steady-state situations. Time-dependent flows of buoyant convection in a cavity have received far less attention (e.g., [29]). As observed by Jischke and Doty in [32], this scarcity does not imply that the time-dependent processes

are in any way less important. Rather, this is reflective of the major difficulties involved in dealing with time-dependent convection problems in general.

The classical framework was then extended by Park and Hyun [51] and Park [50] to include thermal stratification in the study of time-dependent flows. In [51], Park and Hyun used the eigenfunction expansion method to find a formal solution to the unsteady equations of motion for the buoyancy layer generated by an impulsive (step) change of temperature at the infinite vertical wall. A straightforward analysis of the transient buoyancy layer revealed that the transition to the steady state can be monotonic or oscillatory depending on how big (or small) the Prandtl number is compared to the Rayleigh number.

While Park and Hyun [51] and Park [50] considered the flow in the gap between two parallel plates, Shapiro and Fedorovich [61] considered the unsteady flow in the semi-infinite domain bounded by a single plate immersed in a stably stratified fluid. Shapiro and Fedorovich also made provision for pressure work for a perfect gas, a term that is neglected in the conventional Boussinesq approximation. With attention restricted to fluids of Prandtl number unity, Shapiro and Fedorovich obtained analytical solutions for the cases of (1) impulsive (step) change in plate perturbation temperature, (2) sudden application of a plate heat flux, and (3) for arbitrary temporal variations in plate perturbation temperature or plate heat flux. Thermal stratification provided a negative feedback mechanism whereby rising fluid cooled relative to the environment, while subsiding fluid warmed relative to the environment. In a later paper of the same authors [60], analytical solutions of the viscous equations of motion and thermodynamic energy were obtained for Prandtl numbers near unity by the method of Laplace transforms and a regular perturbation

expansion in the Prandtl number. It was shown that the developing boundary layers are thicker, more vigorous, and more sensitive to smaller Prandtl numbers (< 1).

5.1.3 Some Flows in Other Geometries

To address the demands of fast developing engineering applications, researchers have studied a variety of geometrical configurations. Some of the interesting problems in the literature include the study of analytical solutions for time-periodic thermally driven slope flows [74], stability scaling for inclined differentially heated cavity flows [71] and investigation of fluid dynamics and thermal performance in the space between a hot inner cylinder and a cold outer polygonal shape when radiative heat flux is taken into consideration [58].

Convective heat transfer problems about cylindrical bodies have gained increasing attention because of their widely used geometry: in geothermal reservoirs for power generation, heat generating fuel rods in reactors, hot filaments in polymer industries, and others. The early research mainly focused on unstratified media and examined natural convective flows along vertical cylinders with constant or sudden change in heat flux [24, 46] and surface temperature [45, 11]. To add realism to the problem, researchers considered vertical cylinders immersed in stratified media and studied free convection for a sudden change in surface temperature of the cylinder [15] as well as time-periodic surface boundary conditions [62]. Recently, more studies have been conducted for flows along oscillating and moving cylinders in both unstratified [34] and stratified media [16].

5.1.4 Direct Numerical Simulation of Boundary Layers

Unsteady natural convection flows are considerably more difficult to analyze theoretically because of the intrinsic coupling between the temperature and velocity fields. The case of a doubly infinite plate, in which no leading edges are considered, is one of the few scenarios where the Boussinesq equations of motion and the thermodynamic energy may be solved analytically. This owes to the fact that the unsteady natural convection flow along an infinite vertical plate can be assumed laminar one-dimensional and so the equations reduce to a set of linear partial differential equations which may be easier to study theoretically in a number of circumstances.

Flows between infinite vertical walls become much more difficult to analyze when the temperature along each plate is not constant (isothermal case) but increases linearly with height (positive stratification). Moreover, the level of complexity of the problem increases when we want to study a fluid in a rectangular closed container as we lose the one-dimensional property of the flow and instead the full two-dimensional setting should be considered. This led researchers to rely on numerical models to understand these turbulent flows for a variety of regimes and for different boundary conditions (for example, [19, 53, 20, 42]). There has also been increasing interest over the years to use direct numerical simulations to understand the initial stage of laminar to turbulent transition (see, [1, 27, 76, 63]) as well as the problem of evaporation and condensation by mixed convection in vertical channels and rectangular ducts (for example, [6, 48, 10, 47, 66, 30]).

5.1.5 Periodically-Driven Flows

A major issue that will be the main object of our study is the case of a fluid driven by external periodic temperature variations. When a system is subjected to an external excitation with the correct natural frequency, its eigenmodes will be amplified and the system undergoes a physical phenomenon referred to as resonance. This problem statement has serious ramifications from the standpoint of the fundamental dynamics of natural convection. In practical applications, the problem models, for example, natural convection in a room which is heated periodically on a daily basis. Even more appealing is the convection in a confined space in many electronic devices, where time-dependent flows are induced due to the periodic energizing of the on and off modes.

Extensive studies have been conducted for instabilities of natural convection boundary layers in differentially heated cavities and other interesting regimes for both unstratified (for example, [3, 8, 12, 13, 65]) and stratified media (see, [23, 44, 69, 70, 72]). However, resonance of natural convection flows has attracted much less interest and results about resonance in a cavity were initially reported by Kazmierczak and Chinoda [33] and Lage and Bejan [41]. Some of the later investigations were concerned with external periodic-heating-induced resonance of natural convection (for example, [39, 40, 37]) and others examined the resonance induced by a mechanical oscillating boundary [36]. Moreover, Zhao *et al.* [75] used a direct stability analysis to exploit the resonance characteristics of the thermal boundary layer and the effects of the resonance on heat transfer, especially in the nonlinear flow response regime.

In [41], Lage and Bejan's interest was directed at a rectangular cavity with

a constant-temperature cold sidewall and a time-dependent heat flux fluctuating in a square-wave fashion about the mean value at the other vertical wall. Their research mainly focused on the effect of periodicity of the sidewall heating on the time-dependent flow and the possibility of resonance of the fluid system with the oscillation of the externally supplied heat input. The numerical studies in [41] at high Rayleigh numbers clearly established the existence of resonance for periodic heating which was identified by the occurrence of maximal fluctuations of the local velocity and the Nusselt numbers. The study in [41] shows good evidence of the existence of resonance in natural convection when a continuously changing thermal boundary condition is adopted.

In a related problem set-up, Kazmierczak and Chinoda [33] conducted numerical studies of natural convection in a square cavity with one vertical sidewall at a constant temperature while the temperature at the other wall varied sinusoidally in time about the mean value. The numerical simulations produced periodic solutions for one Rayleigh number ($\mathsf{Ra} = 1.4 \times 10^5$) and one Prandtl number ($\mathsf{Pr} = 7$), and for three different frequencies of the temperature oscillations. The solutions demonstrated that the interior flow fluctuations changed monotonically with the frequency of the externally supplied temperature, and no resonance was detected between the temporal temperature variations and the resulting flow oscillations. The numerical account of Kazmierczak and Chinoda [33] was then at variance with the qualitative conclusions of Lage and Bejan [41], although the precise problem formulations may be only slightly different.

Kwak and Hyun [39] performed comprehensive and far-ranging numerical computations for the same problem formulation as the one used in [33] to ob-

tain detailed numerical solutions over a much broader range of the frequency of the hot-wall temperature oscillation. It was shown that the previous computational results in [33] for three different values of frequency represent only a narrow portion of the whole spectrum of solutions. Owing to the limited frequency resolution, distinct evidence of resonance between the flow fluctuation and the frequency of wall temperature oscillation was not found in [33]. However, the numerical results in [39] have illustrated that the fluctuations of flow and heat transfer responses display peak values at certain frequencies, if computations span much more extended ranges of the frequency with considerably finer resolution. These efforts explain the apparent disagreements among the previous works.

5.1.6 Our Problem

In the present part of the dissertation, we study a viscous stably stratified fluid in a channel with time-periodic temperature variations applied at the sidewalls. The fundamental question then concerns the way in which the periodicity of the sidewalls' heating-cooling cycles affect both the time-dependent flow and the heat transfer across the cavity. The crux of the argument is focused on the possibility of 'resonance' of the fluid flow with the periodic oscillations of the externally supplied temperatures at the walls. Although several authors have studied such physical phenomena (for example, [33, 41, 39]), their research heavily relied on numerical studies of natural convection since in most cases they did not have analytical solutions to the time-dependent flow.

For the above set-up, we seek solutions in the form of simple harmonic oscillations to obtain analytical temperature and velocity profiles of the time-

dependent flow for the Boussinesq equations of motion and thermodynamic energy that depend on time and one spatial variable. This enables us to study the vertical motion of the fluid caused by variations in the buoyancy forces as well as the heat transfer across the cavity.

The results presented in the following chapters are a part of an ongoing research aimed at analyzing the existence of resonance of the fluid flow as a function of three parameters: Prandtl number, width of the channel, and frequency of the external temperature oscillations. So far, we consider time-periodic temperature oscillations at the sidewalls to be in direct opposition. As a future project, we wish to consider the set-up in which we make a provision for a phase shift between the heating and cooling cycles of the two vertical walls. In that case, it would be interesting to study how this phase shift affects any resonance in view of different Prandtl numbers. We hope to study this problem in the near future.

5.2 Governing Equations

Consider a Cartesian coordinate system in which the z-axis opposes the gravity vector, the (y, z)-plane coincides with an infinite vertical plate, the x-axis is directed perpendicular to the plates, and the fluid fills an infinite vertical channel of width $2L$. In the initial state, the fluid is at rest with zero horizontal temperature gradient until thermal conditions at the left and right plates are abruptly changed at $t = 0$ (see Figure 5.1). The derivation of the governing equations below follows closely the discussion found in [61]. In full generality, these equations are far more complicated as there are many competing factors. Detailed accounts can be found in the classical works of Prandtl [54] and Schlichting [59]. In the present study, we neglect terms that are small and only consider a simplified version of these equations.

5.2.1 Derivation of the PDEs

The motion of the fluid is assumed laminar, with the only non-zero velocity component, the vertical velocity W, varying only in the x-direction. (Hence, the incompressibility condition is trivially satisfied). In order for the horizontal equations of motion to be satisfied, $\dfrac{\partial p}{\partial x} = 0$ and the local pressure $p(x, z, t) = p_0(z)$ where the environmental pressure $p_0(z)$ satisfies the hydrostatic equation,

$$\frac{\mathrm{d}p_0}{dz} = -\rho_0\, g, \tag{5.1}$$

and $\rho_0(z)$ is the environmental density. Accordingly, p itself satisfies the hydrostatic equation based on the environmental density.

Writing the density as the sum of its environmental and perturbation components

$$\rho(x, z, t) = \rho_0(z) + \rho'(x, t), \tag{5.2}$$

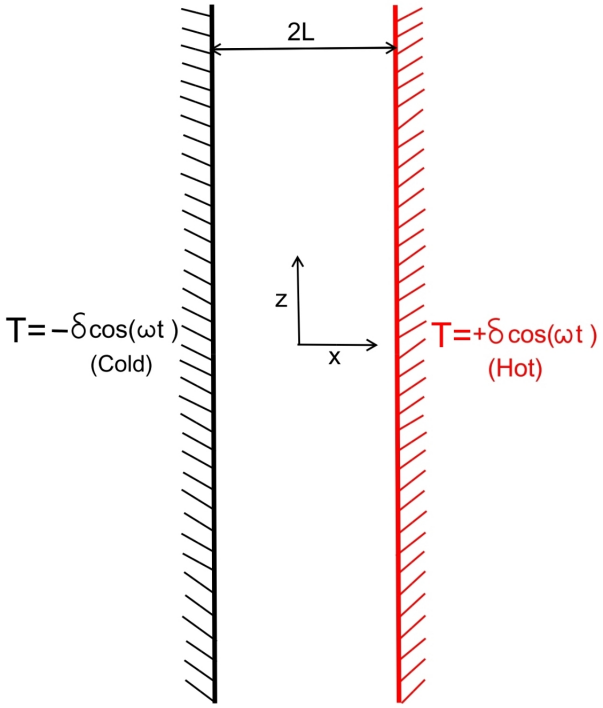

Figure 5.1: Geometric Configuration of a fluid in a channel of width $2L$ with left (cold) wall at temperature $T = -\,\delta\,\cos(\omega t)$ and right (Hot) wall at temperature $T = +\,\delta\,\cos(\omega t)$.

the Boussinesq form of the vertical equation of motion is given by

$$\frac{\partial W}{\partial t} = -g\,\frac{\rho'}{\rho_{\mathrm{r}}} + \nu\,\frac{\partial^2 W}{\partial x^2}. \tag{5.3}$$

Here, the subscript 'r' denotes a constant reference value, and ν is a constant kinematic viscosity coefficient.

We can also decompose the temperature into its environmental and perturbation components,

$$T(x, z, t) = T_0(z) + T'(x, t), \tag{5.4}$$

and use the Boussinesq (linearized) form of the equation of state

$$\rho' = -\frac{\rho_{\mathrm{r}}}{T_{\mathrm{r}}}\, T' \tag{5.5}$$

to eliminate ρ' from (5.3) in favour of T' and get

$$\frac{\partial W}{\partial t} = g\,\frac{T'}{T_{\mathrm{r}}} + \nu\,\frac{\partial^2 W}{\partial x^2}. \tag{5.6}$$

The term $g\,\dfrac{T'}{T_{\mathrm{r}}}$ represents the buoyancy force per unit mass of the fluid.

Now let us turn our attention to the thermodynamic energy equation for a perfect gas of constant thermal conductivity [59],

$$\rho c_{\mathrm{p}}\,\frac{\mathrm{D}T}{\mathrm{D}t} = \frac{\mathrm{D}p}{\mathrm{D}t} + k\,\frac{\partial^2 T}{\partial x^2}, \tag{5.7}$$

where $\dfrac{\mathrm{D}}{\mathrm{D}t} = \dfrac{\partial}{\partial t} + W\,\dfrac{\partial}{\partial z}$ is the one-dimensional total derivative operator, c_p is the specific heat at constant pressure and k is the thermal conductivity.

Note that we have neglected the viscous dissipation term which is generally smaller than the other terms in (5.7), including the pressure work term (see [2, 21, 43]). The pressure work term is itself small and is neglected in the conventional Boussinesq approximation [38]; in our case, however, the retention of the pressure work term amounts to a slight refinement of the Boussinesq model. For a detailed and lucid discussion of this issue, we refer the reader to [61].

Using (5.4) and $p(x, z, t) = p_0(z)$, where p_0 satisfies (5.1), the equation (5.7) becomes

$$\frac{\partial T'}{\partial t} = -\frac{\mathrm{d}T_0}{\mathrm{d}z}\,W - \frac{\rho_0\, g}{\rho\, c_{\mathrm{p}}}\,W + \frac{k}{\rho c_{\mathrm{p}}}\,\frac{\partial^2 T'}{\partial x^2}. \tag{5.8}$$

Approximating $\frac{\rho_0}{\rho}$ by unity and treating the thermal diffusivity $\kappa := \frac{k}{\rho\, c_p}$ as constant, we rewrite (5.8) as

$$\frac{\partial T'}{\partial t} = -\sigma\, W + \kappa\, \frac{\partial^2 T'}{\partial x^2}, \tag{5.9}$$

where $\sigma := \frac{\mathrm{d}T_0}{\mathrm{d}z} + \frac{g}{c_\mathrm{p}}$ is a constant parameter referred to as the *stratification parameter*. The term $-\sigma\, W$ in (5.9), which is a combination of the vertical temperature advection and pressure work, introduces a coupling between W and T'. When $\sigma > 0$, the environment is said to be statically stable and in this case the term $-\sigma\, W$ provides a simple negative feedback in (5.3), (5.6) and (5.9): warm fluid rises, expands and cools relative to the environment, whereas cool fluid subsides, compresses and warms relative to the environment. Thus, the classical problem becomes more realistic when we take into account the effects from thermal stratification.

5.2.2 Boundary Conditions

Recall that in this case we have an incompressible fluid contained in a vertically infinite channel of width $2L$ so that the left plate is located at $x = -L$ and the right plate is located at $x = L$ (see Figure 5.1).

The no-slip boundary condition is imposed at the plate surfaces, that is, for $t > 0$,

$$W(\pm L, t) = 0. \tag{5.10}$$

The perturbation temperature at both of the plate surfaces is a temporal oscillation with circular frequency ω and an amplitude of $-\delta$ on the left (cold) plate and $+\delta$ on the right (hot) plate, that is, for $t > 0$,

$$T'(\pm L, t) = \pm\, \delta\, \cos(\omega t). \tag{5.11}$$

5.3 Energy Balance Equations

In this section, we attach a physical meaning to each of the terms that appear in our governing equations given for $x \in (-L, L)$ and $t > 0$ by the system

$$\frac{\partial W}{\partial t} = -g\,\frac{\rho'}{\rho_r} + \nu\,\frac{\partial^2 W}{\partial x^2}, \tag{5.12}$$

$$\frac{\partial T'}{\partial t} = -\sigma\,W + \kappa\,\frac{\partial^2 T'}{\partial x^2}. \tag{5.13}$$

Multiplying (5.12) by $\rho_{\rm r} W$, integrating with respect to x from x_1 to x_2, where $-L \le x_1 < x_2 \le L$, and using integration by parts, we obtain

$$\begin{aligned}\frac{\rm d}{{\rm d}t}\int_{x_1}^{x_2}\frac{\rho_{\rm r}W^2}{2}\,{\rm d}x + \int_{x_1}^{x_2}\rho' g W\,{\rm d}x = &-\int_{x_1}^{x_2}\rho_{\rm r}\nu\left(\frac{\partial W}{\partial x}\right)^2{\rm d}x \\ &+ \rho_{\rm r}\nu\,W\frac{\partial W}{\partial x}\bigg|_{x_1}^{x_2}.\end{aligned} \tag{5.14}$$

If we use the fact that $g\,\dfrac{\rho'}{\rho_{\rm r}} = -g\,\dfrac{T'}{T_{\rm r}}$, we can rewrite (5.14) in the form

$$\begin{aligned}\frac{\rm d}{{\rm d}t}\int_{x_1}^{x_2}\frac{\rho_{\rm r}W^2}{2}\,{\rm d}x - g\,\frac{\rho_{\rm r}}{T_r}\int_{x_1}^{x_2}T'W\,{\rm d}x = &-\int_{x_1}^{x_2}\rho_{\rm r}\nu\left(\frac{\partial W}{\partial x}\right)^2{\rm d}x \\ &+ \rho_{\rm r}\nu\,W\frac{\partial W}{\partial x}\bigg|_{x_1}^{x_2}.\end{aligned} \tag{5.15}$$

Interpretation of each term in (5.14) and (5.15):

- rate of change of the kinetic energy, $\displaystyle\int_{x_1}^{x_2}\frac{\rho_{\rm r}W^2}{2}\,{\rm d}x$, of the fluid between x_1 and x_2:
$$\frac{\rm d}{{\rm d}t}\int_{x_1}^{x_2}\frac{\rho_{\rm r}W^2}{2}\,{\rm d}x\ ;$$

- rate of increase of the potential energy of the fluid in the gravity field

(heavier fluid is moved higher because of the vertical motion of the fluid):

$$\int_{x_1}^{x_2} \rho' g W \,\mathrm{d}x = -g\,\frac{\rho_\mathrm{r}}{T_r}\int_{x_1}^{x_2} T' W \,\mathrm{d}x \;;$$

- rate of viscous dissipation of the mechanical energy of the fluid:

$$-\int_{x_1}^{x_2} \rho_\mathrm{r}\nu \left(\frac{\partial W}{\partial x}\right)^2 \mathrm{d}x \;;$$

- flux of mechanical energy through the boundaries of the region $[x_1, x_2]$:

$$\rho_\mathrm{r}\nu\, W\frac{\partial W}{\partial x}\bigg|_{x_1}^{x_2} = -\left(-\,\rho_\mathrm{r}\nu\, W\frac{\partial W}{\partial x}\bigg|_{x_2}\right) + \left(-\,\rho_\mathrm{r}\nu\, W\frac{\partial W}{\partial x}\bigg|_{x_1}\right) \;.$$

Multiplying (5.13) by $c_\mathrm{p}\rho_\mathrm{r}$ and integrating with respect to x from x_1 to x_2:

$$\frac{\mathrm{d}}{\mathrm{d}t}\int_{x_1}^{x_2} c_\mathrm{p}\rho_\mathrm{r} T' \,\mathrm{d}x = -\int_{x_1}^{x_2} c_\mathrm{p}\rho_\mathrm{r}\sigma W \,\mathrm{d}x + c_\mathrm{p}\rho_\mathrm{r}\kappa\,\frac{\partial T'}{\partial x}\bigg|_{x_1}^{x_2} \;. \tag{5.16}$$

Interpretation of each term in (5.16):

- rate of change of the excess heat energy, $\displaystyle\int_{x_1}^{x_2} c_\mathrm{p}\rho_\mathrm{r} T' \,\mathrm{d}x$, over the "background" heat energy, $\displaystyle\int_{x_1}^{x_2} c_\mathrm{p}\rho_\mathrm{r} T_\infty \,\mathrm{d}x$, of the fluid between x_1 and x_2:

$$\frac{\mathrm{d}}{\mathrm{d}t}\int_{x_1}^{x_2} c_\mathrm{p}\rho_\mathrm{r} T' \,\mathrm{d}x \;;$$

- rate of change of the heat energy due to the vertical temperature advection and the vertical stratification of the fluid:

$$-\int_{x_1}^{x_2} c_\mathrm{p}\rho_\mathrm{r}\sigma W \,\mathrm{d}x \;;$$

Using that $\sigma = \dfrac{\mathrm{d}T_\infty}{\mathrm{d}z}(z) + \dfrac{g}{c_\mathrm{p}}$, we can write this as

$$-\int_{x_1}^{x_2} c_\mathrm{p}\rho_\mathrm{r}\frac{\mathrm{d}T_\infty}{\mathrm{d}z}(z)\,W\,\mathrm{d}x - \int_{x_1}^{x_2}\rho_\mathrm{r} g W\,\mathrm{d}x\ ,$$

where the first term accounts for the fact that the fluid at different heights has different environmental temperature $T_\infty(z)$, while the second one comes from the pressure work;

- flux of heat energy through the boundaries of the region $[x_1, x_2]$:

$$c_\mathrm{p}\rho_\mathrm{r}\kappa\,\frac{\partial T'}{\partial x}\bigg|_{x_1}^{x_2} = -\left(-\,c_\mathrm{p}\rho_\mathrm{r}\kappa\,\frac{\partial T'}{\partial x}\bigg|_{x_2}\right) + \left(-\,c_\mathrm{p}\rho_\mathrm{r}\kappa\,\frac{\partial T'}{\partial x}\bigg|_{x_1}\right)\ .$$

Note that $c_\mathrm{p}\rho_\mathrm{r}\kappa$ is the coefficient in front of the temperature gradient in the Fourier law of heat conduction,

$$\mathbf{j} = -c_\mathrm{p}\rho_\mathrm{r}\kappa\,\nabla T\ .$$

It is important to note that while the term $-\displaystyle\int_{x_1}^{x_2}\rho_\mathrm{r}\nu\left(\frac{\partial W}{\partial x}\right)^2\mathrm{d}x$ in (5.14) accounts for the loss of mechanical energy due to viscous dissipation, it is neglected in the balance of heat energy in (5.16). This is customary since detailed theoretical considerations and analysis of experimental data show that the viscous dissipation term is typically smaller than the other terms in (5.16), including the pressure work term (see, e.g., Ackroyed [2], Gebhart *et al* [21] and Mahajan and Gebhart [43]).

5.4 Non-dimensionalization

We non-dimensionalize the variables with the intent of clearing the governing equations of all parameters except the Prandtl number. Recall that our governing equations for $x \in (-L, L)$ and $t > 0$ are given by

$$\frac{\partial W}{\partial t} = g\,\frac{T'}{T_r} + \nu\,\frac{\partial^2 W}{\partial x^2}, \tag{5.17}$$

$$\frac{\partial T'}{\partial t} = -\sigma\,W + \kappa\,\frac{\partial^2 T'}{\partial x^2}, \tag{5.18}$$

with the boundary conditions

$$W(\pm L, t) = 0, \tag{5.19}$$

$$T'(\pm L, t) = \pm\,\delta\,\cos(\omega t). \tag{5.20}$$

In what follows, we describe how we non-dimensionalize our variables to reduce the number of degrees of freedom in the governing equations to one. We set

$$x = x^*\,\overline{x}\ , \quad t = t^*\,\overline{t}\ , \quad W = W^*\,\overline{W}\ , \quad \text{and } T' = T^*\,\overline{T}\ .$$

and plug in (5.17) and (5.18) to obtain

$$\frac{\partial \overline{W}}{\partial \overline{t}} = g\,\frac{T^* t^*}{T_{\mathrm{r}} W^*}\,\overline{T} + \nu\,\frac{t^*}{x^{*2}}\,\frac{\partial^2 \overline{W}}{\partial \overline{x}^2}, \tag{5.21}$$

$$\frac{\partial \overline{T}}{\partial \overline{t}} = -\sigma\,\frac{W^* t^*}{T^*}\,\overline{W} + \kappa\,\frac{t^*}{x^{*2}}\,\frac{\partial^2 \overline{T}}{\partial \overline{x}^2}. \tag{5.22}$$

This produces the following system for the coefficients:

$$\begin{aligned}
\frac{g}{T_\mathrm{r}}\,\frac{T^*t^*}{W^*} &= \lambda_1,\\
\nu\,\frac{t^*}{x^{*2}} &= \lambda_2,\\
\sigma\,\frac{W^*t^*}{T^*} &= \lambda_3,\\
\kappa\,\frac{t^*}{x^{*2}} &= \lambda_4.
\end{aligned}$$

Scaling the temperature by the amplitude δ, that is, setting $T^* = \delta$, we get

$$\frac{g\delta}{T_\mathrm{r}}\,\frac{t^*}{W^*} = \lambda_1, \tag{5.23}$$

$$\nu\,\frac{t^*}{x^{*2}} = \lambda_2, \tag{5.24}$$

$$\frac{\sigma}{\delta}\,W^*t^* = \lambda_3, \tag{5.25}$$

$$\kappa\,\frac{t^*}{x^{*2}} = \lambda_4. \tag{5.26}$$

Now,

- choosing $\lambda_2 = 1$, we get a time scale from (5.24): $t^* = \dfrac{x^{*2}}{\nu}$
- the choice of λ_2 fixes the constant λ_4 because of (5.26): $\lambda_4 = \dfrac{\kappa}{\nu} = \dfrac{1}{\mathsf{Pr}}$
- choosing $\lambda_1 = \lambda_3 = 1$, we get:

  the spatial scale: $x^* = \sqrt{\kappa}\left(\dfrac{T_\mathrm{r}}{\sigma g}\right)^{1/4}$

  the velocity scale: $W^* = \delta\sqrt{\dfrac{g}{\sigma T_\mathrm{r}}}$
- as a consequence, we get the time scale: $t^* = \sqrt{\dfrac{T_\mathrm{r}}{\sigma g}}$

Therefore, the scaling:

$$x = \sqrt{\nu}\left(\frac{T_{\mathrm{r}}}{\sigma g}\right)^{1/4}\overline{x}, \quad t = \sqrt{\frac{T_{\mathrm{r}}}{\sigma g}}\,\overline{t}, \quad T' = \delta\,\overline{T}, \quad W = \delta\sqrt{\frac{g}{\sigma T_{\mathrm{r}}}}\,\overline{W}$$

gives the following non-dimensionalized system of differential equations

$$\begin{aligned}\frac{\partial \overline{W}}{\partial \overline{t}} &= \overline{T} + \frac{\partial^2 \overline{W}}{\partial \overline{x}^2},\\ \frac{\partial \overline{T}}{\partial \overline{t}} &= -\overline{W} + \frac{1}{\mathsf{Pr}}\,\frac{\partial^2 \overline{T}}{\partial \overline{x}^2},\end{aligned}$$

where $\mathsf{Pr} = \dfrac{\nu}{\kappa}$ is the Prandtl number. The non-dimensional boundary conditions are

$$\begin{aligned}\overline{W}(\pm\overline{L}, \overline{t}) &= 0,\\ \overline{T}(\pm\overline{L}, \overline{t}) &= \pm\cos(\overline{\omega}\overline{t}),\end{aligned}$$

where $\overline{L} = \dfrac{1}{\sqrt{\nu}}\left(\dfrac{\sigma g}{T_r}\right)^{1/4} L$ and $\overline{\omega} = \sqrt{\dfrac{T_{\mathrm{r}}}{\sigma g}}\,\omega$.

Remark 5.1. *Park and Hyun [51] and Park [50] used the natural length scale L to non-dimensionalize the space variable and their choice corresponds to:*

$$x^* = L\ , \quad t^* = \frac{L^2}{\kappa}\ , \quad W^* = \frac{\kappa}{L}\ , \quad T^* = \sigma L\ ,$$

which gives us

$$\lambda_1 = \mathsf{Ra}\,\mathsf{Pr}\ , \quad \lambda_2 = \mathsf{Pr}\ , \quad \lambda_3 = 1\ , \quad \lambda_4 = 1\ ,$$

where $\mathsf{Ra} = \dfrac{L^4 g\sigma}{\kappa\nu T_{\mathrm{r}}}$.

Therefore, the non-dimensional system for $x \in (-1, 1)$ *and* $t > 0$ *is given by*

$$\begin{aligned} \frac{1}{\mathsf{Pr}} \frac{\partial \overline{W}}{\partial \overline{t}} &= \mathsf{Ra} \overline{T} + \frac{\partial^2 \overline{W}}{\partial \overline{x}^2}, \\ \frac{\partial \overline{T}}{\partial \overline{t}} &= -\overline{W} + \frac{\partial^2 \overline{T}}{\partial \overline{x}^2}, \end{aligned}$$

with the non-dimensional boundary conditions

$$\begin{aligned} \overline{W}(\pm 1, \overline{t}) &= 0, \\ \overline{T}(\pm 1, \overline{t}) &= \pm\, \delta\, \cos(\overline{\omega} \overline{t}). \end{aligned}$$

Chapter 6

Temperature and Velocity Profiles

Consider the non-dimensionalized system of differential equations (from Section 5.4) given for $x \in (-L, L)$ and $t > 0$ by

$$\frac{\partial W}{\partial t} = T + \frac{\partial^2 W}{\partial x^2}, \tag{6.1}$$

$$\frac{\partial T}{\partial t} = -W + \frac{1}{\mathsf{Pr}} \frac{\partial^2 T}{\partial x^2}, \tag{6.2}$$

with the boundary conditions for $t > 0$

$$W(\pm L, t) = 0, \tag{6.3}$$

$$T(\pm L, t) = \pm \cos(\omega t), \tag{6.4}$$

where we dropped the bars to simplify the notation.

Eliminating one of the variables in terms of the other has the advantage of decoupling the system by getting a higher order partial differential equation (PDE) but this poses challenges in terms of deriving the required number of boundary conditions needed to solve the resulting PDEs.

6.1 Transforming the PDEs into ODEs

Using (6.1), we can express T as a function of W and substitute it in (6.2) to get a fourth order PDE for the vertical velocity W given by

$$\frac{\partial^4 W}{\partial x^4} - (1 + \mathsf{Pr}) \frac{\partial^3 W}{\partial t \, \partial x^2} + \mathsf{Pr} \frac{\partial^2 W}{\partial t^2} + \mathsf{Pr} \, W = 0. \tag{6.5}$$

Alternatively, if we choose to express W from (6.2) as a function of T and substitute it in (6.1), we get a fourth order PDE for the temperature T given by

$$\frac{\partial^4 T}{\partial x^4} - (1 + \mathsf{Pr}) \frac{\partial^3 T}{\partial t \, \partial x^2} + \mathsf{Pr} \frac{\partial^2 T}{\partial t^2} + \mathsf{Pr} \, T = 0. \tag{6.6}$$

Note that the structure of the system (6.1)-(6.2) is special in the sense that both the temperature T and the vertical velocity W satisfy the same partial differential equation

$$\frac{\partial^4 \Phi}{\partial x^4} - (1 + \mathsf{Pr}) \frac{\partial^3 \Phi}{\partial t \, \partial x^2} + \mathsf{Pr} \frac{\partial^2 \Phi}{\partial t^2} + \mathsf{Pr} \, \Phi = 0,$$

but corresponding to different boundary conditions and so it does not matter which equation we choose to solve first.

6.1.1 Deriving the ODEs

At this stage, we will focus our attention on equation (6.6) and use (6.2) to find the vertical velocity. We seek solutions of (6.5) and (6.6) in the form of simple harmonic oscillations and so we write:

$$W(x,t) = \Re \left\{ \mathrm{e}^{\mathrm{i}\omega t} \left[A(x) + \mathrm{i} \, B(x) \right] \right\}, \tag{6.7}$$

$$T(x,t) = \Re \left\{ \mathrm{e}^{\mathrm{i}\omega t} \left[C(x) + \mathrm{i} \, D(x) \right] \right\}, \tag{6.8}$$

where A, B, C, $D : (-L, L) \to \mathbb{R}$ are real-valued functions.

Substituting the expression for $T(x,t)$ from (6.36) into (6.6) yields two coupled ordinary differential equations in C and D (fourth-order system) given by

$$C^{(4)} + \mathsf{Pr}\,(1-\omega^2)\,C = -\omega\,(1+\mathsf{Pr})\,D'', \tag{6.9}$$

$$D^{(4)} + \mathsf{Pr}\,(1-\omega^2)\,D = \omega\,(1+\mathsf{Pr})\,C'', \tag{6.10}$$

where $' = \dfrac{d}{dx}$.

Differentiating (6.10) twice (with respect to x), multiplying by $\omega\,(1+\mathsf{Pr})$ and substituting $\omega\,(1+\mathsf{Pr})\,D''$ and $\omega\,(1+\mathsf{Pr})\,D^{(6)}$ obtained from (6.9), we get

$$C^{(8)} + \left[2\,\mathsf{Pr} + \omega^2\,(1+\mathsf{Pr}^2)\right] C^{(4)} + \mathsf{Pr}^2\,(1-\omega^2)^2\,C = 0. \tag{6.11}$$

Similarly, one can easily see that D satisfies the same ordinary differential equation (ODE), that is,

$$D^{(8)} + \left[2\,\mathsf{Pr} + \omega^2\,(1+\mathsf{Pr}^2)\right] D^{(4)} + \mathsf{Pr}^2\,(1-\omega^2)^2\,D = 0. \tag{6.12}$$

6.1.2 Deriving the Boundary Conditions for the ODEs

The boundary conditions for the real-valued functions C and D follow immediately from the expression of $T(x,t)$ (6.36) and the boundary condition (6.4), so that

$$C(\pm L) = \pm 1 \quad \text{and} \quad D(\pm L) = 0. \tag{6.13}$$

To obtain the boundary conditions for the higher derivatives of C and D,

1. Using (6.2), we have

$$\frac{1}{\mathsf{Pr}}\,\frac{\partial^2 T}{\partial x^2}(x,t) - \frac{\partial T}{\partial t}(x,t) = W(x,t).$$

Setting $x = \pm L$ and using the boundary condition $W(\pm L, t) = 0$, we get

$$\frac{1}{\mathsf{Pr}}\,\frac{\partial^2 T}{\partial x^2}(\pm L,t) = \frac{\partial T}{\partial t}(\pm L,t).$$

Using the expression for T from (6.36), we can rewrite this as a condition on $C''(\pm L)$ and $D''(\pm L)$ in terms of $C(\pm L)$ and $D(\pm L)$ given by

$$\left[-\omega\, C(\pm L) + \frac{1}{\mathsf{Pr}}\, D''(\pm L)\right]\sin(\omega t) + \left[-\omega\, D(\pm L) - \frac{1}{\mathsf{Pr}}\, C''(\pm L)\right]\cos(\omega t) = 0,$$

or, using (6.13),

$$\left[\mp\omega + \frac{1}{\mathsf{Pr}}\, D''(\pm L)\right]\sin(\omega t)\; - \frac{1}{\mathsf{Pr}}\, C''(\pm L)\cos(\omega t) = 0\ .$$

This gives the boundary conditions

$$C''(\pm L) = 0 \quad \text{and} \quad D''(\pm L) = \pm\,\omega \mathsf{Pr}. \tag{6.14}$$

2. Setting $x = \pm L$ in (6.9) and using the boundary conditions (6.13) and (6.14), we get

$$\begin{aligned} C^{(4)}(\pm L) &= -\mathsf{Pr}\,(1-\omega^2)\,C(\pm L) - \omega\,(1+\mathsf{Pr})\,D''(\pm L) \\ &= \mp\,\mathsf{Pr}\,(1-\omega^2) \mp\, \omega^2(1+\mathsf{Pr}) \end{aligned}$$

and

$$C^{(4)}(\pm L) = \mp\,\mathsf{Pr}\,(1+\omega^2\,\mathsf{Pr}). \tag{6.15}$$

Similarly, setting $x = \pm L$ in (6.10) and using the boundary conditions (6.13) and (6.14), we get

$$D^{(4)}(\pm L) = -\mathsf{Pr}\,(1-\omega^2)\,D(\pm L) + \omega\,(1+\mathsf{Pr})\,C''(\pm L) = 0. \qquad (6.16)$$

3. Now, taking the second x-derivatives of (6.9) and (6.10) and using the boundary conditions (6.13)-(6.16), we get

$$C^{(6)}(\pm L) = -\mathsf{Pr}\,(1-\omega^2)\,C''(\pm L) - \omega\,(1+\mathsf{Pr})\;D^{(4)}(\pm L) = 0,$$

and respectively,

$$\begin{aligned} D^{(6)}(\pm L) &= -\mathsf{Pr}\,(1-\omega^2)\,D''(\pm L) + \omega\,(1+\mathsf{Pr})\,C^{(4)}(\pm L) \\ &= \mp\,\omega\,\mathsf{Pr}^2\,(1-\omega^2) \mp\,\omega\,\mathsf{Pr}\,(1+\mathsf{Pr})\,(1+\omega^2\,\mathsf{Pr}) \\ &= \mp\,\omega\,\mathsf{Pr}\left[1+\mathsf{Pr}\;\left(2+\omega^2\mathsf{Pr}\right)\right]. \end{aligned}$$

Therefore, C and D satisfy the boundary value problem

$$\Psi^{(8)} + \left[2\,\mathsf{Pr} + \omega^2\,(1+\mathsf{Pr}^2)\right]\Psi^{(4)} + \mathsf{Pr}^2\,(1-\omega^2)^2\,\Psi = 0,$$

with the boundary conditions

$$\begin{aligned} &C(\pm L) = \pm 1, && D(\pm L) = 0, \\ &C''(\pm L) = 0, && D''(\pm L) = \pm\,\omega\,\mathsf{Pr}, \\ &C^{(4)}(\pm L) = \mp\,\mathsf{Pr}\;\left(1+\omega^2\mathsf{Pr}\right) && D^{(4)}(\pm L) = 0, \\ &C^{(6)}(\pm L) = 0, && D^{(6)}(\pm L) = \mp\,\omega\,\mathsf{Pr}\left[1+\mathsf{Pr}\;\left(2+\omega^2\,\mathsf{Pr}\right)\right]. \end{aligned} \qquad (6.17)$$

6.2 Solving the BVPs

Now let's find the general solution of the ODE (6.11) for C (and respectively (6.12) for D). Recall that C and D satisfy the same ODE whose characteristic equation

$$\left(\lambda^4\right)^2 + \left[2\,\mathsf{Pr} + \omega^2\,\left(1 + \mathsf{Pr}^2\right)\right]\,\lambda^4 + \mathsf{Pr}^2\,(1-\omega^2)^2 = 0 \tag{6.18}$$

is a quadratic equation in λ^4 and so

$$\begin{aligned}\lambda^4 &= \frac{1}{2}\left[-2\mathsf{Pr} - \omega^2(1+\mathsf{Pr}^2) \pm \sqrt{\left[2\mathsf{Pr} + \omega^2\,(1+\mathsf{Pr}^2)\right]^2 - 4\mathsf{Pr}^2(1-\omega^2)^2}\right] \\ &= -\mathsf{Pr} - \frac{\omega^2}{2}(1+\mathsf{Pr}^2) \pm \omega\,(1+\mathsf{Pr})\sqrt{\mathsf{Pr} + \frac{\omega^2}{4}\,(1-\mathsf{Pr}^2)^2}.\end{aligned} \tag{6.19}$$

One can easily observe that:

- the discriminant of (6.18) is always strictly positive, hence both values of λ^4 are real, and
- using the fact that both $\left[2\mathsf{Pr} + \omega^2(1+\mathsf{Pr}^2)\right]$ and the discriminant are both strictly positive, we get that

  $$\left[2\,\mathsf{Pr} + \omega^2\,(1+\mathsf{Pr}^2)\right]^2 > \left[2\,\mathsf{Pr} + \omega^2\,(1+\mathsf{Pr}^2)\right]^2 - 4\,\mathsf{Pr}^2\left(1-\omega^2\right)^2 > 0$$

  and

  $$-\,\mathsf{Pr} - \frac{\omega^2}{2}\,(1+\mathsf{Pr}^2) + \omega\,(1+\mathsf{Pr})\sqrt{\mathsf{Pr} + \frac{\omega^2}{4}\,(1-\mathsf{Pr}^2)^2} < 0,$$

  so that both values of λ^4 are negative.

Let us set

$$\Delta := \mathsf{Pr} + \frac{\omega^2}{4}(1-\mathsf{Pr})^2, \tag{6.20}$$

and

$$\gamma_{1,2} := \left\{ \frac{1}{4}\left[\mathsf{Pr} + \frac{\omega^2}{2}(1+\mathsf{Pr}^2) \mp \omega(1+\mathsf{Pr})\sqrt{\Delta} \right] \right\}^{1/4}, \tag{6.21}$$

so that γ_1 and γ_2 are real with $0 < \gamma_1 < \gamma_2$, and

$$\lambda^4 = -4\,\gamma_{1,2}^4.$$

Introducing the notations

$$\lambda_1 := (1+\mathrm{i})\,\gamma_1 \quad \text{and} \quad \lambda_2 := (1+\mathrm{i})\,\gamma_2, \tag{6.22}$$

we can write all eight roots of the characteristic equation (6.18) as

$$\lambda_1,\ -\lambda_1,\ \bar{\lambda_1},\ -\bar{\lambda_1},\ \lambda_2,\ -\lambda_2,\ \bar{\lambda_2},\ -\bar{\lambda_2}.$$

The general solution for C has, therefore, the form

$$\begin{aligned} C(x) = \ & k_1 \mathrm{e}^{\lambda_1 x} + k_2 \mathrm{e}^{-\lambda_1 x} + k_3 \mathrm{e}^{\bar{\lambda}_1 x} + k_4 \mathrm{e}^{-\bar{\lambda}_1 x} \\ & + k_5 \mathrm{e}^{\lambda_2 x} + k_6 \mathrm{e}^{-\lambda_2 x} + k_7 \mathrm{e}^{\bar{\lambda}_2 x} + k_8 \mathrm{e}^{-\bar{\lambda}_2 x}, \end{aligned} \tag{6.23}$$

where k_l $(l = 1, \ldots, 8)$ are arbitrary complex-valued constants.

Since the function C is real-valued, then C must equal its complex conjugate, that is,

$$C(x) = \overline{C(x)}\ ,$$

which implies that the constants k_j satisfy

$$k_3 = \bar{k}_1,\ k_4 = \bar{k}_2,\ k_7 = \bar{k}_5,\ k_8 = \bar{k}_6,$$

and the general solution (6.23) becomes (c.c.="complex conjugate")

$$C(x) = k_1 \mathrm{e}^{\lambda_1 x} + k_2 \mathrm{e}^{-\lambda_1 x} + k_5 \mathrm{e}^{\lambda_2 x} + k_6 \mathrm{e}^{-\lambda_2 x} + \text{c.c.} \ . \tag{6.24}$$

For the case of zero "dephasing" we expect the function C to be also odd,

$$C(-x) = -C(x) \ ,$$

which yields the relations

$$k_2 = -k_1, \ k_6 = -k_5 \ ,$$

and hence restricts the general solution (6.24) even further to give

$$\begin{aligned} C(x) &= k_1 \left(\mathrm{e}^{\lambda_1 x} - \mathrm{e}^{-\lambda_1 x}\right) + k_5 \left(\mathrm{e}^{\lambda_2 x} - \mathrm{e}^{-\lambda_2 x}\right) + \text{c.c.} \\ &= 2\,\Re\left\{k_1 \left(\mathrm{e}^{\lambda_1 x} - \mathrm{e}^{-\lambda_1 x}\right) + k_5 \left(\mathrm{e}^{\lambda_2 x} - \mathrm{e}^{-\lambda_2 x}\right)\right\}, \end{aligned} \tag{6.25}$$

where $\lambda_{1,2}$ are given by (6.21) and (6.22).

Moreover, using expression(6.25) for C and notations (6.21) and (6.22), we can record the 2^{nd}, 4^{th} and 6^{th}-order derivatives of C as follows:

$$\begin{aligned} C(x) =& \quad 2\,\Re\left\{k_1 \left(\mathrm{e}^{\lambda_1 x} - \mathrm{e}^{-\lambda_1 x}\right) + k_5 \left(\mathrm{e}^{\lambda_2 x} - \mathrm{e}^{-\lambda_2 x}\right)\right\}, \\ C''(x) =& \quad 2\gamma_1^2\,\Re\left\{\mathrm{i}k_1 \left(\mathrm{e}^{\lambda_1 x} - \mathrm{e}^{-\lambda_1 x}\right)\right\} + 2\gamma_2^2\,\Re\left\{\mathrm{i}k_5 \left(\mathrm{e}^{\lambda_2 x} - \mathrm{e}^{-\lambda_2 x}\right)\right\}, \\ C^{(4)}(x) =& -4\gamma_1^4\,\Re\left\{k_1 \left(\mathrm{e}^{\lambda_1 x} - \mathrm{e}^{-\lambda_1 x}\right)\right\} - 4\gamma_2^4\,\Re\left\{k_5 \left(\mathrm{e}^{\lambda_2 x} - \mathrm{e}^{-\lambda_2 x}\right)\right\}, \\ C^{(6)}(x) =& -8\gamma_1^6\,\Re\left\{\mathrm{i}k_1 \left(\mathrm{e}^{\lambda_1 x} - \mathrm{e}^{-\lambda_1 x}\right)\right\} - 8\gamma_2^6\,\Re\left\{\mathrm{i}k_5 \left(\mathrm{e}^{\lambda_2 x} - \mathrm{e}^{-\lambda_2 x}\right)\right\}. \end{aligned} \tag{6.26}$$

Let

$$k_\zeta = k_{\zeta \mathrm{r}} + \mathrm{i}k_{\zeta \mathrm{i}} \ , \qquad \zeta = 1, 5,$$

where the subscripts r and i stand for "real part" and "imaginary part," respectively.

Observe that

$$\begin{aligned}\Re\left\{k_1\left(\mathrm{e}^{\lambda_1 x}-\mathrm{e}^{-\lambda_1 x}\right)\right\} &= 2\Re\left\{k_1\sinh(\lambda_1 x)\right\}\\ &= 2\Re\left\{\left[k_{1\mathrm{r}}\sinh(\gamma_1 x)\cos(\gamma_1 x)-k_{1\mathrm{i}}\cosh(\gamma_1 x)\sin(\gamma_1 x)\right]\right.\\ &\quad\left.+\,\mathrm{i}\left[k_{1\mathrm{r}}\cosh(\gamma_1 x)\sin(\gamma_1 x)+k_{1\mathrm{i}}\sinh(\gamma_1 x)\cos(\gamma_1 x)\right]\right\}\\ &= 2\left[k_{1\mathrm{r}}\sinh(\gamma_1 x)\cos(\gamma_1 x)-k_{1\mathrm{i}}\cosh(\gamma_1 x)\sin(\gamma_1 x)\right],\end{aligned}$$

where we used $\sinh(\lambda_1 x)=\sinh(\gamma_1 x)\cos(\gamma_1 x)+\mathrm{i}\cosh(\gamma_1 x)\sin(\gamma_1 x)$. Therefore, the expression (6.25) for C can be rewritten as

$$\begin{aligned}C(x) = 4\big[&k_{1\mathrm{r}}\sinh(\gamma_1 x)\cos(\gamma_1 x)-k_{1\mathrm{i}}\cosh(\gamma_1 x)\sin(\gamma_1 x)\\ &+k_{5\mathrm{r}}\sinh(\gamma_2 x)\cos(\gamma_2 x)-k_{5\mathrm{i}}\cosh(\gamma_2 x)\sin(\gamma_2 x)\big].\end{aligned}\tag{6.27}$$

Moreover, introducing the notations

$$\begin{aligned}&\alpha_\zeta(x) := \cosh(\gamma_\zeta x)\sin(\gamma_\zeta x),\\ &\beta_\zeta(x) := \sinh(\gamma_\zeta x)\cos(\gamma_\zeta x),\end{aligned}\qquad \zeta=1,2,\tag{6.28}$$

we can simplify the expression (6.25) for C and write

$$C(x) = 4\big[k_{1\mathrm{r}}\,\beta_1(x)-k_{1\mathrm{i}}\,\alpha_1(x)+k_{5\mathrm{r}}\,\beta_2(x)-k_{5\mathrm{i}}\,\alpha_2(x)\big].\tag{6.29}$$

It remains now to impose the boundary conditions on C. Since we have already implemented the fact that C is an odd function, we need to impose only the boundary conditions at $x=L$.

At this point, it is convenient to introduce the temporary notations

$$\begin{aligned} a_\zeta &:= \alpha_\zeta(L) = \cosh(\gamma_\zeta L)\sin(\gamma_\zeta L), \\ & \qquad\qquad\qquad\qquad \zeta = 1, 2, \\ b_\zeta &:= \beta_\zeta(L) = \sinh(\gamma_\zeta L)\cos(\gamma_\zeta L), \end{aligned} \tag{6.30}$$

and write the system from which we solve for the coefficients k_{lr} and k_{li}, $l = 1, 5$, as

$$\begin{aligned} \tfrac{1}{4}\, C(L) = &\quad a_1\, k_{1\mathrm{r}} - \quad a_1\, k_{1\mathrm{i}} + \quad b_2\, k_{5\mathrm{r}} - \quad a_2\, k_{5\mathrm{i}} = \tfrac{1}{4}, \\ -\tfrac{1}{8}\, C''(L) &= \gamma_1^2 a_1\, k_{1\mathrm{r}} + \gamma_1^2 b_1\, k_{1\mathrm{i}} + \gamma_2^2 a_2\, k_{5\mathrm{r}} + \gamma_2^2 b_2\, k_{5\mathrm{i}} = 0, \\ -\tfrac{1}{16}\, C^{(4)}(L) &= \gamma_1^4 b_1\, k_{1\mathrm{r}} - \gamma_1^4 a_1 k_{1\mathrm{i}} + \gamma_2^4 b_2\, k_{5\mathrm{r}} - \gamma_2^4 a_2\, k_{5\mathrm{i}} = \tfrac{1}{16}\mathsf{Pr}(1 + \omega^2 \mathsf{Pr}), \\ \tfrac{1}{32}\, C^{(6)}(L) &= \gamma_1^6 a_1\, k_{1\mathrm{r}} + \gamma_1^6 b_1\, k_{1\mathrm{i}} + \gamma_2^6 a_2\, k_{5\mathrm{r}} + \gamma_2^6 b_2\, k_{5\mathrm{i}} = 0. \end{aligned}$$

The solution of this system is

$$\begin{bmatrix} k_{1\mathrm{r}} & k_{1\mathrm{i}} \\ k_{5\mathrm{r}} & k_{5\mathrm{i}} \end{bmatrix} = \frac{1}{16(\gamma_1^4 - \gamma_2^4)} \begin{bmatrix} \dfrac{\mathsf{Pr} - 4\,\gamma_2^4 + \omega^2\mathsf{Pr}^2}{a_1^2 + b_1^2}\, b_1 & -\dfrac{\mathsf{Pr} - 4\,\gamma_2^4 + \omega^2\mathsf{Pr}^2}{a_1^2 + b_1^2}\, a_1 \\ -\dfrac{\mathsf{Pr} - 4\,\gamma_1^4 + \omega^2\mathsf{Pr}^2}{a_2^2 + b_1^2}\, b_2 & \dfrac{\mathsf{Pr} - 4\,\gamma_1^4 + \omega^2\mathsf{Pr}^2}{a_2^2 + b_2^2}\, a_2 \end{bmatrix}.$$

Going back to the original notations:

1. Using the expressions (6.21) and (6.22), we have

$$\frac{1}{16(\gamma_1^4 - \gamma_2^4)} = -\frac{1}{8\,\omega\,(1 + \mathsf{Pr})\,\sqrt{\Delta}}\,.$$

2. Similarly,

$$\begin{aligned} \mathsf{Pr} - 4\,\gamma_1^4 + \omega^2\mathsf{Pr}^2 &= \quad \omega\sqrt{\Delta}\,(1 + \mathsf{Pr})\left[1 - \frac{w}{2\sqrt{\Delta}}\,(1 - \mathsf{Pr})\right], \\ \mathsf{Pr} - 4\,\gamma_2^4 + \omega^2\mathsf{Pr}^2 &= -\omega\sqrt{\Delta}\,(1 + \mathsf{Pr})\left[1 + \frac{w}{2\sqrt{\Delta}}\,(1 - \mathsf{Pr})\right]. \end{aligned}$$

3. Moreover, using the definitions of a_ζ and b_ζ for $\zeta = 1, 2$, we can write

$$\begin{aligned} a_\zeta^2 + b_\zeta^2 &= \cosh^2(\gamma_\zeta L)\, \sin^2(\gamma_\zeta L) + \sinh^2(\gamma_\zeta L)\, \cos^2(\gamma_\zeta L) \\ &= \left[1 + \sinh^2(\gamma_\zeta L)\right] \sin^2(\gamma_\zeta L) + \sinh^2(\gamma_\zeta L)\, \cos^2(\gamma_\zeta L) \\ &= \sinh^2(\gamma_\zeta L) + \sin^2(\gamma_\zeta L). \end{aligned}$$

Incidentally, $a_\zeta^2 + b_\zeta^2$ can be factorized as

$$a_\zeta^2 + b_\zeta^2 = \cosh^2(\gamma_\zeta L) - \cos^2(\gamma_\zeta L).$$

Using these expressions, we can write

$$\begin{aligned} k_{1\mathrm{r}} &= -\frac{1}{8\,\omega\,(1+\mathsf{Pr})\,\sqrt{\Delta}}\, \frac{-\omega\sqrt{\Delta}\,(1+\mathsf{Pr})\left[1 + \frac{w}{2\sqrt{\Delta}}\,(1-\mathsf{Pr})\right]}{a_1^2 + b_1^2}\, b_1 \\ &= \frac{1}{8}\left[1 + \frac{\omega}{2\sqrt{\Delta}}\,(1-\mathsf{Pr})\right]\, \frac{\sinh(\gamma_1 L)\cos(\gamma_1 L)}{\sinh^2(\gamma_1 L) + \sin^2(\gamma_1 L)}. \end{aligned}$$

Similarly, the other coefficients of C can be written as

$$\begin{aligned} k_{1\mathrm{i}} &= -\frac{1}{8}\left[1 + \frac{\omega}{2\sqrt{\Delta}}\,(1-\mathsf{Pr})\right]\, \frac{\cosh(\gamma_1 L)\sin(\gamma_1 L)}{\sinh^2(\gamma_1 L) + \sin^2(\gamma_1 L)}, \\ k_{5\mathrm{r}} &= \frac{1}{8}\left[1 - \frac{\omega}{2\sqrt{\Delta}}\,(1-\mathsf{Pr})\right]\, \frac{\sinh(\gamma_2 L)\cos(\gamma_2 L)}{\sinh^2(\gamma_2 L) + \sin^2(\gamma_2 L)}, \\ k_{5\mathrm{i}} &= -\frac{1}{8}\left[1 - \frac{\omega}{2\sqrt{\Delta}}\,(1-\mathsf{Pr})\right]\, \frac{\cosh(\gamma_2 L)\sin(\gamma_2 L)}{\sinh^2(\gamma_2 L) + \sin^2(\gamma_2 L)}. \end{aligned}$$

Substituting these expression in (6.29), we obtain

$$\begin{aligned} C(x) = \; & \frac{1}{2}\left[1 + \frac{\omega}{2\sqrt{\Delta}}\,(1-\mathsf{Pr})\right]\, \frac{\alpha_1(L)\,\alpha_1(x) + \beta_1(L)\,\beta_1(x)}{\sinh^2(\gamma_1 L) + \sin^2(\gamma_1 L)} \\ & + \frac{1}{2}\left[1 - \frac{\omega}{2\sqrt{\Delta}}\,(1-\mathsf{Pr})\right]\, \frac{\alpha_2(L)\,\alpha_2(x) + \beta_2(L)\,\beta_2(x)}{\sinh^2(\gamma_2 L) + \sin^2(\gamma_2 L)}. \end{aligned} \tag{6.31}$$

The function D satisfies the same differential equation as C (namely, (6.12)), so its general solution has the form

$$\begin{aligned} D(x) = \; & k_1' \mathrm{e}^{\lambda_1 x} + k_2' \mathrm{e}^{-\lambda_1 x} + k_3' \mathrm{e}^{\bar{\lambda}_1 x} + k_4' \mathrm{e}^{-\bar{\lambda}_1 x} \\ & + k_5' \mathrm{e}^{\lambda_2 x} + k_6' \mathrm{e}^{-\lambda_2 x} + k_7' \mathrm{e}^{\bar{\lambda}_2 x} + k_8' \mathrm{e}^{-\bar{\lambda}_2 x}, \end{aligned} \tag{6.32}$$

where k_l' $(l = 1, \ldots, 8)$ are arbitrary complex-valued constants.

Similarly to C, the function D must be real and odd, so the general solution for D becomes

$$\begin{aligned} D(x) &= k_1' \left(\mathrm{e}^{\lambda_1 x} - \mathrm{e}^{-\lambda_1 x} \right) + k_5' \left(\mathrm{e}^{\lambda_2 x} - \mathrm{e}^{-\lambda_2 x} \right) + \text{c.c.} \\ &= 2\,\Re \left\{ k_1' \left(\mathrm{e}^{\lambda_1 x} - \mathrm{e}^{-\lambda_1 x} \right) + k_5' \left(\mathrm{e}^{\lambda_2 x} - \mathrm{e}^{-\lambda_2 x} \right) \right\}, \end{aligned} \tag{6.33}$$

and by writing

$$k_l' = k_{l\mathrm{r}}' + \mathrm{i} k_{l\mathrm{i}}\,, \quad l = 1, 5$$

and using the notations (6.28), we can write

$$D(x) = 4\big[k_{1\mathrm{r}}'\, \beta_1(x) - k_{1\mathrm{i}}'\, \alpha_1(x) + k_{5\mathrm{r}}'\, \beta_2(x) - k_{5\mathrm{i}}'\, \alpha_2(x) \big]. \tag{6.34}$$

Imposing the boundary conditions and using notations (6.30), we have

$$\begin{aligned} b_1\, k_{1\mathrm{r}}' - \quad a_1\, k_{1\mathrm{i}}' + \quad b_2\, k_{5\mathrm{r}}' - \quad a_2\, k_{5\mathrm{i}}' &= 0, \\ \gamma_1^2 a_1\, k_{1\mathrm{r}}' + \gamma_1^2 b_1\, k_{1\mathrm{i}}' + \gamma_2^2 a_2\, k_{5\mathrm{r}}' + \gamma_2^2 b_2\, k_{5\mathrm{i}}' &= -\frac{1}{8}\,\omega\,\mathsf{Pr}, \\ \gamma_1^4 b_1\, k_{1\mathrm{r}}' - \gamma_1^4 a_1\, k_{1\mathrm{i}}' + \gamma_2^4 b_2\, k_{5\mathrm{r}}' - \gamma_2^4 a_2\, k_{5\mathrm{i}}' &= 0, \\ \gamma_1^6 a_1\, k_{1\mathrm{r}}' + \gamma_1^6 \beta_1\, k_{1\mathrm{i}}' + \gamma_2^6 a_2\, k_{5\mathrm{r}}' + \gamma_2^6 b_2\, k_{5\mathrm{i}}' &= -\frac{1}{32}\,\omega \mathsf{Pr} \left[1 + \mathsf{Pr} \left(2 + \omega^2 \mathsf{Pr} \right) \right]. \end{aligned}$$

The solution of this system is

$$\begin{bmatrix} k'_{1\mathrm{r}} & k'_{1\mathrm{i}} \\ k'_{5\mathrm{r}} & k'_{5\mathrm{i}} \end{bmatrix} = \frac{\omega \mathsf{Pr}}{32(\gamma_1^4 - \gamma_2^4)} \begin{bmatrix} -\dfrac{1 - 4\,\gamma_2^4 + \mathfrak{p}}{\gamma_1^2\,(a_1^2 + b_1^2)}\,a_1 & -\dfrac{1 - 4\,\gamma_2^4 + \mathfrak{p}}{\gamma_1^2\,(a_1^2 + b_1^2)}\,b_1 \\ \dfrac{1 - 4\,\gamma_1^4 + \mathfrak{p}}{\gamma_2^2\,(a_2^2 + b_2^2)}\,a_2 & \dfrac{1 - 4\,\gamma_1^4 + \mathfrak{p}}{\gamma_2^2\,(a_2^2 + b_2^2)}\,b_2 \end{bmatrix},$$

where $\mathfrak{p} = 2\mathsf{Pr} + \omega^2 \mathsf{Pr}^2$.

Going back to the original notations and similarly as in the case of solving for the coefficients for C, we can write the coefficients of D as

$$\begin{aligned}
k'_{1\mathrm{r}} &= -\frac{\mathsf{Pr}}{16\gamma_1^2}\left[\omega + \frac{\omega^2}{2\sqrt{\Delta}}\,(1 - \mathsf{Pr}) - \frac{1}{\sqrt{\Delta}}\right] \frac{\cosh(\gamma_1 L)\sin(\gamma_1 L)}{\sinh^2(\gamma_1 L) + \sin^2(\gamma_1 L)}, \\
k'_{1\mathrm{i}} &= -\frac{\mathsf{Pr}}{16\gamma_1^2}\left[\omega + \frac{\omega^2}{2\sqrt{\Delta}}\,(1 - \mathsf{Pr}) - \frac{1}{\sqrt{\Delta}}\right] \frac{\sinh(\gamma_1 L)\cos(\gamma_1 L)}{\sinh^2(\gamma_1 L) + \sin^2(\gamma_1 L)}, \\
k'_{5\mathrm{r}} &= -\frac{\mathsf{Pr}}{16\gamma_2^2}\left[\omega - \frac{\omega^2}{2\sqrt{\Delta}}\,(1 - \mathsf{Pr}) + \frac{1}{\sqrt{\Delta}}\right] \frac{\cosh(\gamma_2 L)\sin(\gamma_2 L)}{\sinh^2(\gamma_2 L) + \sin^2(\gamma_2 L)}, \\
k'_{5\mathrm{i}} &= -\frac{\mathsf{Pr}}{16\gamma_2^2}\left[\omega - \frac{\omega^2}{2\sqrt{\Delta}}\,(1 - \mathsf{Pr}) + \frac{1}{\sqrt{\Delta}}\right] \frac{\sinh(\gamma_2 L)\cos(\gamma_2 L)}{\sinh^2(\gamma_2 L) + \sin^2(\gamma_2 L)}.
\end{aligned}$$

Substituting these expressions in (6.34), we get

$$\begin{aligned}
D(x) = &-\frac{\mathsf{Pr}}{4\gamma_1^2}\left[\omega + \frac{\omega^2}{2\sqrt{\Delta}}\,(1 - \mathsf{Pr}) - \frac{1}{\sqrt{\Delta}}\right] \frac{\alpha_1(L)\,\beta_1(x) - \beta_1(L)\,\alpha_1(x)}{\sinh^2(\gamma_1 L) + \sin^2(\gamma_1 L)} \\
&- \frac{\mathsf{Pr}}{4\gamma_2^2}\left[\omega - \frac{\omega^2}{2\sqrt{\Delta}}\,(1 - \mathsf{Pr}) + \frac{1}{\sqrt{\Delta}}\right] \frac{\alpha_2(L)\beta_2(x) - \beta_2(L)\alpha_2(x)}{\sinh^2(\gamma_2 L) + \sin^2(\gamma_2 L)}.
\end{aligned} \tag{6.35}$$

We can therefore write an expression for the temperature $T(x,t)$ as

$$T(x,t) = C(x)\,\cos(\omega t) - D(x)\,\sin(\omega t), \tag{6.36}$$

where

$$C(x) = \frac{1}{2}\Big[\, Q_1\,\frac{\alpha_1(L)\,\alpha_1(x) + \beta_1(L)\,\beta_1(x)}{\sinh^2(\gamma_1 L) + \sin^2(\gamma_1 L)} + Q_2\,\frac{\alpha_2(L)\,\alpha_2(x) + \beta_2(L)\,\beta_2(x)}{\sinh^2(\gamma_2 L) + \sin^2(\gamma_2 L)}\Big],$$

$$\begin{aligned} D(x) = &-\frac{\mathsf{Pr}}{4\gamma_1^2}\left[\omega Q_1 - \frac{1}{\sqrt{\Delta}}\right]\,\frac{\alpha_1(L)\,\beta_1(x) - \beta_1(L)\,\alpha_1(x)}{\sinh^2(\gamma_1 L) + \sin^2(\gamma_1 L)} \\ &-\frac{\mathsf{Pr}}{4\gamma_2^2}\left[\omega Q_2 + \frac{1}{\sqrt{\Delta}}\right]\,\frac{\alpha_2(L)\,\beta_2(x) - \beta_2(L)\,\alpha_2(x)}{\sinh^2(\gamma_2 L) + \sin^2(\gamma_2 L)}, \end{aligned}$$

and

$$Q_1 = 1 + \frac{\omega}{2\sqrt{\Delta}}\,(1 - \mathsf{Pr})\,, \tag{6.37}$$

$$Q_2 = 1 - \frac{\omega}{2\sqrt{\Delta}}\,(1 - \mathsf{Pr})\,, \tag{6.38}$$

In order to solve for the vertical velocity $W(x,t)$, we'll use equation (6.2) and the expression for $T(x,t)$ from (6.36) to write

$$\begin{aligned} W(x,t) &= \frac{1}{\mathsf{Pr}}\frac{\partial^2 T}{\partial x^2}(x,t) - \frac{\partial T}{\partial t}(x,t) \\ &= \Big[\frac{1}{\mathsf{Pr}}\,C''(x) - \omega\,D(x)\Big]\cos(\omega t) - \Big[\frac{1}{\mathsf{Pr}}\,D''(x) + \omega\,C(x)\Big]\sin(\omega t) \\ &= A(x)\,\cos(\omega t) - B(x)\,\sin(\omega t). \end{aligned}$$

Now, using the expressions of $C(x)$ and $D(x)$ from (6.36), we have an expression for the vertical velocity $W(x,t)$ given by

$$W(x,t) = A(x)\,\cos(\omega t) - B(x)\,\sin(\omega t), \tag{6.39}$$

where

$$A(x) = -\frac{1}{\mathsf{Pr}}\frac{1}{4\gamma_1^2}\left[Q_1\left(\omega^2\mathsf{Pr}^2 - 4\gamma_1^4\right) - \frac{\omega\mathsf{Pr}^2}{\sqrt{\Delta}}\right]\frac{\alpha_1(L)\,\beta_1(x) - \beta_1(L)\,\alpha_1(x)}{\sinh^2(\gamma_1 L) + \sin^2(\gamma_1 L)}$$
$$-\frac{1}{\mathsf{Pr}}\frac{1}{4\gamma_2^2}\left[Q_2\left(\omega^2\mathsf{Pr}^2 - 4\gamma_2^2\right) + \frac{\omega\mathsf{Pr}^2}{\sqrt{\Delta}}\right]\frac{\alpha_2(L)\,\beta_2(x) - \beta_2(L)\,\alpha_2(x)}{\sinh^2(\gamma_2 L) + \sin^2(\gamma_2 L)},$$

and

$$B(x) = -\frac{1}{2\sqrt{\Delta}}\left[\frac{\alpha_1(L)\,\alpha_1(x) + \beta_1(L)\,\beta_1(x)}{\sinh^2(\gamma_1 L) + \sin^2(\gamma_1 L)} - \frac{\alpha_2(L)\,\alpha_2(x) + \beta_2(L)\,\beta_2(x)}{\sinh^2(\gamma_2 L) + \sin^2(\gamma_2 L)}\right],$$

with Q_1 and Q_2 are given by (6.37) and (6.38), respectively.

Chapter 7

Physical Interpretation

7.1 Temperature Distribution

Using the expression for $T(x,t)$ from (6.36), we can study the effect of the frequency of the external temperature oscillations ω and the width of the channel L on the temperature distribution of the fluid at some fixed instant t. In Figure 7.1, we consider a fluid of Prandtl number $\mathsf{Pr} = 0.07$ in two different regimes. When $L = 3$ (Figure 7.1(top)), the temperature $T(x,0)$ is almost linear for $\omega = 4$ and we see less uniform temperature distribution when we take a larger frequency $\omega = 40$. Although there is less time for heat to propagate across the cavity, the fact that the walls are relatively close to each other allows us to see some temperature variations throughout the fluid.

The effect of the width of the channel becomes more prominent when we consider sidewalls that are relatively far from each other (Figure 7.1(bottom)). In this case, even for smaller frequency $\omega = 4$, temperature variations are confined to layers close to the right (hot) wall. This can be seen evidently for the large frequency $\omega = 40$ when only a thin layer adjacent to the wall

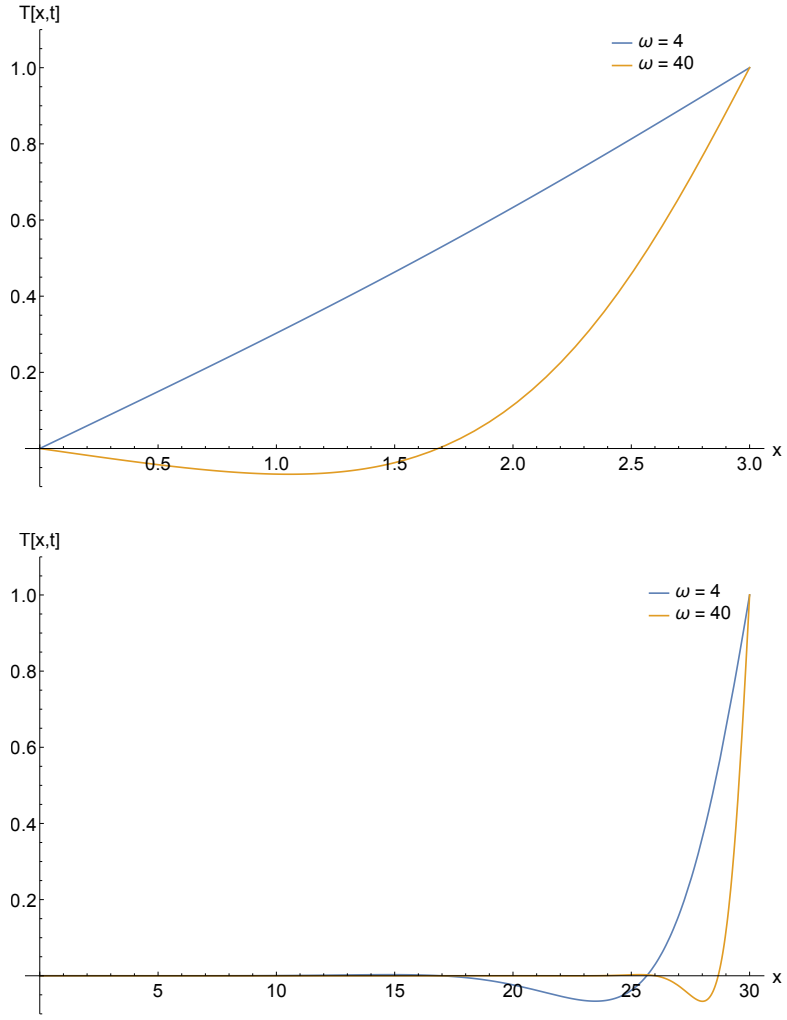

Figure 7.1: $T(x,0)$ vs. x for $\mathsf{Pr} = 0.07$, $\omega = 0.4$ and 40, and $L = 3$ (top) and 30 (bottom).

gets heated. Thus, the impact of the oscillating temperature wall condition is confined to a narrow region adjacent to the hot wall.

7.2 Vertical Motion of the Fluid

In Figure 7.2, we study the vertical motion of the fluid by plotting the analytical solution $W(x,t)$ from equation (6.39) as a function of x at a fixed instant t.

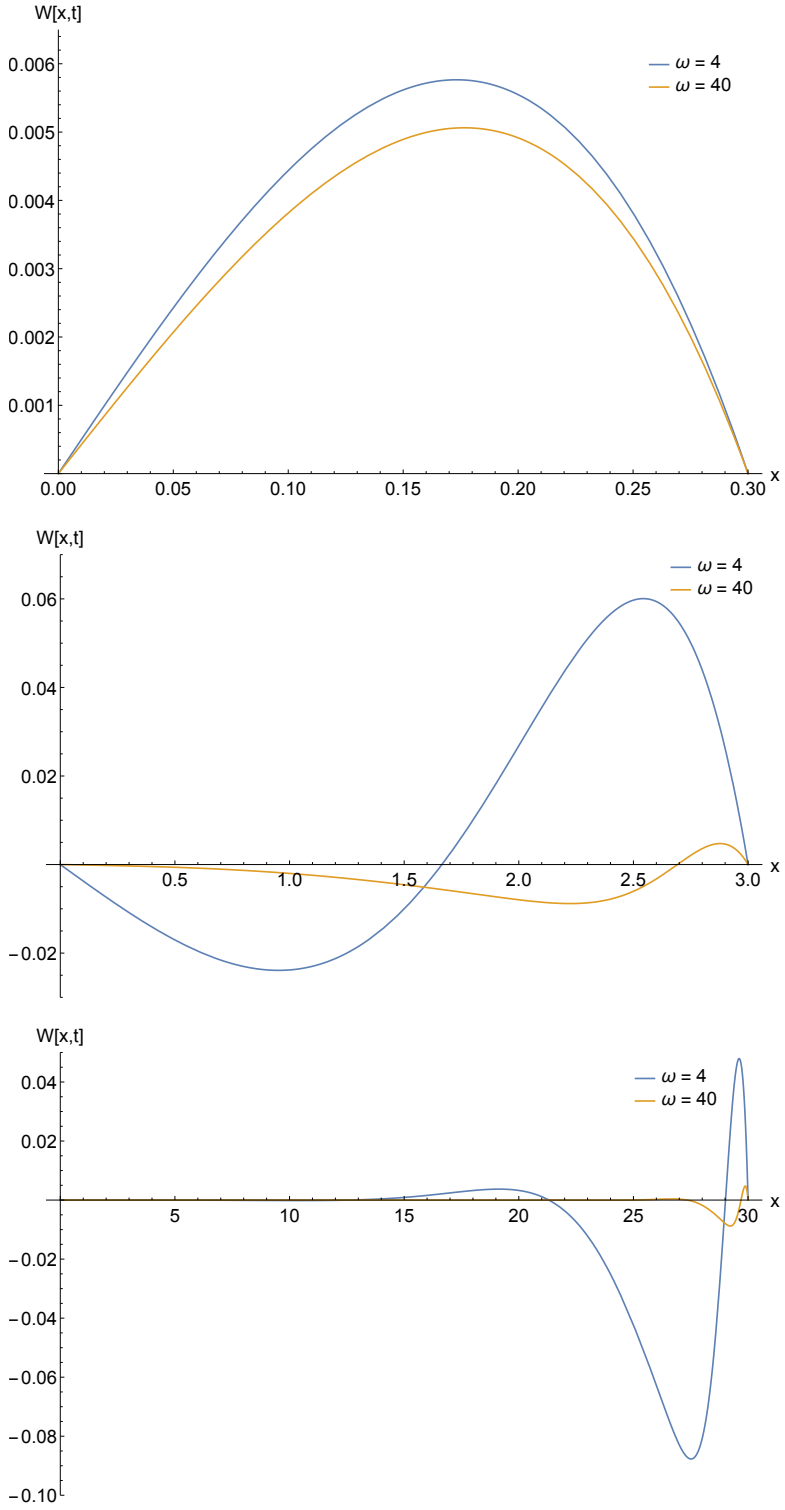

Figure 7.2: $W(x,0)$ vs. x for $\mathsf{Pr} = 0.07$, $\omega = 0.4$ and 40, and $L = 0.3$ (top), 3 (middle), and 30 (bottom).

For Prandtl number $\mathsf{Pr} = 0.07$, we see that the response of the fluid flow is in line with the heat transfer. For smaller widths of the channel (see Figure 7.2(top) for $L = 0.3$), changing the frequency ω from 4 to 40 does not produce drastic changes in the vertical velocity of the fluid. The amplitude of $W(x, 0)$ is slightly smaller for $\omega = 40$ but the overall behaviour of the interior velocity is the same.

The impact of the wall temperature oscillations becomes more interesting for wider cavities. We get moderate effects on the fluid motion for lower frequency (see Figure 7.2(middle) and (bottom) for $\omega = 4$) and negligibly small effects for higher frequency (see Figure 7.2(middle) and (bottom) for $\omega = 40$). It is also worth pointing out that similar to the case of heat transfer, changes in the interior velocity are confined to a thin boundary layer adjacent to the right (hot) wall.

7.3 Energy Balance

Using equations (6.1) and (6.2), we can write the non-dimensionalized equations of mechanical and heat energy balance for any $x_1, x_2 \in (-L, L)$ as

$$\underbrace{\frac{\mathrm{d}}{\mathrm{d}t}\int_{x_1}^{x_2} \frac{W^2}{2}\,\mathrm{d}x}_{\text{r.o.c. of kin. energy}} - \underbrace{\int_{x_1}^{x_2} TW\,\mathrm{d}x}_{\text{r.o.c. of pot. energy}} = -\underbrace{\int_{x_1}^{x_2} \left(\frac{\partial W}{\partial x}\right)^2 \mathrm{d}x}_{\text{rate of viscous dissipation}} + \underbrace{W\frac{\partial W}{\partial x}\bigg|_{x_1}^{x_2}}_{\text{flux through boundaries}}, \tag{7.1}$$

$$\underbrace{\frac{\mathrm{d}}{\mathrm{d}t}\int_{x_1}^{x_2} T\,\mathrm{d}x}_{\text{r.o.c. of heat energy}} + \underbrace{\int_{x_1}^{x_2} W\,\mathrm{d}x}_{\text{r.o.c. of energy by advection}} = \underbrace{\frac{1}{\mathsf{Pr}}\,\frac{\partial T}{\partial x}\bigg|_{x_1}^{x_2}}_{\text{heat flux through boundaries}}. \tag{7.2}$$

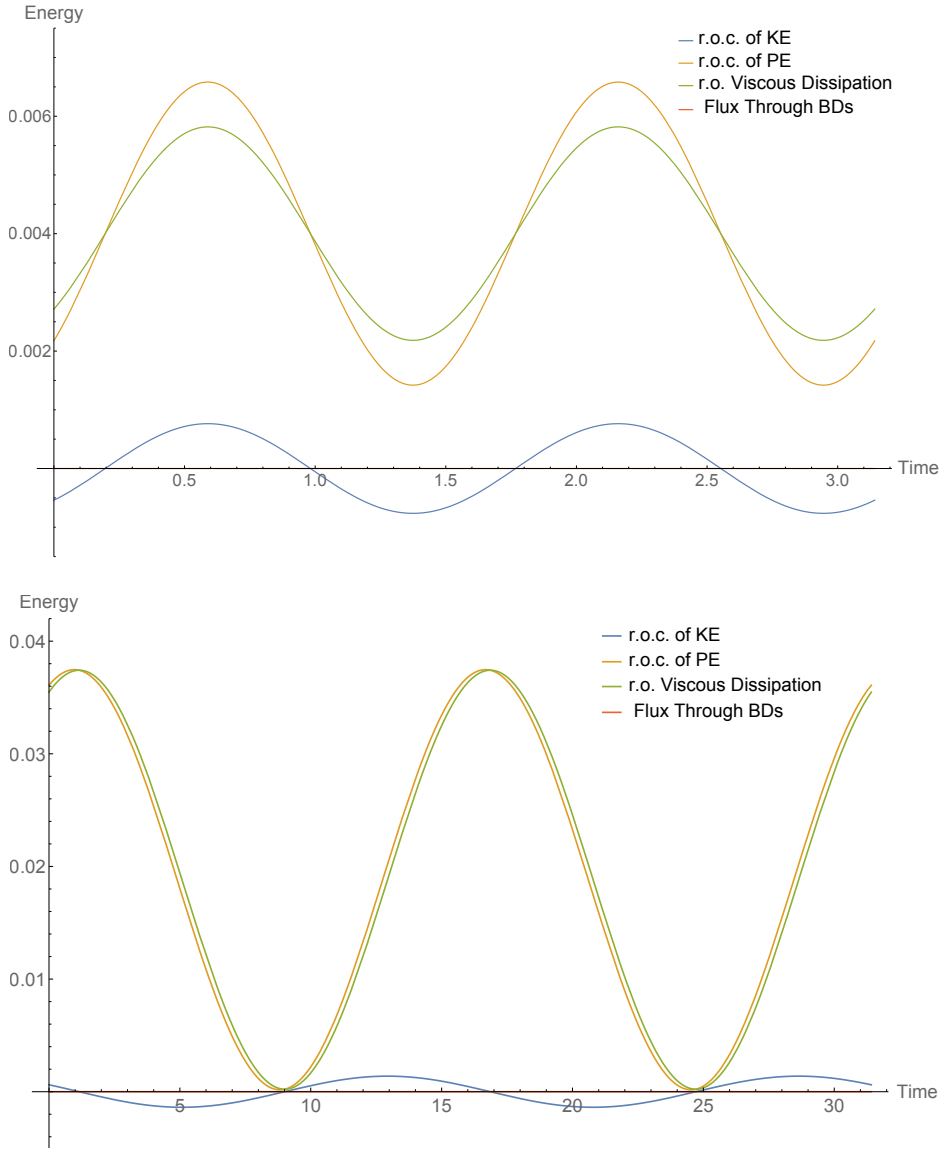

Figure 7.3: Plot of the individual energy quantities from mechanical equation for $\mathsf{Pr} = 7$, $L = 20$, and $\omega = 2$ (top) and 0.2 (bottom).

To study the effect of the frequency of the temperature oscillations on the energy of the fluid, we plot the temporal behaviour of the individual energy quantities from equations (7.1) and (7.2) for $\mathsf{Pr} = 7$, $L = 20$ and for two different ω-values. In this case, we focus our attention to the right half of the cavity, that is, from $x_1 = 0$ to $x_2 = L$.

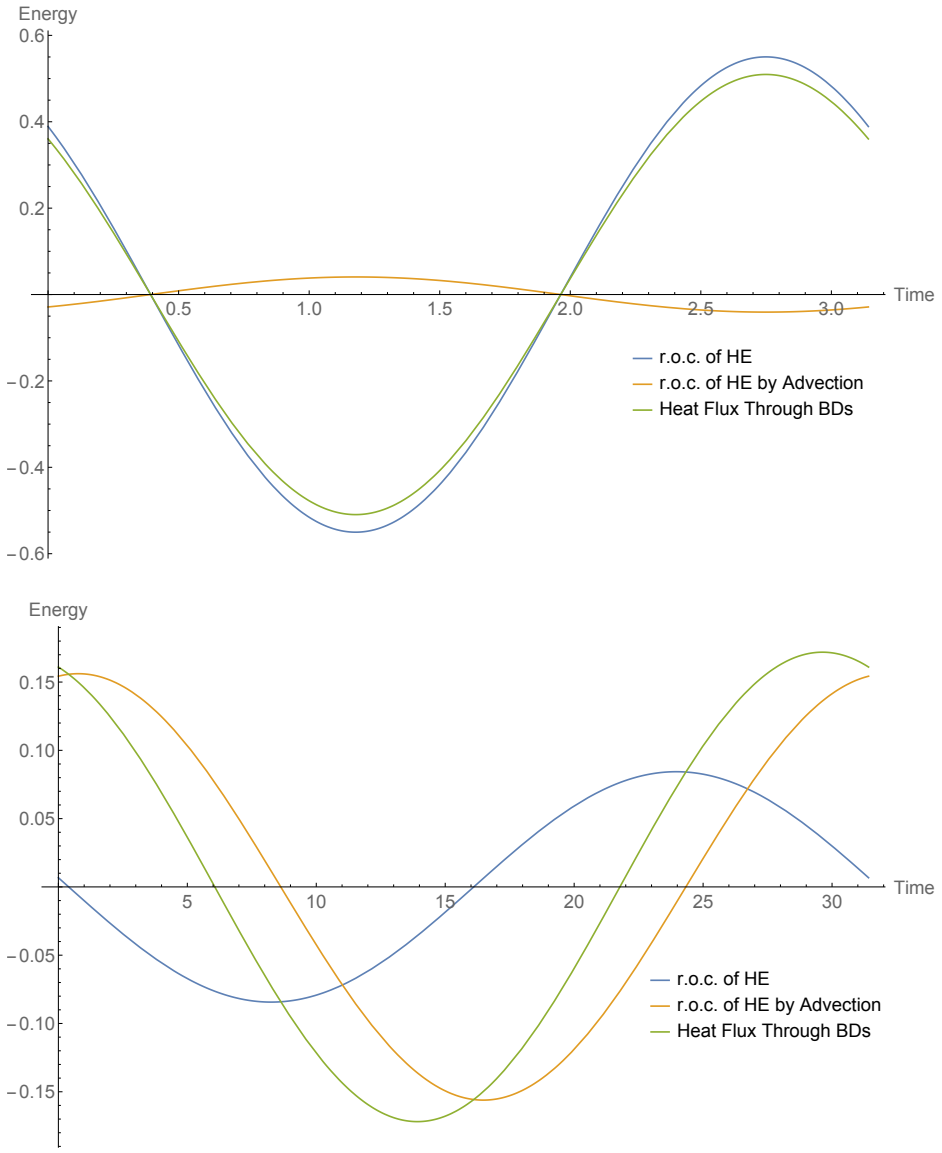

Figure 7.4: Plot of the individual energy quantities from heat equation for $\mathsf{Pr} = 7$, $L = 20$, and $\omega = 2$ (top) and 0.2 (bottom).

In Figure 7.3, we observe two main differences in the energy quantities for higher and lower frequencies (compare Figure 7.3(top) for $\omega = 2$ and (bottom) for $\omega = 0.2$). The rate at which the amount of energy is stored in the fluid decreases as we increase the frequency of oscillations. This is depicted by maxima of rate of change of energy quantities for $\omega = 2$ occurring at lower

values than those considered for $\omega = 0.2$. There also appears to be a shift in the peaks of the rate of change of the kinetic and potential energies for $\omega = 2$ whereas this shift is almost negligible when $\omega = 0.2$. Since we are technically comparing the rate of change of two different types of energies (kinetic vs. potential), it is not quite obvious why such a shift would be more prominent for higher frequencies. Also, notice that for both high and low frequencies, the flux through the boundaries is negligible.

Another interesting behaviour is detected when we focus our attention to studying the rate of change of heat energy, rate of change of heat energy by advection and the heat flux through the boundaries from equation (7.2). We notice that for $\omega = 2$ the rate at which heat energy is retained in the fluid due to advection is lower than that for $\omega = 0.2$ (compare the amplitude of the orange curves of Figure 7.4(top) for $\omega = 2$ and (bottom) for $\omega = 0.2$). This is because smaller frequencies ω allow more time for heat to propagate across the cavity by the movement of bulk fluid causing more advection to occur. On the contrary, the heat flux through the boundaries and the rate of change of heat energy are considerably bigger for the higher frequency $\omega = 2$ because heat transfer in this case will be restricted to the fluid layer adjacent to the wall as seen in Figure 7.1.

7.4 Resonance Effects

7.4.1 Space-Time Average of Kinetic Energy

By symmetry of the vertical velocity $W(x,t)$, it is enough to study the kinetic energy for the right-half of the cavity from $x = 0$ to $x = L$. To remove

the space and time dependence, we take the space-time average of the kinetic energy, denoted by $\langle\, \mathsf{KE} \,\rangle_{x,t}$

$$\begin{aligned} \langle\, \mathsf{KE} \,\rangle_{x,t} &:= \frac{\omega}{2\pi L} \int_0^L \int_0^{2\pi/\omega} W^2(x,t)\ \mathrm{d}t\ \mathrm{d}x \\ &= \frac{1}{4L} \int_0^L \left[A^2(x) + B^2(x)\right] \mathrm{d}x\ , \end{aligned} \tag{7.3}$$

which is then a function of Prandtl number Pr, the frequency of the oscillations ω and the width L of the channel.

The effects of Pr and L on the behaviour of $\langle\, \mathsf{KE} \,\rangle_{x,t}$ are shown in Figure 7.5 for three different Pr-values: $\mathsf{Pr} = 7$, 0.7 and 0.007. Although the results display quantitative differences, the overall qualitative features remain unchanged. For each of these Pr-values, there is some width of the channel L for which $\langle\, \mathsf{KE} \,\rangle_{x,t}$ monotonically decreases as a function of ω (for example, see, Figure 7.5(top) for $L = 2$). This is reasonable because for higher frequencies ω the movement of the fluid is confined to the boundary layer adjacent to the hot wall thus causing the average kinetic energy of the fluid across the channel to decrease.

For each fixed Prandtl number, Figure 7.5 shows the existence of resonance identified by the occurrence of peak values of the space-time average of the kinetic energy around $\omega = 1$. These peaks become sharper and more pronounced as L increases (for example, see, Figure 7.5(middle) for $L = 40$). When L is relatively small (see Figure 7.5(top) for $L = 4$), resonance is less clear-cut. Also, there does not appear to be another peak forming for $\omega > 1$ as $\langle\, \mathsf{KE} \,\rangle_{x,t}$ becomes vanishingly small at high frequencies. Such resonance effects have been studied numerically for more complicated problems such as fluids in square cavities (see for example, [39]).

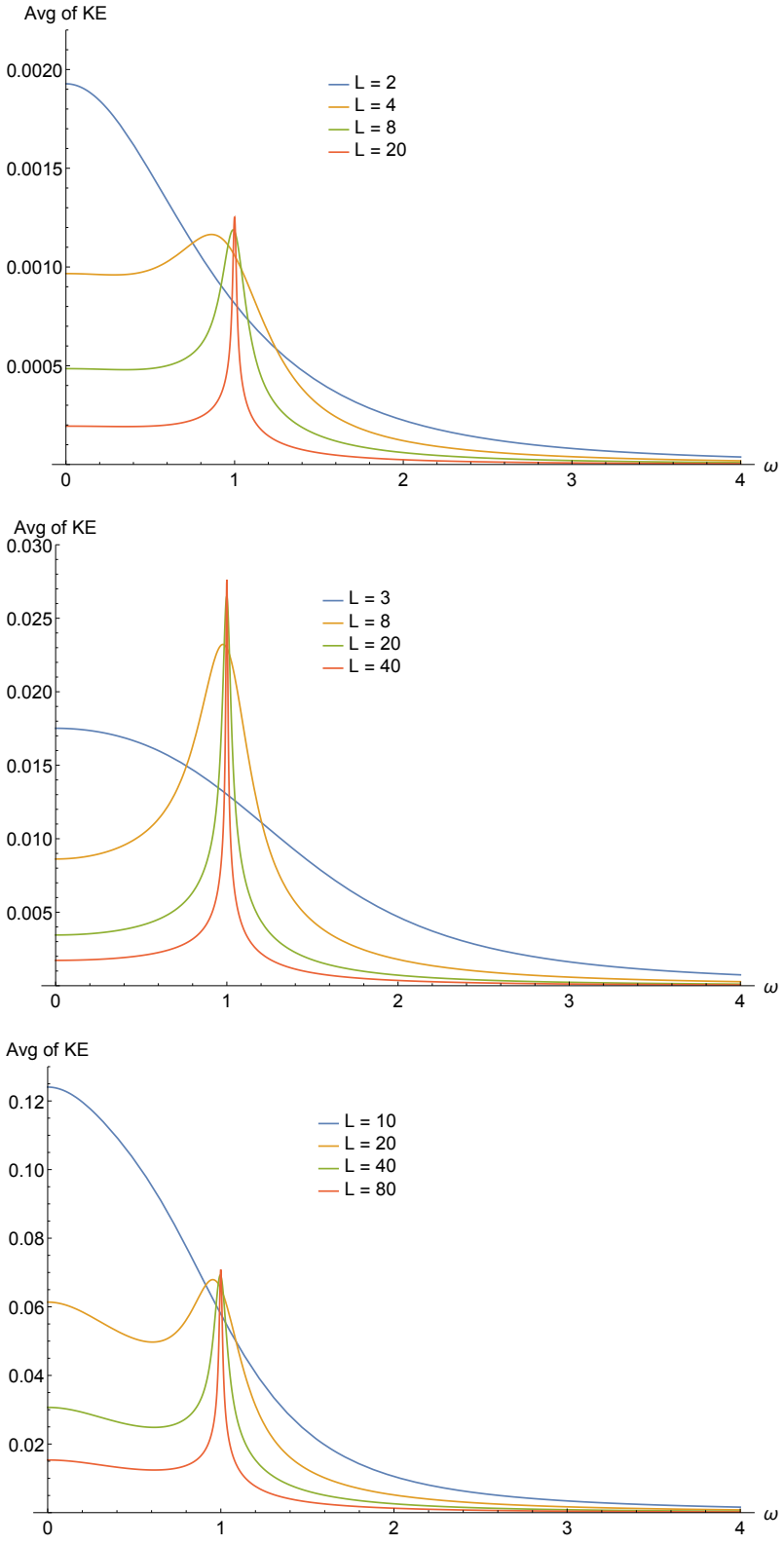

Figure 7.5: Space-time average of the kinetic energy vs. ω for different width L of the channel and $\mathsf{Pr} = 7$ (top), 0.7 (middle), and 0.07 (bottom).

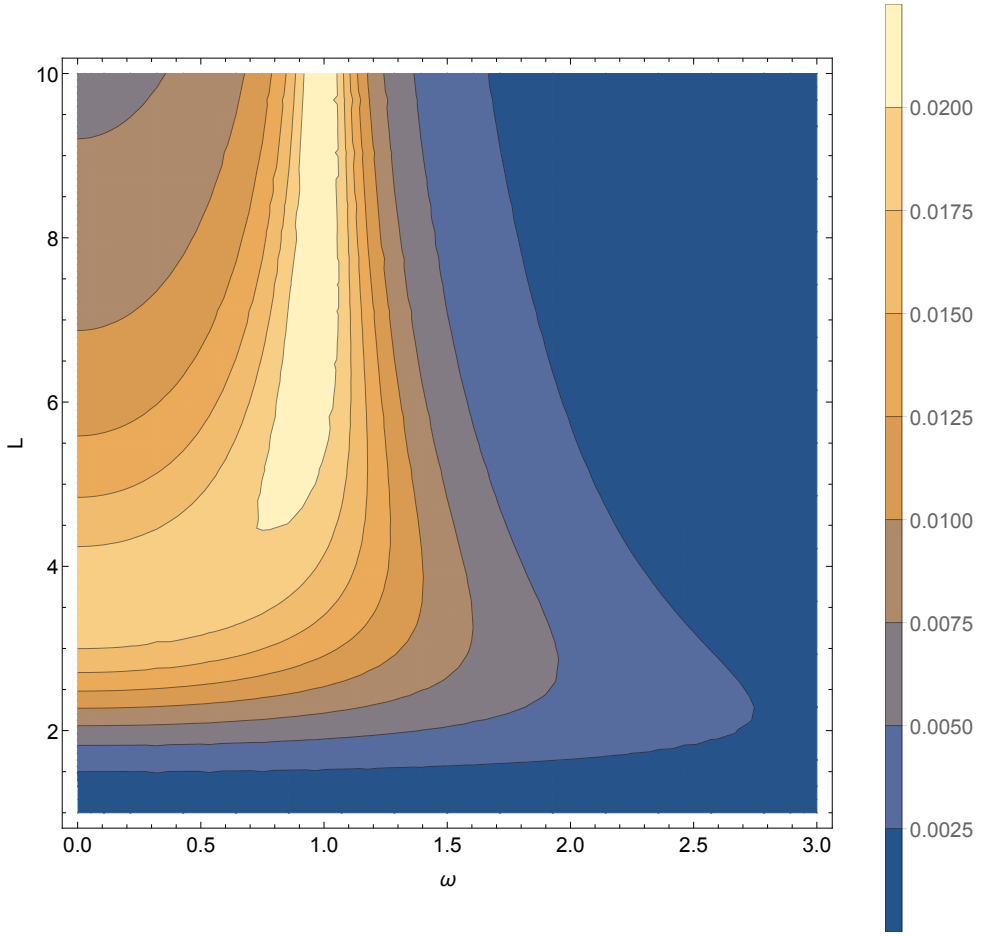

Figure 7.6: Contour plot of the space-time average of the kinetic energy in the (ω, L) plane for $\mathsf{Pr} = 0.7$.

Plots in Figure 7.5 give a strong indication that in order to see resonance in fluids with smaller Prandtl numbers, we need to consider channels with bigger widths L. Moreover, if we look at Figure 7.5(bottom) for $\mathsf{Pr} = 0.007$ and $L = 20$, we notice that the curve of $\langle \mathsf{KE} \rangle_{x,t}$ dips before forming the peak around $\omega = 1$. Another interesting observation is that the values of $\langle \mathsf{KE} \rangle_{x,t}$ are comparatively bigger for smaller Prandtl numbers. To validate these observation, we draw the contour plots of $\langle \mathsf{KE} \rangle_{x,t}$ in the (ω, L)-plane for both $\mathsf{Pr} = 0.7$ and $\mathsf{Pr} = 0.07$ in which darker colours indicate smaller

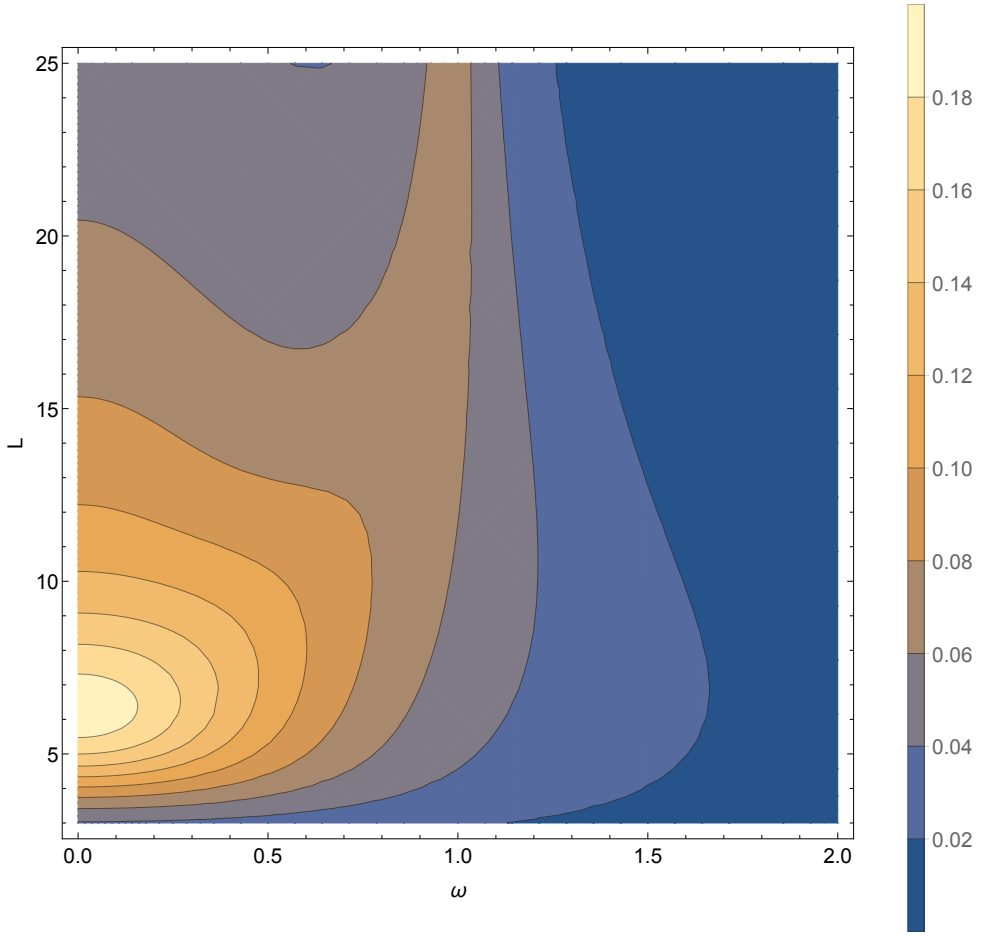

Figure 7.7: Contour plot of the space-time average of the kinetic energy in the (ω, L) plane for $\mathsf{Pr} = 0.07$.

values of $\langle \mathsf{KE} \rangle_{x,t}$. In fact, for $\mathsf{Pr} = 0.7$, it seems that there is some critical width L between 4 and 5 beyond which $\langle \mathsf{KE} \rangle_{x,t}$ forms a peak around $\omega = 1$ (see Figure 7.6). Similarly, looking at the contour plot from Figure 7.7 for $\mathsf{Pr} = 0.07$, we notice that for $L > 16$ (roughly) $\langle \mathsf{KE} \rangle_{x,t}$ dips first before forming a peak indicating the existence of resonance.

7.4.2 Heat Transfer Across the Cavity

In general, we expect the heat flux at the right (hot) wall to be the same as the one computed at the vertical mid-plane between the sidewalls. The explicit solution for the temperature $T(x,t)$ from equation (6.36) enables us to write down the time-average of the heat flux over one period

$$\langle\, \phi_q \,\rangle_t := \frac{\omega}{2\pi} \int_0^{2\pi/\omega} |\partial_x T(x,t)|\, \mathrm{d}x = \frac{2}{\pi} \sqrt{C'(x)^2 + D'(x)^2}$$

and hence study the ratio of time-average of the heat flux at the center ($x = 0$) to the time-average of the heat flux at the hot wall ($x = L$), that is,

$$\mathcal{R}_{\phi_q} = \frac{\langle\, \phi_q \,\rangle_t|_{x=0}}{\langle\, \phi_q \,\rangle_t|_{x=L}}.$$

In Figure 7.8, we plot $\mathcal{R}_{\phi_q}$ as a function of the frequency ω for $\mathsf{Pr} = 0.7$ and $L = 2$. In the steady state case corresponding to $\omega = 0$, we notice that this ratio is around 0.65 indicating that only about 65 % of the heat at the hot boundary is conducted to the center of the cavity. This is because heating of fluid causes it to move vertically and, in the case of thermal stratification, some of the heat energy will be transformed into potential energy due to lifting some of the heavier (cooler) fluid from below. Moreover, as the frequency ω increases, $\mathcal{R}_{\phi_q}$ monotonically decreases indicating the inverse proportionality between ω and the amount of heat transferred across the cavity.

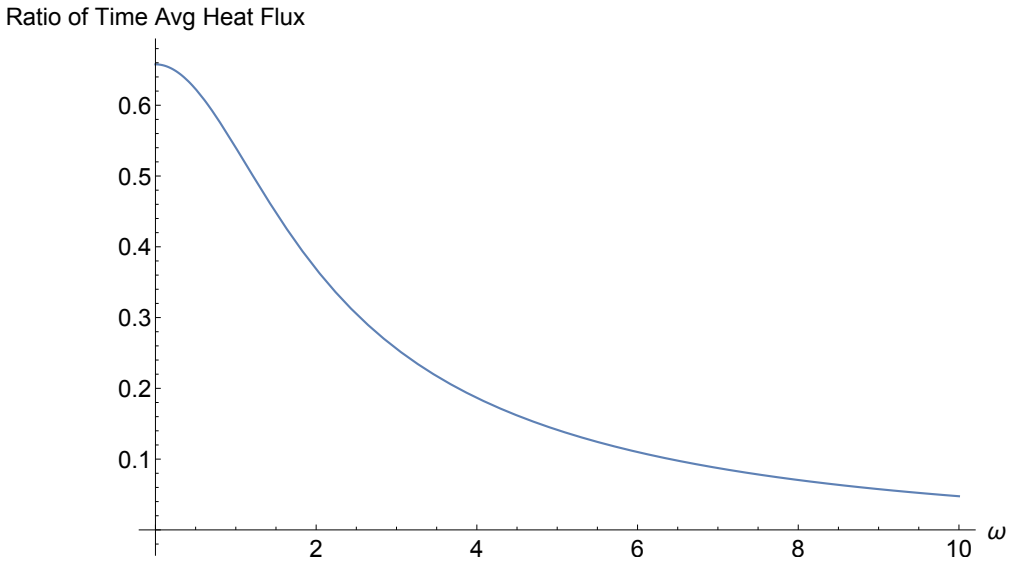

Figure 7.8: (Center-to-right wall) ratio of the time average of the heat flux vs. ω for $\mathsf{Pr} = 0.7$ and $L = 2$.

To study the effect of the width L on the heat transferred across the cavity, for each fixed Pr number we plot $\mathcal{R}_{\phi_q}$ vs. ω for different values of L as shown in Figure 7.9. As we increase the width of the channel L, we notice that $\mathcal{R}_{\phi_q}$ starts to lose its monotonic behaviour by gradually forming a peak (see Figure 7.9(top) for $L = 4$) indicating the start of the resonance phenomenon. One interesting feature to point out is that these peaks seem to shrink in amplitude but tend to be more concentrated around $\omega = 1$ for larger values of L. This concentration around $\omega = 1$ is in accordance with what we observed when we studied the resonance effects in the case of space-time average of the kinetic energy.

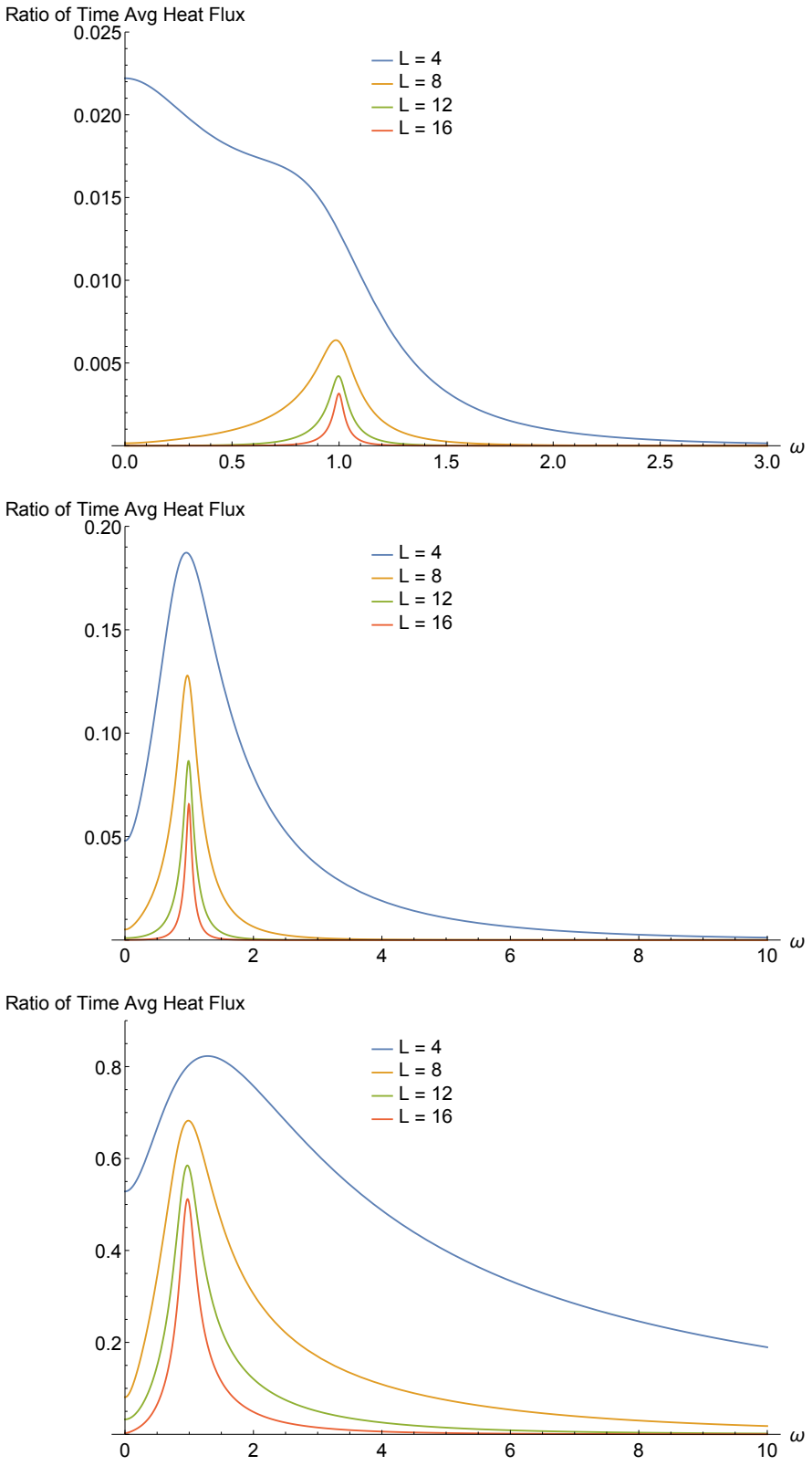

Figure 7.9: (Center-to-right wall) ratio of the time average of the heat flux vs. ω for different width L of the channel and $\mathsf{Pr} = 7$ (top), 0.7 (middle), and 0.07 (bottom).

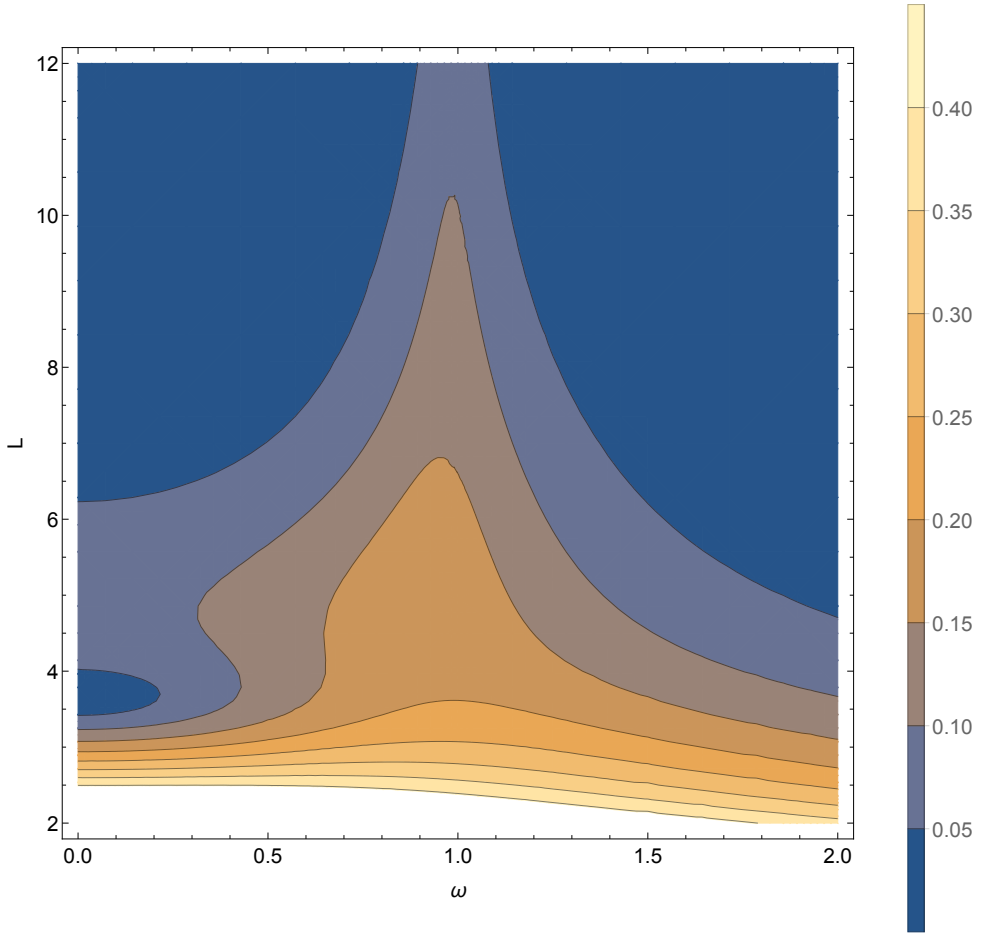

Figure 7.10: Contour plot of the (center-to-right wall) ratio of the time average of heat flux in the (ω, L) plane for $\mathsf{Pr} = 0.7$.

To get more details about when a resonance may occur, we draw the contour plots of $\mathcal{R}_{\phi_q}$ in the (ω, L)-plane for $\mathsf{Pr} = 0.7$ and $\mathsf{Pr} = 0.07$ as shown in Figures 7.10 and 7.11, respectively. Both contour plots show that there appears to be a critical length L after which we see resonance depicted by a single peak in the $\mathcal{R}_{\phi_q}$-curve around $\omega = 1$.

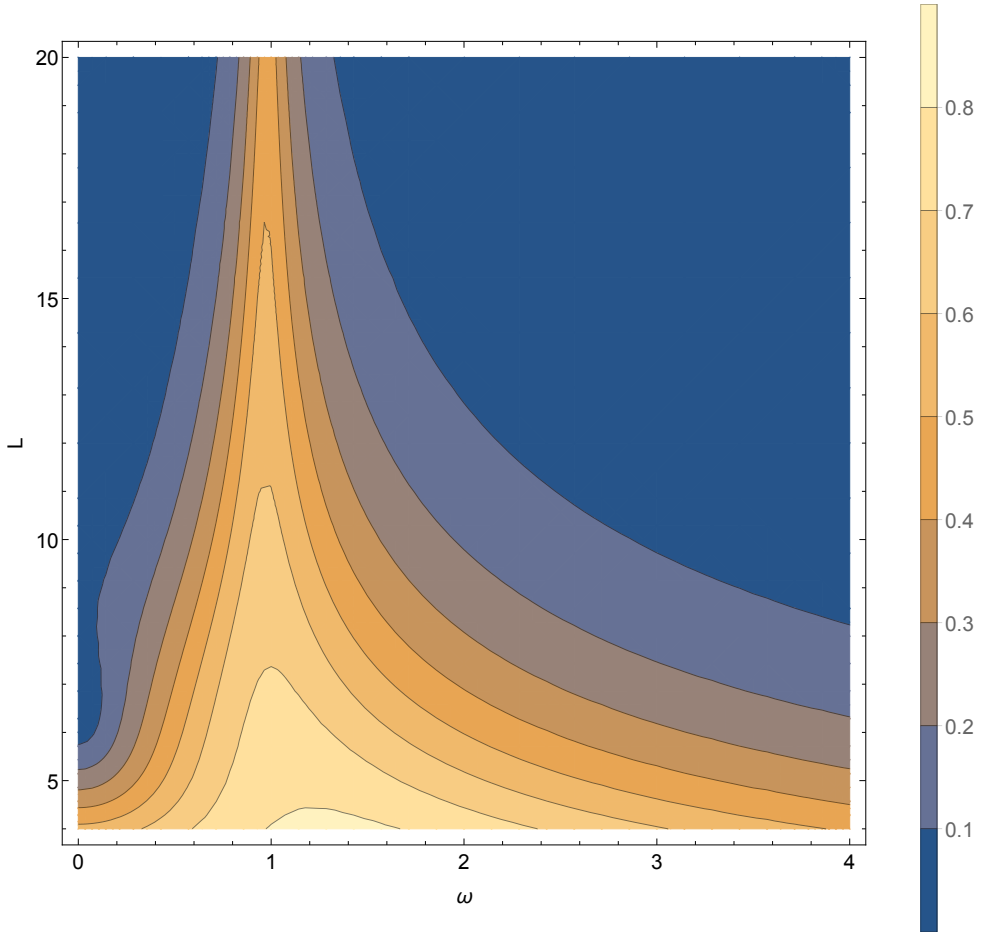

Figure 7.11: Contour plot of the (center-to-right wall) ratio of the time average of heat flux in the (ω, L) plane for $\mathsf{Pr} = 0.07$.

7.5 Concluding Remarks

Although the flow of the fluid is assumed to be one-dimensional, the coupling of the system by the stratification parameter adds complexity to the problem and appears to be one of the reasons why we see resonance effects. The analytical solutions for the vertical velocity and the temperature allow us to study the behaviour of the physical quantities and obtain plenty of observations some of which need more detailed interpretation. All performed studies indicate that the resonance frequency seems to be $\omega = 1$ but we do not have a rigorous

explanation for this. Moreover, we wish to obtain a somewhat explicit relation between Prandtl number Pr, the width of the channel L and the frequency ω. For each fixed Pr, we can then obtain the critical width L after which we see resonance in the fluid.

Appendix A

Coefficient Matrices for Numerical Scheme

Substituting the representations (3.20) in equations (3.16)-(3.19), we get the following numerical scheme :

For $\psi \in \{ \frac{1}{h} \chi_j,\, j = 0, \cdots, J-1\}$,

$$\begin{aligned} \sum_{j=0}^{J} \langle \psi \,,\, \phi_j \rangle \, \partial_t \rho_j = & - \mathrm{i}\, k_x \sum_{j=1}^{J-1} \langle \psi \,,\, \phi_j \rangle \, V_{x,j} + \frac{G}{T_0} \sum_{j=1}^{J-1} \langle \psi \,,\, \phi_j \rangle V_{z,j} \\ & - \sum_{j=1}^{J-1} \langle \psi \,,\, \partial_z \phi_j \rangle \, V_{z,j}. \end{aligned} \tag{A.1}$$

For $\psi \in \{ \frac{1}{h} \phi_j,\, j = 1, \cdots, J-1\}$,

$$\begin{aligned} \sum_{j=1}^{J-1} \langle \psi \,,\, \phi_j \rangle \, \partial_t V_{x,j} = & - \mathrm{i}\, k_x \, T_0 \, \sum_{j=0}^{J-1} \langle \psi \,,\, \chi_j \rangle \, \rho_j \\ & - \mathrm{i}\, k_x \, \sum_{j=1}^{J} \langle \psi \,,\, \phi_j \rangle \, S_j \\ & - \nu_0 \sum_{j=1}^{J-1} \langle \partial_z \left(\frac{1}{\bar{n}} \, \psi \right) , \, \partial_z \phi_j \rangle \, V_{x,j} \\ & - \nu_0 \, k_x^2 \, \sum_{j=1}^{J-1} \langle \psi \,,\, \frac{1}{\bar{n}} \, \phi_j \rangle V_{x,j}, \end{aligned} \tag{A.2}$$

and

$$\begin{aligned}\sum_{j=1}^{J-1}\langle\,\psi\,,\,\phi_j\,\rangle\;\partial_t V_{z,j} = \quad & T_0\sum_{j=0}^{J-1}\langle\,\partial_z\psi\,,\,\chi_j\,\rangle\;\rho_j + \frac{G}{T_0}\sum_{j=1}^{J}\langle\,\psi\,,\,\phi_j\,\rangle\,S_j \\ & - \sum_{j=1}^{J}\langle\,\psi\,,\,\partial_z\phi_j\,\rangle\;S_j \\ & - \nu_0\sum_{j=1}^{J-1}\langle\,\partial_z\left(\frac{1}{\bar{n}}\,\psi\right),\,\partial_z\phi_j\,\rangle V_{z,j} \\ & - \nu_0\,k_x^2\;\sum_{j=1}^{J-1}\langle\,\psi\,,\,\frac{1}{\bar{n}}\,\phi_j\,\rangle\;V_{z,j}.\end{aligned} \tag{A.3}$$

For $\psi\;\in\;\{\;\dfrac{1}{h}\;\phi_j,\;j=1,\cdots,J\}$,

$$\begin{aligned}\sum_{j=1}^{J}\langle\,\psi\,,\,\phi_j\,\rangle\,\partial_t\,S_j = & -\,\mathrm{i}\,k_x\,T_0\;\sum_{j=1}^{J-1}\langle\,\psi\,,\,\phi_j\,\rangle\;V_{x,j} - T_0\;\sum_{j=1}^{J-1}\langle\,\psi\,,\,\partial_z\phi_j\,\rangle\,V_{z,j} \\ & - \kappa_0\;\sum_{j=1}^{J}\langle\,\partial_z\left(\frac{1}{\bar{n}}\,\psi\right),\,\partial_z\phi_j\,\rangle\;S_j \\ & - \kappa_0\,k_x^2\;\sum_{j=1}^{J}\langle\,\psi\,,\,\frac{1}{\bar{n}}\,\phi_j\,\rangle S_j.\end{aligned} \tag{A.4}$$

In what follows, we introduce some notation that would help us translate the numerical scheme into matrix form to be used later in the stability analysis. Note first that there are $4J-1$ equations in $4J-1$ unknowns and it is useful to divide the indexing set $1\;\leq\;i\;\leq\;4J-1$ into four regions each associated with the corresponding coefficients used in the finite element representation of the Fourier coefficients n_k', u_k', w_k' and T_k'.

Define the regions $\mathcal{I}_\rho$, $\mathcal{I}_{V_x}$, $\mathcal{I}_{V_z}$ and $\mathcal{I}_S$ and the corresponding indexing functions σ_ρ, σ_{V_x}, σ_{V_z} and σ_S as follows:

$$\mathcal{I}_\rho = \{\, j,\ 1 \le j \le J+1 \,\} \qquad \sigma_\rho(j) = j-1, \qquad j \in \mathcal{I}_\rho$$

$$\mathcal{I}_{V_x} = \{\, j,\ J+2 \le j \le 2J \,\} \qquad \sigma_{V_x}(j) = j-J-1, \qquad j \in \mathcal{I}_{V_x}$$

$$\mathcal{I}_{V_z} = \{\, j,\ 2J+1 \le j \le 3J-1 \,\} \qquad \sigma_{V_z}(j) = j-2J, \qquad j \in \mathcal{I}_{V_z}$$

$$\mathcal{I}_S = \{\, j,\ 3J \le j \le 4J-1 \,\} \qquad \sigma_S(j) = j-3J+1, \qquad j \in \mathcal{I}_S$$

Let C be a column vector containing the coefficients used in the finite element representations of n'_k, u'_k, w'_k and T'_k, that is

$$C = \Big(\rho_0(t) \cdots \rho_J(t) \;\; V_{x,1}(t) \cdots V_{x,J-1}(t) \;\; V_{z,1}(t) \cdots V_{z,J-1}(t) \;\; S_1(t) \cdots S_J(t) \Big)^T ,$$

where $(\ )^T$ is a short notation for transpose.

Define the $(4J-1) \times (4J-1)$ matrices $M = \{\, M_{l,j}\,,\ 1 \le l,j \le 4J-1 \,\}$ by

$$M_{l,j} = \frac{1}{h} \begin{cases} \langle\, \phi_{\sigma_\rho(l)}\,,\, \phi_{\sigma_\rho(j)} \,\rangle, & l,\, j \in \mathcal{I}_\rho \\ \langle\, \phi_{\sigma_{V_x}(l)}\,,\, \phi_{\sigma_{V_x}(j)} \,\rangle, & l,\, j \in \mathcal{I}_{V_x} \\ \langle\, \phi_{\sigma_{V_z}(l)}\,,\, \phi_{\sigma_{V_z}(j)} \,\rangle, & l,\, j \in \mathcal{I}_{V_z} \\ \langle\, \phi_{\sigma_S(l)}\,,\, \phi_{\sigma_S(j)} \,\rangle, & l,\, j \in \mathcal{I}_S \end{cases}$$

and $A = \{\, A_{l,j}\,,\ 1 \le l,j \le 4J-1 \,\}$ as follows:

For $l \in \mathcal{I}_\rho$,

$$A_{l,j} = \frac{1}{h} \begin{cases} -\,\mathrm{i}\,k_x \,\langle\, \phi_{\sigma_\rho(l)}\,,\, \phi_{\sigma_{V_x}(j)} \,\rangle, & j \in \mathcal{I}_{V_x} \\ +\,\frac{G}{T_0}\,\langle\, \phi_{\sigma_\rho(l)}\,,\, \phi_{\sigma_{V_z}(j)} \,\rangle - \langle\, \phi_{\sigma_\rho(l)}\,,\, \partial_z \phi_{\sigma_{V_z}(j)} \,\rangle, & j \in \mathcal{I}_{V_z} \\ \quad 0, \quad \text{otherwise} \end{cases}$$

For $l \in \mathcal{I}_{V_x}$,

$$A_{l,j} = \frac{1}{h} \begin{cases} -\mathrm{i}\,\mathrm{k_x}\,\mathrm{T}_0 \left\langle \phi_{\sigma_{\mathrm{V_x}}(\mathrm{l})}\,,\, \phi_{\sigma_\rho(\mathrm{j})} \right\rangle, \mathrm{j} \in \mathcal{I}_\rho \\ -\mathrm{i}\,k_x \left\langle \phi_{\sigma_{V_x}(l)}\,,\, \phi_{\sigma_S(j)} \right\rangle, j \in \mathcal{I}_S \\ -\nu_0 \big[\left\langle \partial_z \left(\frac{1}{\bar{n}}\,\phi_{\sigma_{V_x}(l)} \right),\, \partial_z \phi_{\sigma_{V_x}(j)} \right) \big\rangle + k_x^2 \left\langle \phi_{\sigma_{V_x}(l)}\,,\, \frac{1}{\bar{n}}\,\phi_{\sigma_{V_x}(j)} \right\rangle \big], j \in \mathcal{I}_{V_x} \\ \quad 0, \quad \text{otherwise} \end{cases}$$

For $l \in \mathcal{I}_{V_z}$,

$$A_{l,j} = \frac{1}{h} \begin{cases} T_0 \left\langle \partial_z \phi_{\sigma_{V_z}(l)}\,,\, \phi_{\sigma_\rho(j)} \right\rangle, j \in \mathcal{I}_\rho \\ \frac{G}{T_0} \left\langle \phi_{\sigma_{V_z}(l)}\,,\, \phi_{\sigma_S(j)} \right\rangle - \left\langle \phi_{\sigma_{V_z}(l)}\,,\, \partial_z \phi_{\sigma_S(j)} \right\rangle, j \in \mathcal{I}_S \\ -\nu_0 \big[\left\langle \partial_z \left(\frac{1}{\bar{n}}\,\phi_{\sigma_{V_z}(l)} \right),\, \partial_z \phi_{\sigma_{V_z}(j)} \right) \big\rangle + k_x^2 \big\langle \phi_{\sigma_{V_z}(l)}\,,\, \frac{1}{\bar{n}}\,\phi_{\sigma_{V_z}(j)} \big\rangle \big], j \in \mathcal{I}_{V_z} \\ \quad 0, \quad \text{otherwise} \end{cases}$$

For $l \in \mathcal{I}_S$,

$$A_{l,j} = \frac{1}{h} \begin{cases} -\mathrm{i}\; k_x\, T_0 \left\langle \phi_{\sigma_S(l)}\,,\, \phi_{\sigma_{V_x}(j)} \right\rangle, j \in \mathcal{I}_{V_x} \\ -T_0 \left\langle \phi_{\sigma_S(l)}\,,\, \partial_z \phi_{\sigma_{V_z}(j)} \right\rangle, j \in \mathcal{I}_{V_z} \\ -\kappa_0 \left[\left\langle \partial_z \left(\frac{1}{\bar{n}}\,\phi_{\sigma_S(l)} \right)\,,\, \partial_z \phi_{\sigma_S(j)} \right\rangle + k_x^2 \left\langle \phi_{\sigma_S(l)}\,,\, \frac{1}{\bar{n}}\,\phi_{\sigma_S(j)} \right\rangle \right], j \in \mathcal{I}_S \\ \quad 0. \quad \text{otherwise} \end{cases}$$

Bibliography

[1] T. Aberra, S.W. Armfield, M. Behnia, and G.D. McBain. Boundary layer instability of the natural convection flow on a uniformly heated vertical plate. *International Journal of Heat and Mass Transfer*, 55(21-22):6097–6108, 2012.

[2] J. A. D. Ackroyd. Stress work effects in laminar flat-plate natural convection. *Journal of Fluid Mechanics*, 62(4):677–695, 1974.

[3] S. W. Armfield and J. C. Patterson. Wave properties of natural-convection boundary layers. *Journal of Fluid Mechanics*, 239(195):195–211, 1992.

[4] E. Bacharoudis, M. G. Vrachopoulos, M. K. Koukou, D. Margaris, A. E. Filios, and S. A. Mavrommatis. Study of the natural convection phenomena inside a wall solar chimney with one wall adiabatic and one wall under a heat flux. *Applied Thermal Engineering*, 27:2266–2275, 2007.

[5] G. K. Batchelor. Heat transfer by free convection across a closed cavity between vertical boundaries at different temperatures. *Quarterly of Applied Mathematics*, 12:209–233, 1954.

[6] A. Belhadj Mohamed, J. Orfi, C. Debissi, and S. Ben Nasrallah. Heat and mass transfer during condensation in a vertical channel under mixed convection. *Heat and Mass Transfer*, 43(9):851–861, 2007.

[7] R. F. Bergholz. Instability of steady natural convection in a vertical fluid layer. *Journal of Fluid Mechanics*, 84:743–768, 1978.

[8] A. M. H. Brooker, J. C. Patterson, and S. W. Armfield. Non-parallel linear stability analysis of the vertical boundary layer in a differentially heated cavity. *Journal of Fluid Mechanics*, 352:265–281, 1997.

[9] S. Chandrasekhar. *Hydrodynamic and Hydromagnetic Stability.* Clarendon Press, Oxford, 1961.

[10] A. S. Cherif, M. A. Kassim, B. Benhamou, S. Harmand, J. P. Corriou, and S. Ben Jabrallah. Experimental and numerical study of mixed convection heat and mass transfer in a vertical channel with film evaporation. *International Journal of Thermal Sciences*, 50(6):942–953, 2011.

[11] L. Crane. Natural convection from a vertical cylinder at very large Prandtl numbers. *Journal of Engineering Mathematics*, 10(2):115–124, 1976.

[12] P. G. Daniels and J. C. Patterson. On the long-wave instability of natural-convection boundary layers. *Journal of Fluid Mechanics*, 335:57–73, 1997.

[13] P. G. Daniels and J. C. Patterson. On the short-wave instability of natural convection boundary layers. *The Royal Society of London. Proceedings. Series A. Mathematical, Physical and Engineering Sciences*, 457(2007):519–538, 2001.

[14] U. N. Das, R. K. Deka, and V. M. Soundalgekar. Transient free convection flow past an infinite vertical plate with periodic temperature variation. *Journal of Heat Transfer*, 121(4):1091–1094, 1999.

[15] R. K. Deka and A. Paul. Transient free convection flow past an infinite vertical cylinder with thermal stratification. *Journal of Mechanical Science and Technology*, 26(8):2229–2237, 2012.

[16] R. K. Deka and A. Paul. Convectively driven flow past an infinite moving vertical cylinder with thermal and mass stratification. *Pramana - Journal of Physics*, 81(4):641–665, 2013.

[17] P. G. Drazin and W. H. Reid. *Hydrodynamic Stability*. Cambridge University Press, Cambridge, 2nd edition, 2004.

[18] J. W. Elder. Laminar free convection in a vertical slot. *Journal of Fluid Mechanics*, 23:77–98, 1965.

[19] E. Fedorovich and A. Shapiro. Turbulent natural convection along a vertical plate immersed in a stably stratified fluid. *Journal of Fluid Mechanics*, 636:41–57, 2009.

[20] E. Fedorovich and A. Shapiro. Oscillations in Prandtl slope flow started from rest. *Quarterly Journal of the Royal Meteorological Society*, 143(703):670–677, 2017.

[21] B. Gebhart, Y. Jaluria, R. L. Mahajan, and B. Sammakia. *Buoyancy-Induced Flows and Transport*. Hemisphere Publishing Co., 1988.

[22] A. E. Gill. The boundary-layer regime for convection in a rectangular cavity. *Journal of Fluid Mechanics*, 26(3):515–536, 1966.

[23] A. E. Gill and A. Davey. Instabilities of a buoyancy-driven system. *Journal of Fluid Mechanics*, 35(4):775–798, 1969.

[24] R. J. Goldstein and D. G. Briggs. Transient free convection about vertical plates and circular cylinders. *Journal of Heat Transfer*, 86(4):490–500, 1964.

[25] G. H. Hardy, J. E. Littlewood, and G. Pólya. *Inequalities*. Cambridge University Press, Cambridge, 1988.

[26] Tae Hattori, S. Armfield, M. P. Kirkpatrick, S. Maruyama, and A. Komiya. Numerical study of a transitional natural ventilation flow driven by a line source plume with varied Reynolds and Prandtl numbers. *Computational Thermal Sciences*, 3(6):511–519, 2011.

[27] Tae Hattori, S. Norris, M. Kirkpatrick, and S. Armfield. Prandtl number dependence and instability mechanism of the near-field flow in a planar thermal plume. *Journal of Fluid Mechanics*, 732:105–127, 2013.

[28] D. Henry. *Geometric Theory of Semilinear Parabolic Equations*, volume 840 of *Lecture Notes in Mathematics*. Springer-Verlag, Berlin-New York, 1981.

[29] Jae Min Hyun. Unsteady buoyant convection in an enclosure. *Advances in Heat Transfer*, 24(4):277–320, 1994.

[30] M. Ihdene, T. Ben Malek, S. Aberkane, M. Mouderes, P. Spitéri, and A. Ghezal. Analytical and numerical study of the evaporation on mixed convection in vertical rectangular cavity. *Fluid Dynamics and Materials Processing Journal*, 13(2):85–105, 2017.

[31] C. R. Illingworth. Unsteady laminar flow of gas near an infinite flat plate. *Mathematical Proceedings of the Cambridge Philosophical Society*, 46(4):603–613, 1950.

[32] M. C. Jischke and R. T. Doty. Linearized buoyant motion in a closed container. *Journal of Fluid Mechanics*, 71(4):729–754, 1975.

[33] M. Kazmierczak and Z. Chinoda. Buoyancy-driven flow in an enclosure with time periodic boundary conditions. *International Journal of Heat and Mass Transfer*, 35(6):1507–1518, 1992.

[34] I. Khan, N. Ali Shah, A. Tassaddiq, N. Mustapha, and S. Awang Kechil. Natural convection heat transfer in an oscillating vertical cylinder. *PLoS ONE*, 13(1):e0188656, 2018.

[35] R. Khanal and C. Lei. A scaling investigation of the laminar convective flow in a solar chimney for natural ventilation. *International Journal of Heat and Fluid Flow*, 45:98–108, 2014.

[36] Sung Ki Kim, Seo Young Kim, and Young Don Choi. Resonance of natural convection in a side heated enclosure with a mechanically oscillating bottom wall. *International Journal of Heat and Mass Transfer*, 45(15):3155–3162, 2002.

[37] Sung Ki Kim, Seo Young Kim, and Young Don Choi. Amplification of boundary layer instability by hot wall thermal oscillation in a side heated cavity. *Physics of Fluids*, 17(1), 2005.

[38] P. K. Kundu and I. M. Cohen. *Fluid Mechanics*. Academic Press, San Diego, 2nd edition, 2002.

[39] Ho Sang Kwak and Jae Min Hyun. Natural convection in an enclosure having a vertical sidewall with time-varying temperature. *Journal of Fluid Mechanics*, 329:65–88, 1996.

[40] Ho Sang Kwak, Kunio Kuwahara, and Jae Min Hyun. Resonant enhancement of natural convection heat transfer in a square enclosure. *International Journal of Heat and Mass Transfer*, 41(18):2837–2846, 1998.

[41] J. L. Lage and A. Bejan. The resonance of natural convection in an enclosure heated periodically from the side. *International Journal of Heat and Mass Transfer*, 36(8):2027–2038, 1993.

[42] Jia Ma, Bingchuan Nie, and Feng Xu. Transient flows on an evenly heated wall with a fin. *International Journal of Heat and Mass Transfer*, 118:235–246, 2018.

[43] R. L. Mahajan and B. Gebhart. Viscous dissipation effects in buoyancy induced flows. *International Journal of Heat and Mass Transfer*, 32(7):1380–1382, 1989.

[44] G. D. McBain, S. W. Armfield, and G. Desrayaud. Instability of the buoyancy layer on an evenly heated vertical wall. *Journal of Fluid Mechanics*, 587:453–469, 2007.

[45] W. J. Minkowycz and Ping Cheng. Free convection about a vertical cylinder embedded in a porous medium. *International Journal of Heat and Mass Transfer*, 19(7):805–813, 1976.

[46] H. R. Nagendra, M. A. Tirunarayanan, and A. Ramachandran. Laminar free convection from vertical cylinders with uniform heat flux. *Journal of Heat Transfer*, 92(1):191–194, 1970.

[47] A. Nait Alla, M. Feddaoui, and H. Meftah. Numerical study of the evaporation by mixed convection of ethanol in partially heated plate along a vertical channel. *International Journal of Heat and Mass Transfer*, 89:206–215, 2015.

[48] A. Nasr, C. Debbissi, and S. Ben Nasrallah. Evaporation of a thin binary liquid film by forced convection into air and superheated steam. *Journal of Thermal Science*, 19(4):346–356, 2010.

[49] H. F. Nouanégué and E. Bilgen. Heat transfer by convection, conduction and radiation in solar chimney systems for ventilation of dwellings. *International Journal of Heat and Fluid Flow*, 30(1):150–157, 2009.

[50] Jun Sang Park. Transient buoyant flows of a stratified fluid in a vertical channel. *KSME International Journal*, 15:656–664, 2001.

[51] Jun Sang Park and Jae Min Hyun. Transient behavior of vertical buoyancy layer in a stratified fluid. *International Journal of Heat and Mass Transfer*, 41:4393–4397, 1998.

[52] K. Petersen. *Ergodic Theory*. Cambridge University Press, Cambridge, 1983.

[53] B. Podvin and P. Le Quéré. Nonlinear dynamics between two differentially heated vertical plates in the presence of stratification. *Theoretical and Computational Fluid Dynamics*, 27:89–114, 2013.

[54] L. Prandtl. *Essentials of Fluid Dynamics. With applications to hydraulics, aeronautics, meteorology, and other subjects*. Blackie & Son Limited, London, 1952.

[55] S. Punyasompun, J. Hirunlabh, J. Khedari, and B. Zeghmati. Investigation on the application of solar chimney for multi-storey buildings. *Renewable Energy*, 34(12):2545–2561, 2009.

[56] A. Rényi. On measures of entropy and information. In *Proc. 4th Berkeley Sympos. Math. Statist. and Prob., Vol. I*, pages 547–561. Univ. California Press, Berkeley, Calif., 1961.

[57] A. Rényi. *Probability Theory*. North-Holland, Amsterdam-London, 1970.

[58] H. Saleh, A. I. Alsabery, and I. Hashim. Natural convection in polygonal enclosures with inner circular cylinder. *Advances in Mechanical Engineering*, 7(12):1–10, 2015.

[59] H. Schlichting. *Boundary-Layer Theory*. McGraw-Hill, New York, 7th edition, 1979.

[60] A. Shapiro and E. Fedorovich. Prandtl number dependence of unsteady natural convection along a vertical plate in a stably stratified fluid. *International Journal of Heat and Mass Transfer*, 47:4911–4927, 2004.

[61] A. Shapiro and E. Fedorovich. Unsteady convectively driven flow along a vertical plate immersed in a stably stratified fluid. *Journal of Fluid Mechanics*, 498:333–352, 2004.

[62] A. Shapiro and E. Fedorovich. Natural convection in a stably stratified fluid along vertical plates and cylinders with temporally periodic surface temperature variations. *Journal of Fluid Mechanics*, 546:295–311, 2006.

[63] J. Singh and R. Bajaj. Stability of temperature modulated convection in a vertical fluid layer. *Applied Mathematical Modelling*, 61:408–420, 2018.

[64] E. V. Starikov, V. A. Klimova, and S. E. Shcheklein. Study of natural convection development in narrow vertical channels. *Journal of Physics: Conference Series*, 1105:012005, Nov 2018.

[65] M. Tadie Fogaing, L. Nana, O. Crumeyrolle, and I. Mutabazi. Wall effects on the stability of convection in an infinite vertical layer. *International Journal of Thermal Sciences*, 100:240–247, 2016.

[66] A. Terzi, S. Ben Jabrallah, and S. Harmand. Experimental study of heat and mass transfer for liquid film evaporation along a vertical plate covered with a porous layer. *Journal of Applied Fluid Mechanics*, 9:113–120, 2016.

[67] J. A. Walker. *Dynamical Systems and Evolution Equations*. Plenum Press, New York-London, 1980.

[68] G. F. Webb. Compactness of bounded trajectories of dynamical systems in infinite-dimensional spaces. *Proceedings of the Royal Society of Edinburgh. Section A. Mathematical and Physical Sciences*, 84(1-2):19–33, 1979.

[69] N. Williamson, S. W Armfield, and M. P. Kirkpatrick. Transition to oscillatory flow in a differentially heated cavity with a conducting partition. *Journal of Fluid Mechanics*, 693:93–114, 2012.

[70] N. Williamson, S. W. Armfield, M. P. Kirkpatrick, and S. E. Norris. Transition to stably stratified states in open channel flow with radiative surface heating. *Journal of Fluid Mechanics*, 766:528–555, 2015.

[71] N. Williamson, S. W. Armfield, Wenxian Lin, and M. P. Kirkpatrick. Stability and Nusselt number scaling for inclined differentially heated cavity flow. *International Journal of Heat and Mass Transfer*, 97:787–793, 2016.

[72] N. Williamson, M. Kirkpatrick, and S. Armfield. Entrainment across a sheared density interface in a cavity flow. *Journal of Fluid Mechanics*, 835:999–1021, 2018.

[73] B. Zamora and A. S. Kaiser. Optimum wall-to-wall spacing in solar chimney shaped channels in natural convection by numerical investigation. *Applied Thermal Engineering*, 29(4):762–769, 2009.

[74] D. Zardi and S. Serafin. An analytic solution for time-periodic thermally driven slope flows. *Quarterly Journal of the Royal Meteorological Society*, 141:1968–1974, 2015.

[75] Yongling Zhao, Chengwang Lei, and J. Patterson. Resonance of the thermal boundary layer adjacent to an isothermally heated vertical. *Journal of Fluid Mechanics*, 724:305–336, 2013.

[76] Yongling Zhao, Chengwang Lei, and J. Patterson. The k-type and h-type transitions of natural convection boundary layers. *Journal of Fluid Mechanics*, 824:352–387, 2017.